

The Low-Temperature Geothermal Resource  
and Stratigraphy of Portions of Yakima County, Washington

by

John Biggane

Prepared for  
Washington State Department of Natural Resources

Under Contract No. DE-AC07-79ET27014  
with the U.S. Department of Energy

Washington Division of Geology and Earth Resources

Open File Report 82-6

Geological Engineering Section  
Washington State University  
Pullman, Washington  
July 30, 1982

WSU College of Engineering Research Report 82/15-7



## Acknowledgements

I wish to express my gratitude to the following people: to Professor James W. Crosby III for acting as chairman of my Master's committee, for his suggestions and review of this report, and for his advice and guidance while I was studying at Washington State University; to Diane Weber for making the completion of this report possible, for serving as project manager, for editing, typing, and proof-reading this report, and for her patience with the author; to Jeff Brown and Tom Weber for their insights and discussions concerning geophysical borehole logging and stratigraphic correlation of the Columbia River Basalts; to J. Eric Schuster and Mike Korosec of the Washington State Department of Natural Resources for their encouragement, assistance, and discussions; to Dr. Gary Webster and Professor Howard Copp for reviewing this report and serving as members of my Master's committee; to Newell Campbell for leading a field trip in the Yakima region; to all the people, most unknown to me, who have collected the geophysical data utilized in this report; and special thanks to my wife, Lesley, for enduring the trials and burdens of my graduate study.

This research was funded through a subcontract from the Washington State Department of Natural Resources under Contract No. DE-AC07-79ET27014 from the U. S. Department of Energy.



## Abstract

The low-temperature geothermal resource of portions of Yakima County, south-central Washington, is defined by several least squares linear regression analyses of bottom-hole temperature and depth data. Intra-borehole flow prevents the use of borehole temperature gradients for geothermal resource assessment. The traditional method of calculating geothermal gradients by utilizing bottom-hole temperatures and assumed land-surface temperatures proved unsatisfactory.

Bottom-hole temperature and depth data were separated into fourteen well data groups based on geographic proximity, land slope azimuth, and position within the regional ground-water flow system. The depths of these wells range from over 50m to almost 600m.

The regression analyses of these well data groups indicate that the projected land-surface temperature and geothermal gradient range from 10.6 to 14.0°C and from 24.9 to 52.2°C/km, respectively. The depth to the 20°C isotherm ranges from 142 to 346m. The average projected land-surface temperature and geothermal gradient are approximately 11.3°C and 43.0°C/km, respectively. The average depth to the 20°C isotherm is approximately 202m. The projected land-surface temperature appears to decrease and the depth to the 20°C isotherm appears to increase as the land-surface elevation of the well data group increases.

Stratigraphic correlation diagrams developed from borehole geophysical and lithologic logs are given for localities within the lower Yakima, Black Rock, Moxee, Ahtanum, Cowiche, and Naches valleys. These correlation diagrams are combined with their respective borehole temperature logs and well data group predicted temperature curves to assess the validity of the regression analyses and to determine aquifer locations, temperatures, and directions of intra-borehole flow.

A regression analysis of data from wells of south-central Washington with bottom-hole depths of over 700m to almost 3km suggests that the projected land-surface temperature and geothermal gradient of this depth interval are 21.8°C and 31.3°C/km, respectively. The depth to the 100°C isotherm is approximately 2513m.



Table of Contents

	Page
Acknowledgements . . . . .	i
Abstract . . . . .	iif
List of Figures . . . . .	ix
List of Plates . . . . .	xiii
List of Tables . . . . .	xv
Introduction . . . . .	1
Geology, Stratigraphy, and Geologic Structures of the Yakima Region .	1
Geology . . . . .	1
Columbia River Basalt Group . . . . .	1
Columbia River Basalt Group Intraflow Structures . . . . .	1
Ellensburg Formation . . . . .	4
Stratigraphy . . . . .	5
Grande Ronde Formation . . . . .	46
Vantage Member of the Ellensburg Formation . . . . .	46
Wanapum Formation . . . . .	47
Frenchman Springs Member . . . . .	47
Squaw Creek Member of the Ellensburg Formation . . . . .	47
Roza Member . . . . .	49
Quincy Member(?) of the Ellensburg Formation . . . . .	49
Priest Rapids Member of the Wanapum Formation . . . . .	49
Mabton Member of the Ellensburg Formation . . . . .	49

Table of Contents (cont.)

	Page
Saddle Mountains Formation . . . . .	49
Umatilla Member of the Saddle Mountains Formation . . .	49
Huntzinger Valley Flow (Asotin Member?) of the Saddle Mountains Formation . . . . .	50
Selah Member of the Ellensburg Formation . . . . .	50
Pomona Member of the Saddle Mountains Formation . . . .	50
Rattlesnake Ridge Member of the Ellensburg Formation .	51
Elephant Mountain Member of the Saddle Mountains Formation . . . . .	51
Upper Ellensburg Formation and Quaternary Sediments . .	51
Tieton Andesite . . . . .	52
Geologic Structure . . . . .	52
Ground-Water Hydrology of the Yakima Region . . . . .	53
Ground-Water Flow Model in the Yakima Region . . . . .	53
Ground-Water Occurrence in the Yakima Region . . . . .	54
The Sedimentary Aquifer . . . . .	54
The Basalt Aquifer . . . . .	54
Geothermal Resources of the Yakima Region . . . . .	56
Introduction . . . . .	56
Previous Geothermal Research in the Yakima Region . . . . .	63
Temperature Data . . . . .	64
Calculation of Geothermal Gradients in the Yakima Region . . . . .	65
Geothermal Gradients in the Yakima Region . . . . .	70
Projected Land Surface Temperatures, Mean Elevations, Land Slope Azimuths, and Dip Angles of Well Data Groups . . . . .	105
Deep vs. Shallow Geothermal Gradients . . . . .	109
Heat Flow in the Yakima Region . . . . .	112

Table of Contents (cont.)

	Page
Conclusions . . . . .	114
References . . . . .	115
Appendix	
Locations, Designations, Bottom-hole Temperatures, and Bottom-hole Depths of Selected Wells in the Yakima Region . . . . .	123



## List of Figures

Figure		Page
1.	Location of the study area . . . . .	2
2.	Idealized basalt intraflow structures . . . . .	3
3.	Generalized stratigraphic column . . . . .	6
4.	Stratigraphic correlation diagram, Line 1 . . . . .	7
5.	Stratigraphic correlation diagram, Line 2 . . . . .	8
6.	Stratigraphic correlation diagram, Line 3 . . . . .	9
7.	Stratigraphic correlation diagram, Line 4 . . . . .	10
8.	Stratigraphic correlation diagram, Line 5 . . . . .	11
9.	Stratigraphic correlation diagram, Line 6 . . . . .	12
10.	Stratigraphic correlation diagram, Line 7 . . . . .	13
11.	Stratigraphic correlation diagram, Line 8 . . . . .	14
12.	Stratigraphic correlation diagram, Line 9 . . . . .	15
13.	Stratigraphic correlation diagram, Line 10 . . . . .	16
14.	Stratigraphic correlation diagram, Line 11 . . . . .	17
15.	Stratigraphic correlation diagram, Line 12 . . . . .	18
16.	Stratigraphic correlation diagram, Line 13 . . . . .	19
17.	Stratigraphic correlation diagram, Line 14 . . . . .	20
18.	Stratigraphic correlation diagram, Line 15 . . . . .	21
19.	Stratigraphic correlation diagram, Line 16 . . . . .	22
20.	Stratigraphic correlation diagram, Line 17 . . . . .	23
21.	Typical natural gamma response of the Umatilla and Squaw Creek members . . . . .	48
22.	Relationship between the ground-water flow system and the geothermal gradient . . . . .	62

List of Figures (cont.)

Figure		Page
23.	Step-like distortion of the borehole temperature log . . . . .	66
24.	Plot of bottom-hole temperature vs. bottom-hole depth for well data group 1 . . . . .	71
25.	Plot of bottom-hole temperature vs. bottom-hole depth for well data group 2 . . . . .	72
26.	Plot of bottom-hole temperature vs. bottom-hole depth for well data group 3 . . . . .	73
27.	Plot of bottom-hole temperature vs. bottom-hole depth for well data group 4 . . . . .	74
28.	Plot of bottom-hole temperature vs. bottom-hole depth for well data group 5 . . . . .	75
29.	Plot of bottom-hole temperature vs. bottom-hole depth for well data group 6 . . . . .	76
30.	Plot of bottom-hole temperature vs. bottom-hole depth for well data group 7 . . . . .	77
31.	Plot of bottom-hole temperature vs. bottom-hole depth for well data group 8 . . . . .	78
32.	Plot of bottom-hole temperature vs. bottom-hole depth for well data group 9 . . . . .	79
33.	Plot of bottom-hole temperature vs. bottom-hole depth for well data group 10 . . . . .	80
34.	Plot of bottom-hole temperature vs. bottom-hole depth for well data group 11 . . . . .	81
35.	Plot of bottom-hole temperature vs. bottom-hole depth for well data group 12 . . . . .	82
36.	Plot of bottom-hole temperature vs. bottom-hole depth for well data group 13 . . . . .	83
37.	Plot of bottom-hole temperature vs. bottom-hole depth for well data group 14 . . . . .	84
38.	Borehole temperature logs and well data group predicted temperature curves, Line 1 . . . . .	87
39.	Borehole temperature logs and well data group predicted temperature curves, Line 2 . . . . .	88

List of Figures (cont.)

Figure		Page
40.	Borehole temperature logs and well data group predicted temperature curves, Line 3 . . . . .	89
41.	Borehole temperature logs and well data group predicted temperature curves, Line 4 . . . . .	90
42.	Borehole temperature logs and well data group predicted temperature curves, Line 5 . . . . .	91
43.	Borehole temperature logs and well data group predicted temperature curves, Line 6 . . . . .	92
44.	Borehole temperature logs and well data group predicted temperature curves, Line 7 . . . . .	93
45.	Borehole temperature logs and well data group predicted temperature curves, Line 8 . . . . .	94
46.	Borehole temperature logs and well data group predicted temperature curves, Line 9 . . . . .	95
47.	Borehole temperature logs and well data group predicted temperature curves, Line 10 . . . . .	96
48.	Borehole temperature logs and well data group predicted temperature curves, Line 11 . . . . .	97
49.	Borehole temperature logs and well data group predicted temperature curves, Line 12 . . . . .	98
50.	Borehole temperature logs and well data group predicted temperature curves, Line 14 . . . . .	99
51.	Borehole temperature logs and well data group predicted temperature curves, Line 15 . . . . .	100
52.	Borehole temperature logs and well data group predicted temperature curves, Line 16 . . . . .	101
53.	Borehole temperature logs and well data group predicted temperature curves, Line 17 . . . . .	102
54.	Mean elevation vs. projected land surface temperature of the well data groups . . . . .	107
55.	Mean elevation vs. depth to the 20°C isotherm of the well data groups . . . . .	108
56.	Plot of bottom-hole temperature vs. bottom-hole depth for the deep well data group . . . . .	110

List of Figures (cont.)

Figure		Page
57.	Plot of bottom-hole temperature vs. bottom-hole depth for the shallow well data group . . . . .	111
58.	Plot of bottom-hole temperature vs. bottom-hole depth for the shallow and the deep well data groups . . . . .	113

List of Plates

Plate

1. Preliminary structural geology and locations  
of stratigraphic correlation lines . . . . . in pocket
2. Well data group locations and pertinent  
parameters . . . . . in pocket
3. Location of bottom-hole temperature data  
points . . . . . in pocket
4. Location of bottom-hole temperature data  
points from depths greater than 700m . . . . . in pocket



## List of Tables

Table		Page
1.	Elevations at the tops of the geologic units in the Lower Yakima, Ahtanum, Moxee, and Black Rock valleys . . . . .	24
2.	Elevations at the tops of the geologic units in the Cowiche and Naches valleys . . . . .	33
3.	Thicknesses of the geologic units in the Lower Yakima, Ahtanum, Moxee, and Black Rock valleys . . . . .	35
4.	Thicknesses of the geologic units in the Cowiche and Naches valleys . . . . .	44
5.	Transmissivities, specific capacities, and pumping yields of the Yakima region sedimentary aquifer . . . . .	55
6.	Transmissivities, specific capacities, and pumping yields of the basalt aquifer of the Columbia Plateau . . . . .	57
7.	Transmissivities, specific capacities, and pumping yields of wells that penetrate the basalts in the Yakima region . . . . .	59
8.	Error in the geothermal gradient resulting from incorrect land surface temperatures as a function of depth . . . . .	68
9.	Quality designations, geothermal gradients, land surface temperatures, and depth to 20°C isotherm of well data groups . . . . .	85
10.	Well data group geothermal gradients, mean geothermal gradients G1 and G2, errors in geothermal gradient G2, and corrected mean geothermal gradient G2 . . . . .	104
11.	Mean elevations and azimuths of well data groups . . . . .	106



## Introduction

The low-temperature geothermal resource within the aquifers of the Columbia Plateau has become a significant, albeit minor, energy source during the last decade. Utilization of this resource is expected to increase as other energy sources become more costly and as the number and depth of the water wells of the Columbia Plateau increases.

The study area, the Yakima region, is located in south-central Washington state, as shown in Figure 1. The region lies in the Yakima Folds geomorphic province on the western edge of the Columbia Plateau. A series of southeastward-trending anticlinal ridges and synclinal valleys dominate the topography of the region. This investigation is limited primarily to the valleys of the region.

The research which culminated in this report was aimed at describing the nature of the low-temperature ground water of the Yakima region. A review of the geology, stratigraphy, and ground-water hydrology precedes the description of the geothermal resource of the region.

## Geology, Stratigraphy, and Geologic Structures of the Yakima Region

### Geology

The lava flows of the Columbia River Basalt Group (CRBG) and the interbedded and overlying sediments of the Ellensburg Formation comprise the bulk of the near-surface stratigraphic section of the Yakima region. The deposition of the lava flows and interbedded sediments occurred during the early to late Miocene, approximately 16.5 to 10.5 million years B.P. (Swanson and Wright, 1978; Swanson and others, 1979a). These deposits formed during a period of coeval basaltic and calc-alkaline volcanism and alluvial sedimentation (Schmincke, 1967a; Swanson and Wright, 1978). Valley-filling Pliocene and Quaternary sediments overlie the older formations throughout most of the region. Quaternary andesitic flows occur in the Cowiche Valley.

### Columbia River Basalt Group

The CRBG consists of numerous fine-grained, tholeiitic basalt flows which erupted in the eastern two-thirds of the Columbia Plateau (Swanson and Wright, 1978). These basalt flows moved into the Yakima region over gentle paleoslopes that dipped to the south, west, and northwest (Schmincke, 1967a; Long and others, 1980). The thickness of the CRBG in the region is unknown but probably exceeds 1,000m (Bentley, 1977; Bentley and others, 1980).

The typical CRBG flow averages 30 to 40m in thickness and commonly exhibits three major zones of intraflow structures (Swanson, 1967; Diery and McKee, 1969). These zones--the entablature, the colonnade, and the pillow-palagonite complex--and their distinguishing features are illustrated in Figure 2.

### Columbia River Basalt Group Intraflow Structures

The following description of basalt intraflow structures has been obtained primarily from Swanson (1967) and Swanson and Wright (1978) and for the sake of brevity is presented below without appropriate citations. Detailed information about basalt intraflow structures is given by Myers and others (1979) and Myers and Price (1981).

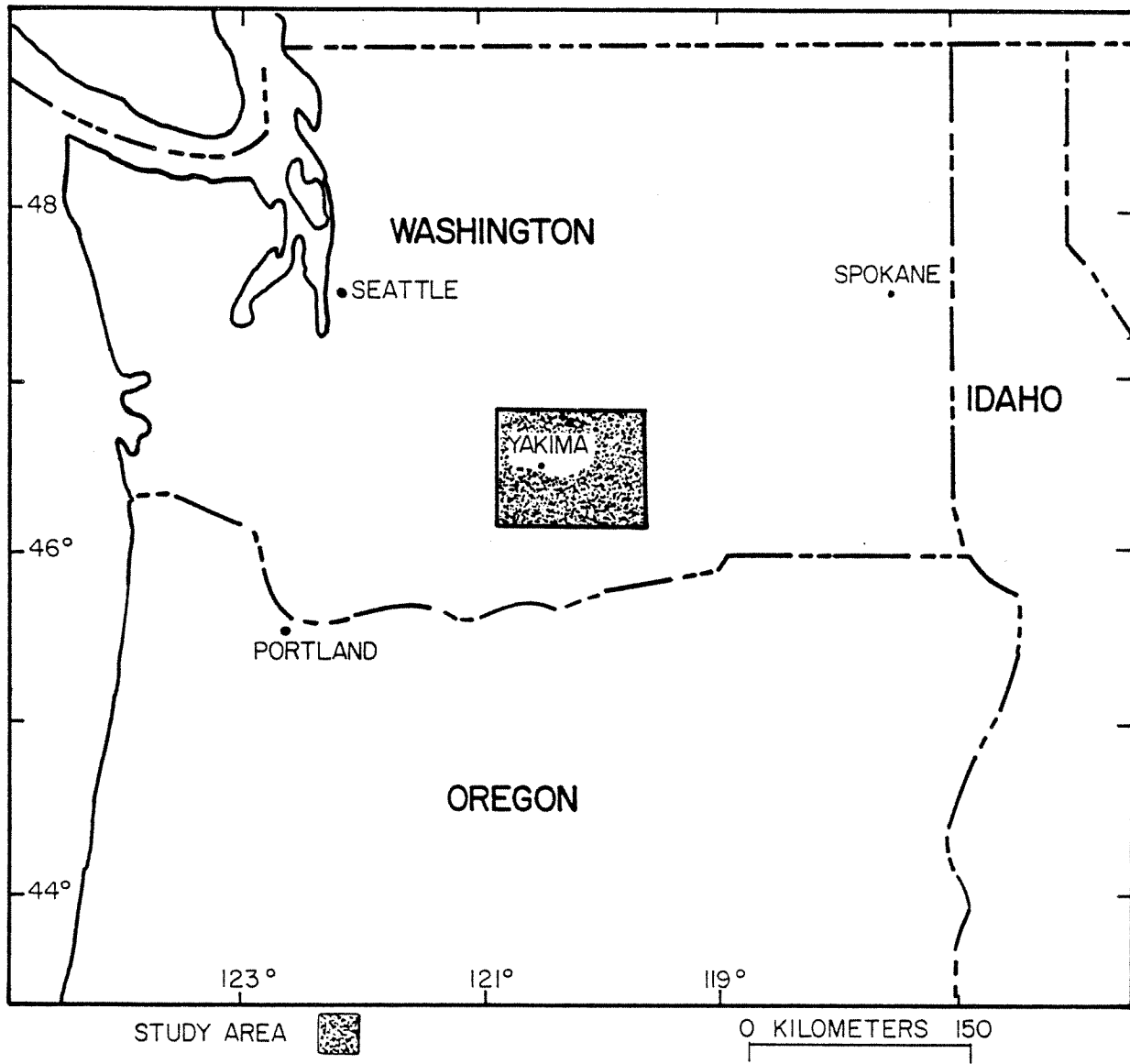


FIGURE 1 LOCATION OF THE STUDY AREA

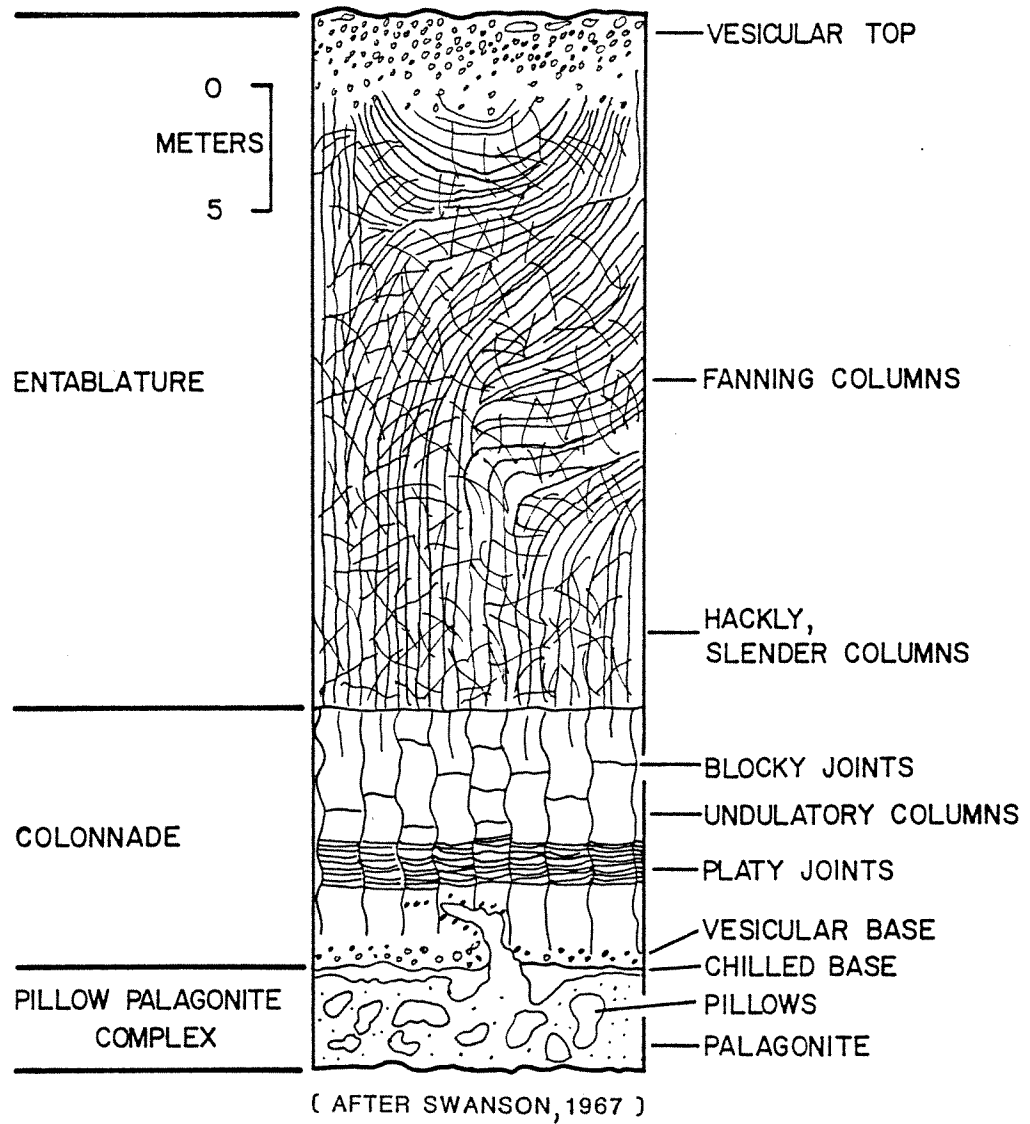


FIGURE 2 IDEALIZED BASALT INTRAFLOW STRUCTURES

The colonnade consists of nearly vertical, three- to eight-sided columns which average 1m in diameter and 5 to 10m in length. Columns within the colonnade range from 10cm to 5m in diameter and may reach a length of 50 to 75m. Columnar contacts are planar to undulatory, and the columns are commonly subdivided by cross-cutting, blocky, and platy joints. A vesicular zone often occurs in the lower several centimeters of the colonnade.

The contact between the colonnade and the overlying entablature is normally sharp, with the transition occurring over 1 to 2cm, but it can be gradational over several meters. The diameter of the entablature columns is generally less than 25cm, and the contacts are commonly highly undulatory. The columns are often described as being in fan-, tent-, or synclinal-shaped arrangements. Hackly joints are common and, when abundant, may obliterate the columnar structures. The upper portion of the entablature is often vesicular and may grade into a poorly-defined zone of larger diameter columns called the upper colonnade. A pillow-palagonite complex, which indicates that deposition occurred in water, may be found at the base of a basalt flow.

The sequence of an entablature overlying the colonnade does not occur in every flow. Myers and others (1979) described Grande Ronde intraflow structures in the Pasco Basin and defined three flow types which were based on the presence of these structures. Type 1 flows are thin (10-30m) and lack a distinct entablature. Type 2 flows are thick (45-76m) and consist of alternating tiers of entablature and colonnade-type columns which grade upward into a hackly entablature. Type 3 flows are moderately thick (30-80m) and possess a well-defined colonnade, entablature, and a crude upper colonnade.

Depending upon position within the flow, the difference in intraflow structures causes the basalt flow to exhibit a wide range of porosity. Estimated effective porosities range from less than 1 percent for dense basalt to 16 percent for fractured basalt (Gephart and others, 1979). Fracture measurements of the Grande Ronde basalt flows in the Pasco Basin indicate that most fractures are less than 1mm wide and that 85 percent of them are filled (Gephart and others, 1979). Rare, unfilled fractures of up to 12mm width were also noted (Gephart and others, 1979).

### Ellensburg Formation

The sediments that are interbedded with and overlie the CRBG have been grouped together as the Ellensburg Formation (Swanson and others, 1979a). In general, the thickness and frequency of the interbeds increase as the stratigraphic section becomes younger. Interbed thicknesses average less than 20m but may be greater than 100m or absent altogether.

The composition of the sediments reflects four different sources: volcanoclastic, plutonic-metamorphic, basaltic, and biogenetic (Schmincke, 1967a; Swanson and Wright, 1978). The volcanoclastic sediments were transported into the region by rivers and lahars and as ashfalls from the Cascade region. Sediments of plutonic-metamorphic origin were transported into the region from the north by the ancestral Columbia River and from the west by rivers and streams. Sediments of basaltic and biogenetic origin were derived locally.

The interbed sediments may range from cobble to clay-size material and, in some localities, may be fused to glass by a succeeding lava flow (Schmincke, 1967b). An average estimated effective porosity for the interbeds is reported to be less than 10 percent (Gephart and others, 1979) and would vary according to the interbed composition.

## Stratigraphy

Geologic studies in the Yakima region were initiated near the turn of the century by Russell (1893) and Smith (1901). Early attempts at regional stratigraphic correlation were based on the petrology of the interbeds, especially the diatomite deposits, and the basalt flows (Smith, 1903; Waring, 1913; Waters, 1955). Lateral variations in the composition of the interbeds and similarities in the exposed basalt flows led to confusion and inaccurate correlations (Waters, 1955). More recent studies have utilized bulk rock chemistry, paleomagnetism, and borehole geophysics and have culminated in the publication of a revised stratigraphic nomenclature for the CRBG and reconnaissance geologic maps of the Columbia Plateau (Swanson and others, 1979a; Swanson and others, 1979b). Geologic studies have progressed beyond the reconnaissance level in the Pasco Basin.

The CRBG has been divided into one subgroup, five formations, and fourteen members (Swanson and others, 1979a). The three youngest formations--the Grande Ronde, the Wanapum, and the Saddle Mountains--have been mapped in this region and comprise the Yakima Basalt Subgroup (Swanson and others, 1979b). Members of the CRBG present in the Yakima region include the Elephant Mountain, Pomona, Huntzinger (Asotin?), and the Unatilla members of the Saddle Mountains Formation, and the Priest Rapids, Roza, and Frenchman Springs members of the Wanapum Formation. Many unnamed flows occur in the Grande Ronde Formation.

The Vantage, Squaw Creek, Quincy(?), Mabton, Selah, and Rattlesnake Ridge members along with several unnamed interbeds comprise the Ellensburg Formation in the Yakima region. The boundary between the Miocene and Pliocene Ellensburg Formation and the overlying Quaternary sediments is poorly defined, at least in terms of regional borehole geophysical studies, because of the similarity in lithology. In this report, those sediments that lie above the youngest basalt flow, normally the Elephant Mountain Member, have been grouped as the upper Ellensburg and Quaternary sediments.

Quaternary deposits include valley-filling alluvial sands and gravels and landslide debris. The Tieton Andesite, a Pleistocene volcanic flow or flows, extends into the Naches Valley in the western portion of the study area.

A generalized stratigraphic section is given in Figure 3. The younger CRBG flows are absent from the stratigraphic section in the western portion of the Yakima region.

Stratigraphic correlation diagrams (Figures 4 to 20) have been prepared for localities within the lower Yakima, Black Rock, Moxee, Ahtanum, Cowiche, and Naches valleys. The locations of the correlation lines are shown in Plate 1. These correlation diagrams have been developed by interpreting borehole geophysical logs in combination with drillers' (lithologic) logs and available reconnaissance geologic mapping. The elevations and thicknesses of the individual flows and interbeds are given in Tables 1 through 4.

Borehole geophysical logs have been collected on the Columbia Plateau by the Geological Engineering Section of the Department of Civil and Environmental Engineering at Washington State University since 1967. Previous borehole stratigraphic studies in the Yakima region include Crosby and others (1972), Siems and others (1973), Robinette and others (1977), Lobdell and Brown (1977), and Brown (1978, 1979a, 1980). The correlation diagrams given in Figures 4 to 20 rely greatly on the information provided by these earlier studies.

Neutron-epithermal neutron borehole logs are shown in Figures 4 through 20, but it should be noted that natural gamma, gamma-gamma, neutron-gamma, and

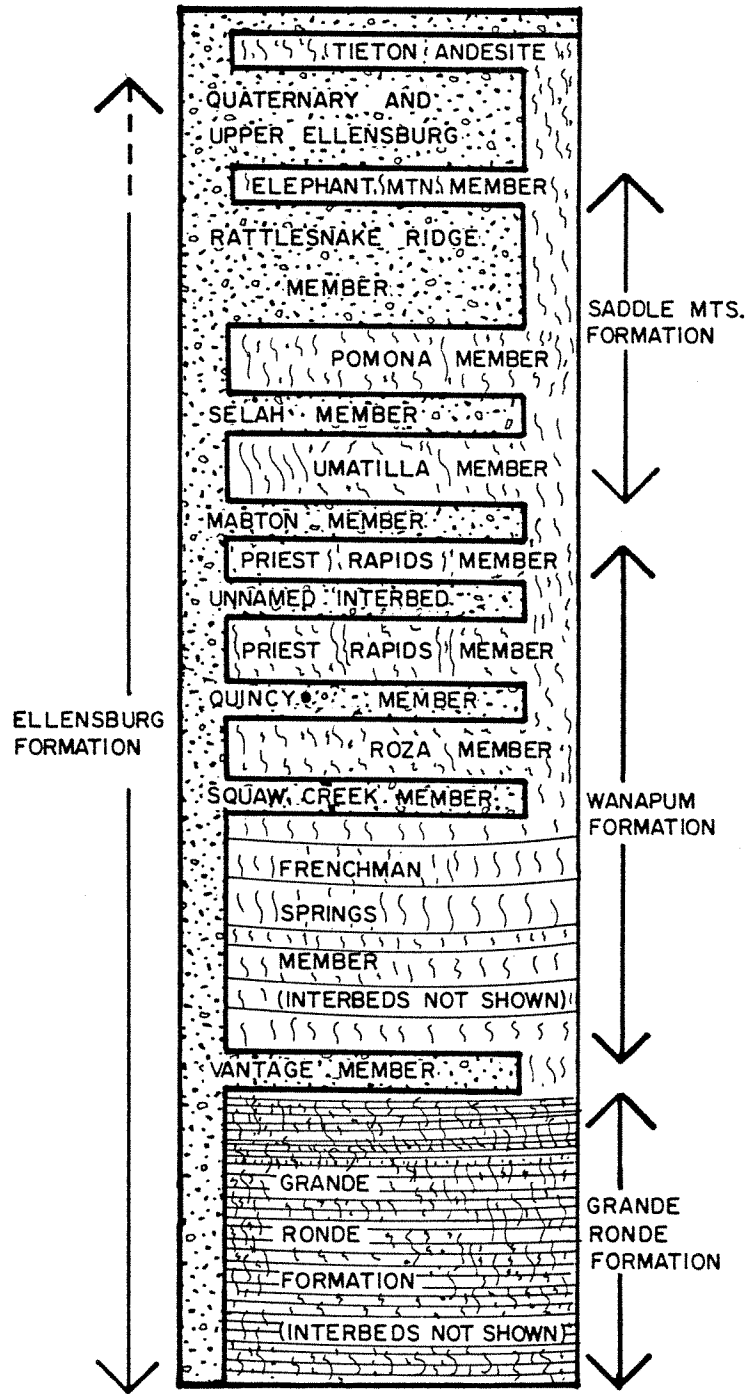


FIGURE 3 GENERALIZED STRATIGRAPHIC COLUMN



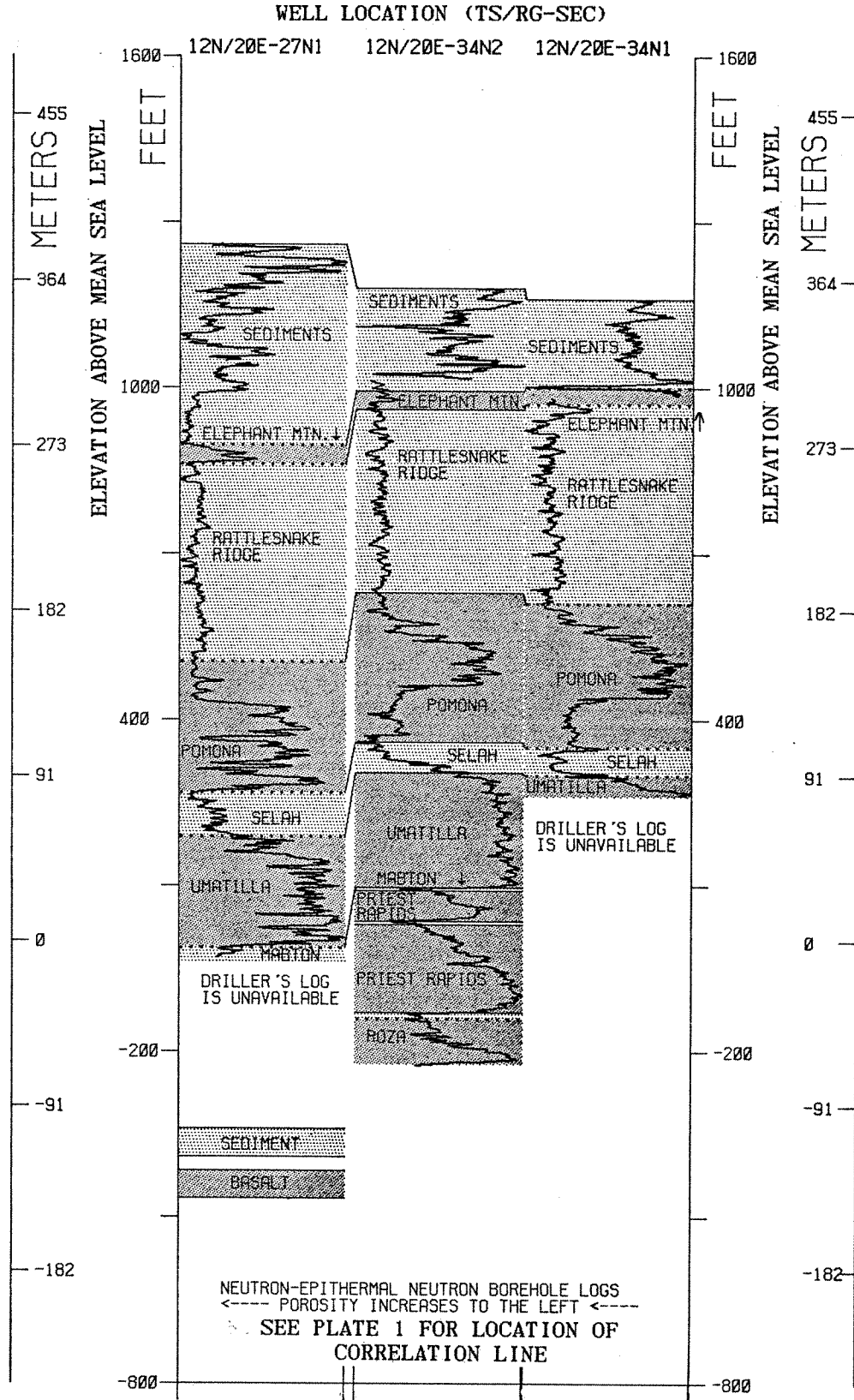
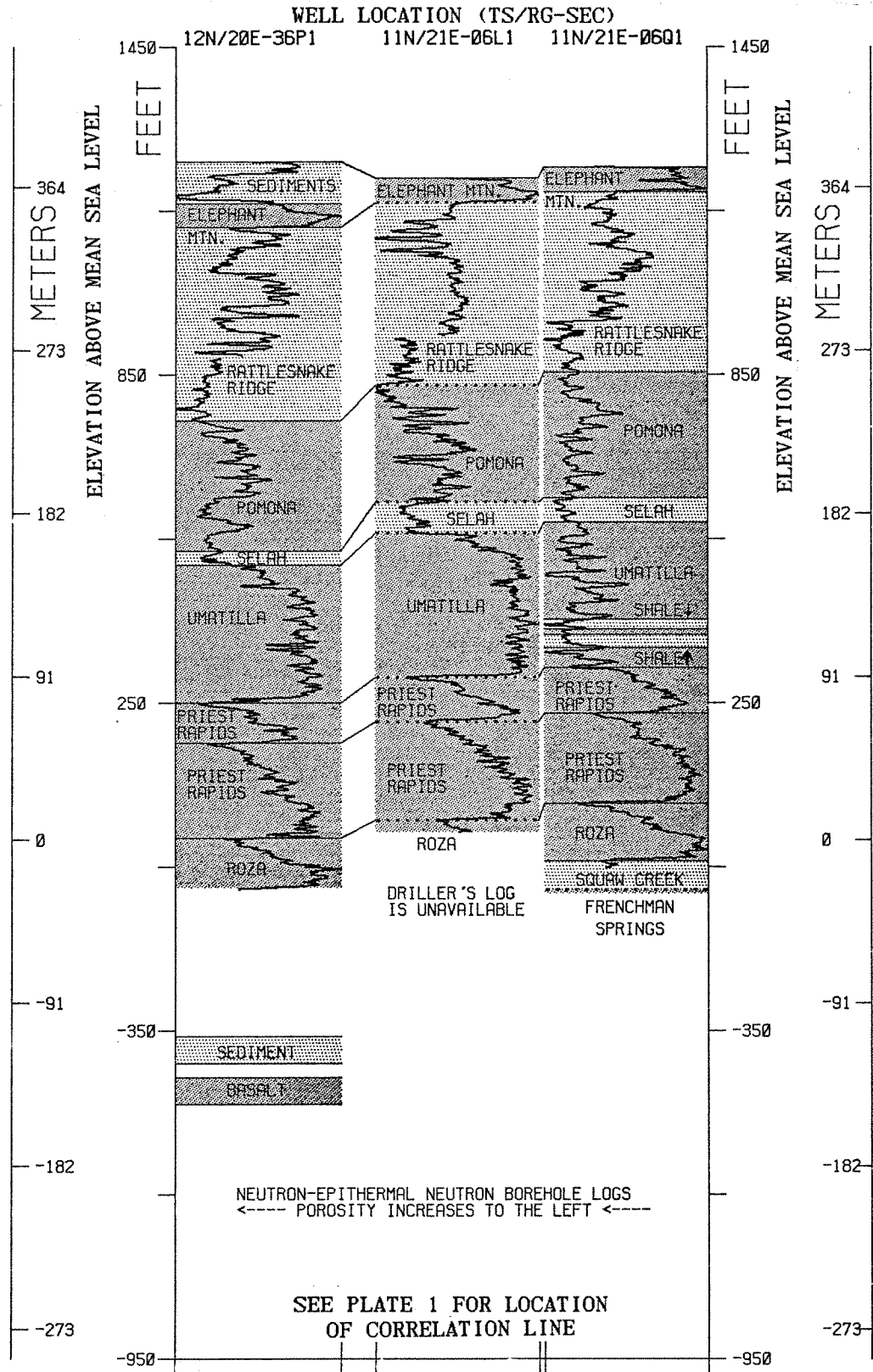


FIGURE 5 STRATIGRAPHIC CORRELATION DIAGRAM - LINE 2



**FIGURE 6 STRATIGRAPHIC CORRELATION DIAGRAM - LINE 3**

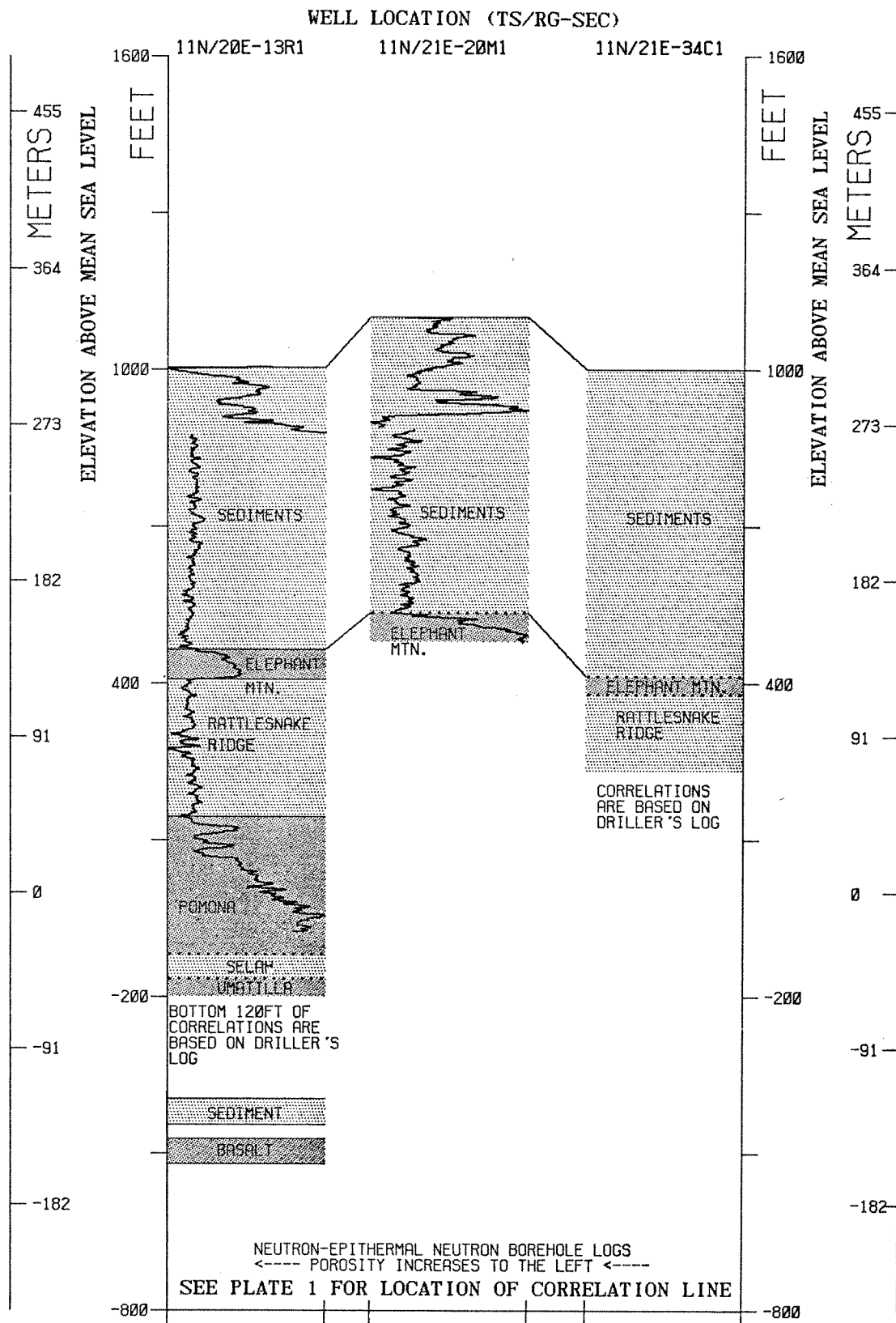


FIGURE 7 STRATIGRAPHIC CORRELATION DIAGRAM - LINE 4

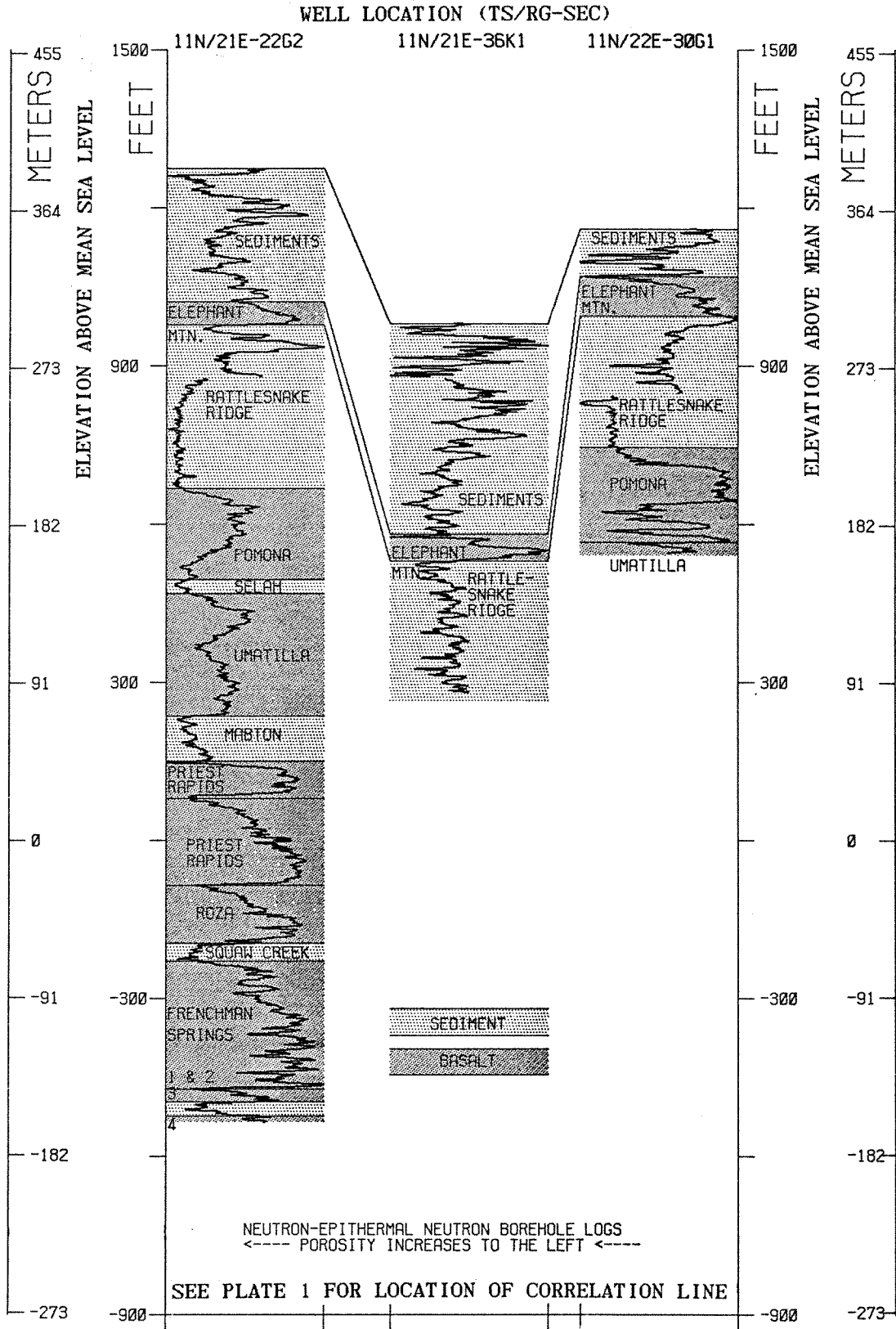
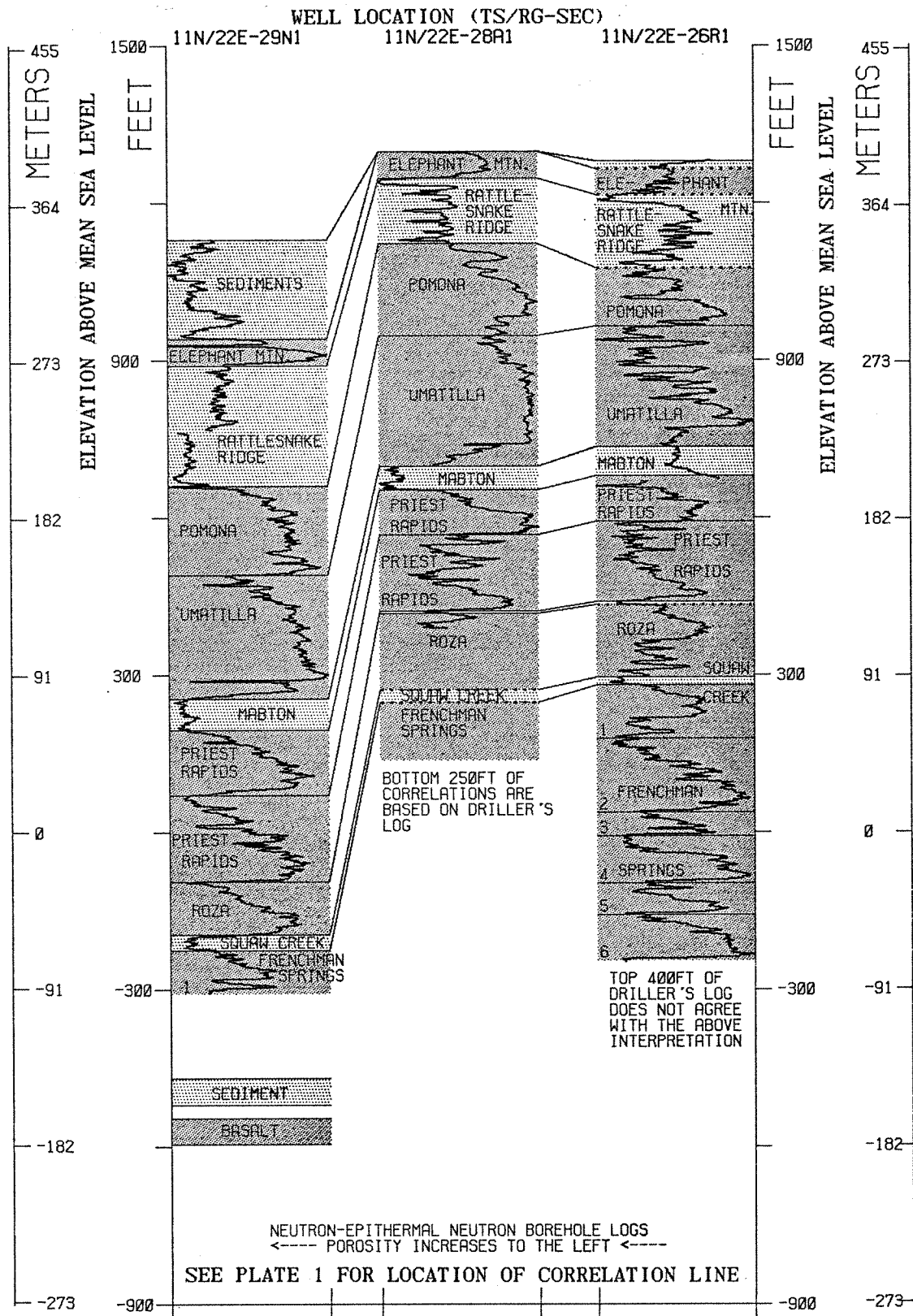


FIGURE 8 STRATIGRAPHIC CORRELATION DIAGRAM - LINE 5



**FIGURE 9 STRATIGRAPHIC CORRELATION DIAGRAM - LINE 6**

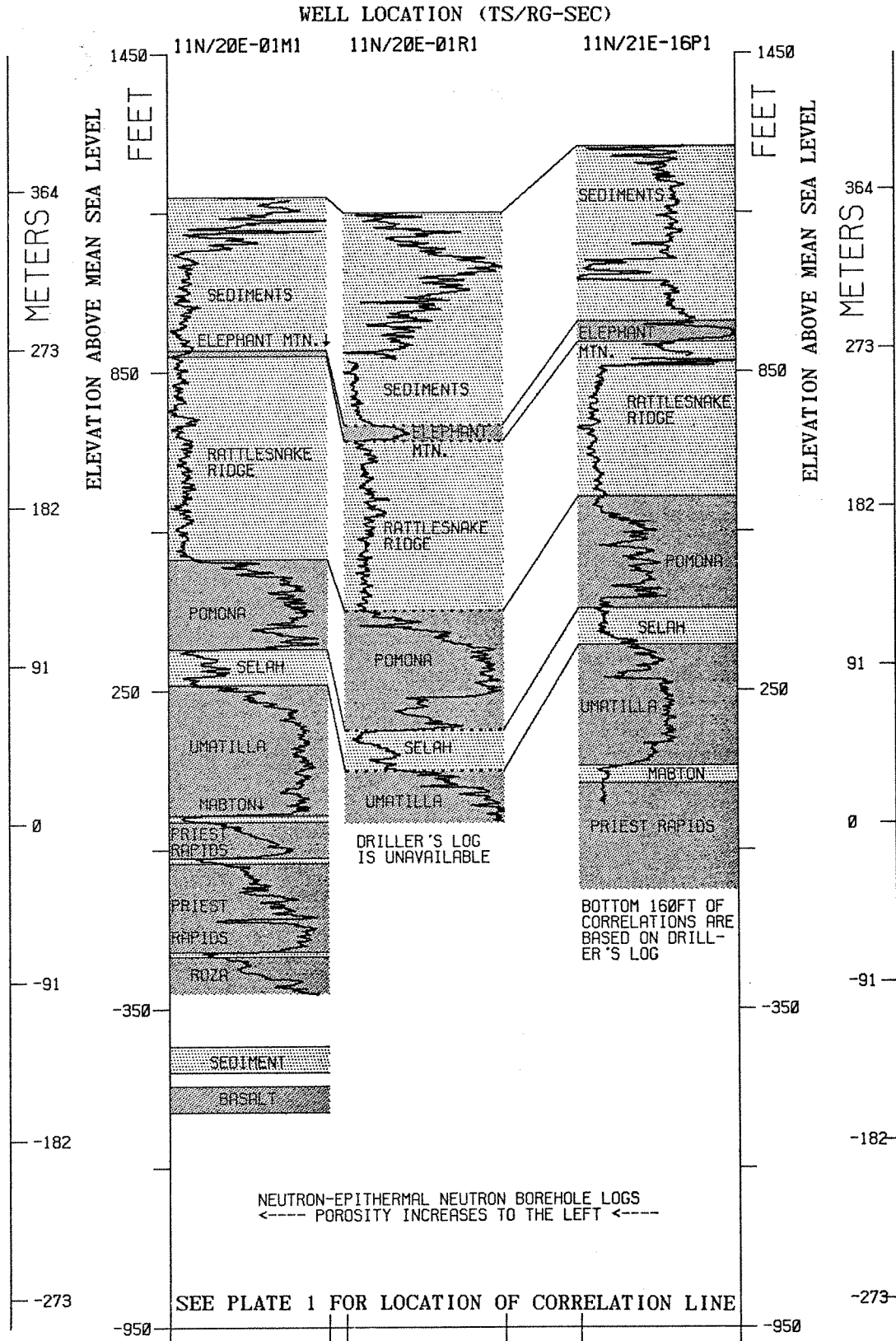


FIGURE 10 STRATIGRAPHIC CORRELATION DIAGRAM - LINE 7

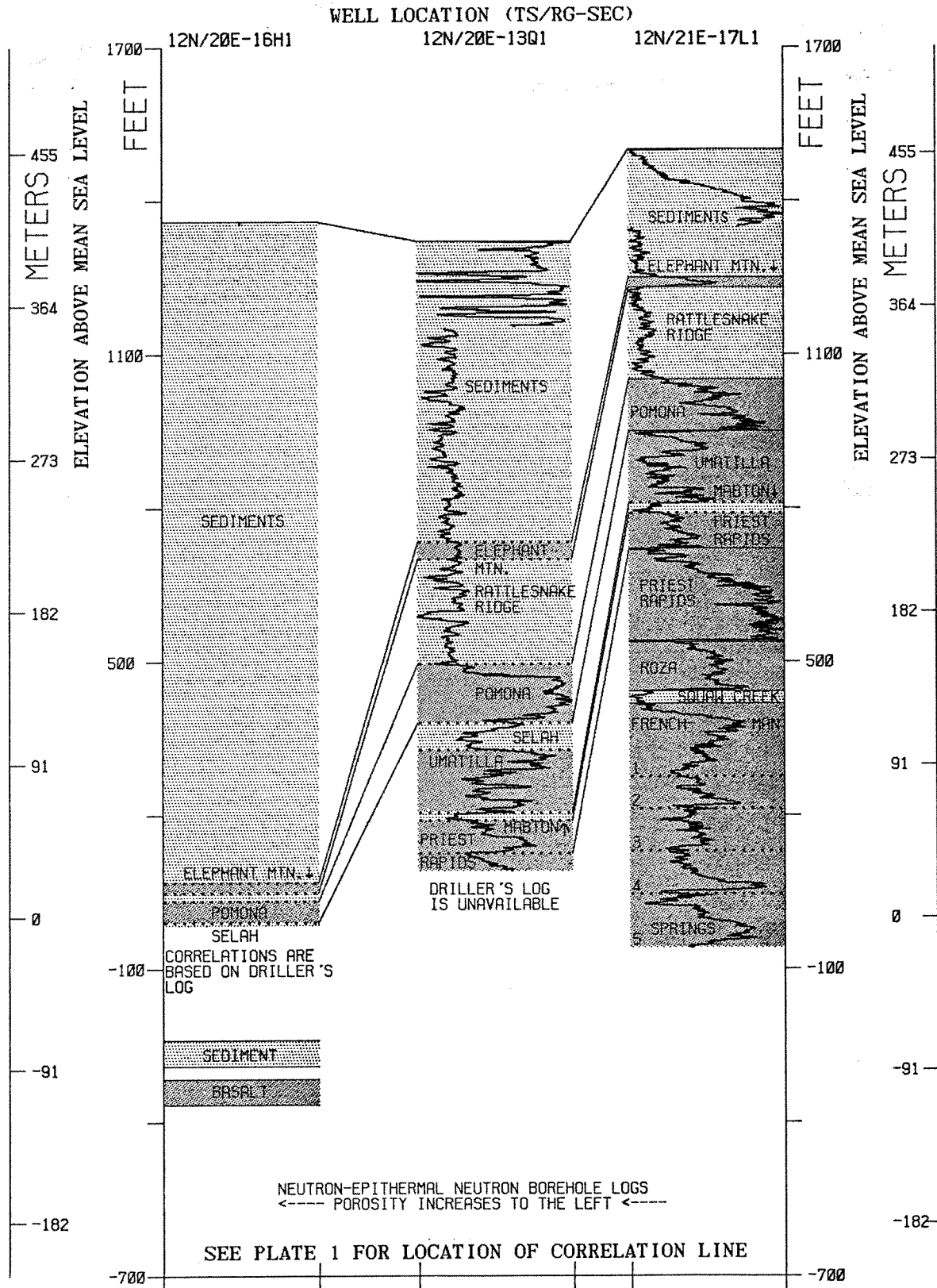


FIGURE 11 STRATIGRAPHIC CORRELATION DIAGRAM - LINE 8

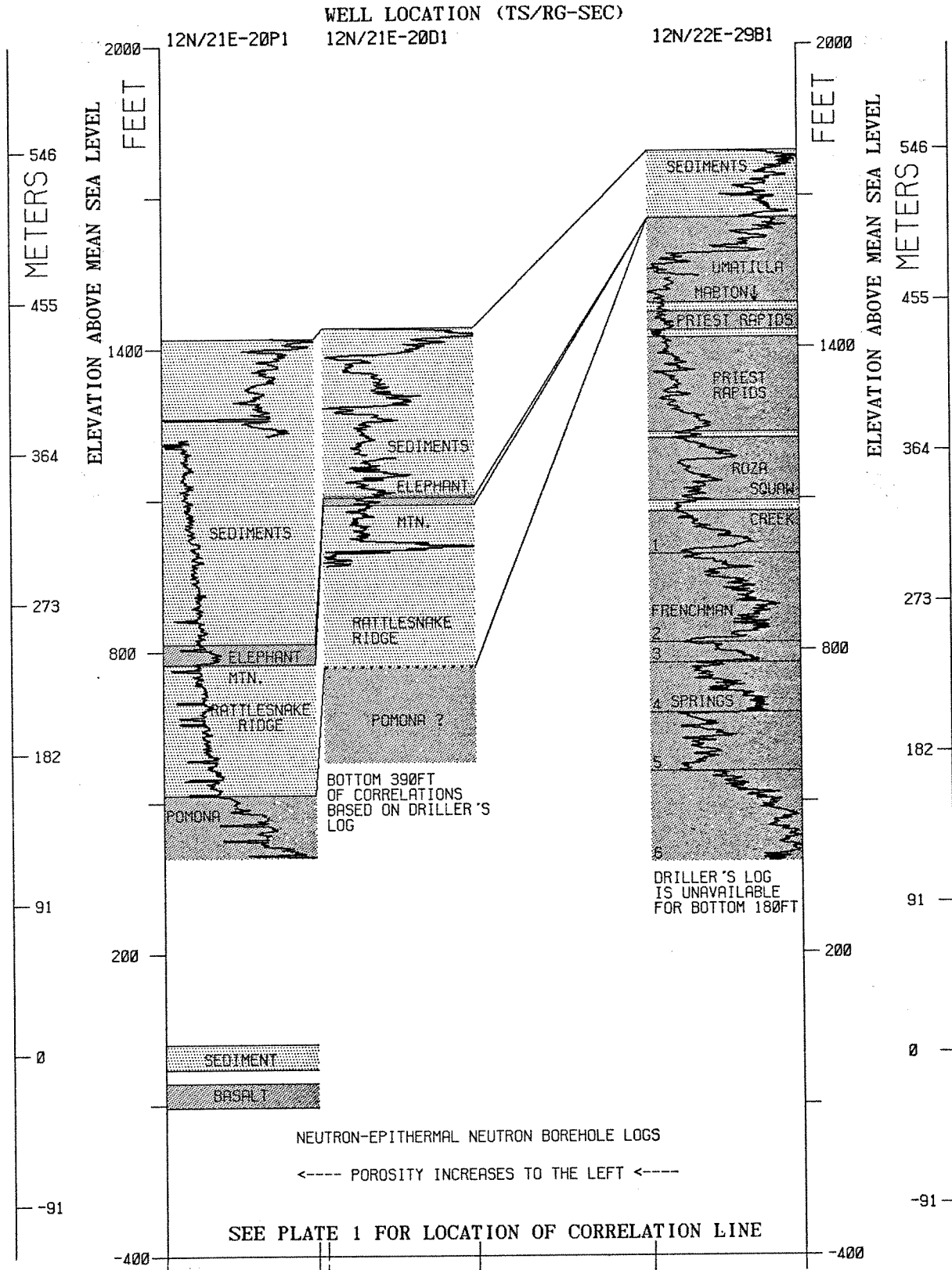


FIGURE 12 STRATIGRAPHIC CORRELATION DIAGRAM - LINE 9

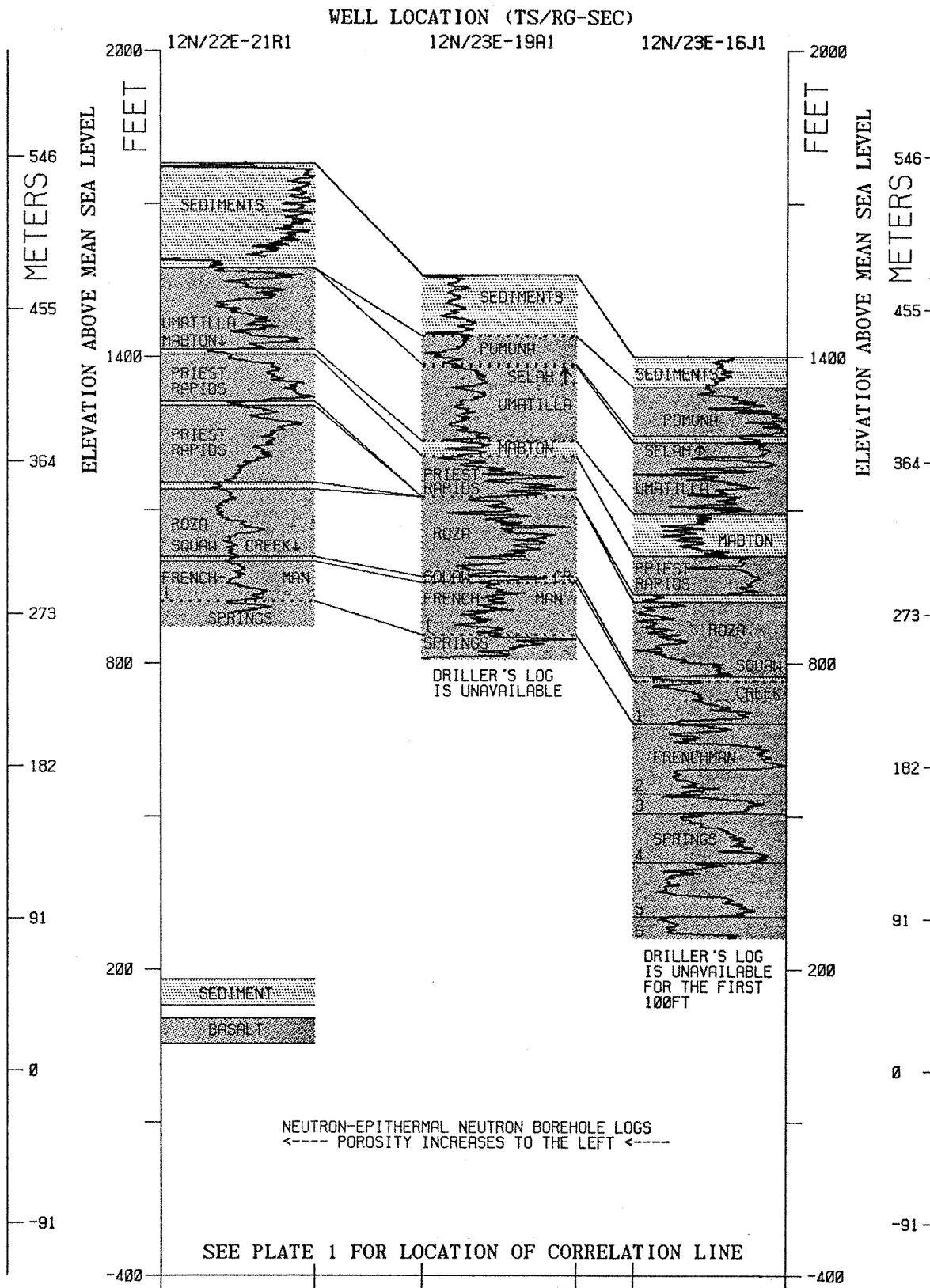


FIGURE 13 STRATIGRAPHIC CORRELATION DIAGRAM - LINE 10



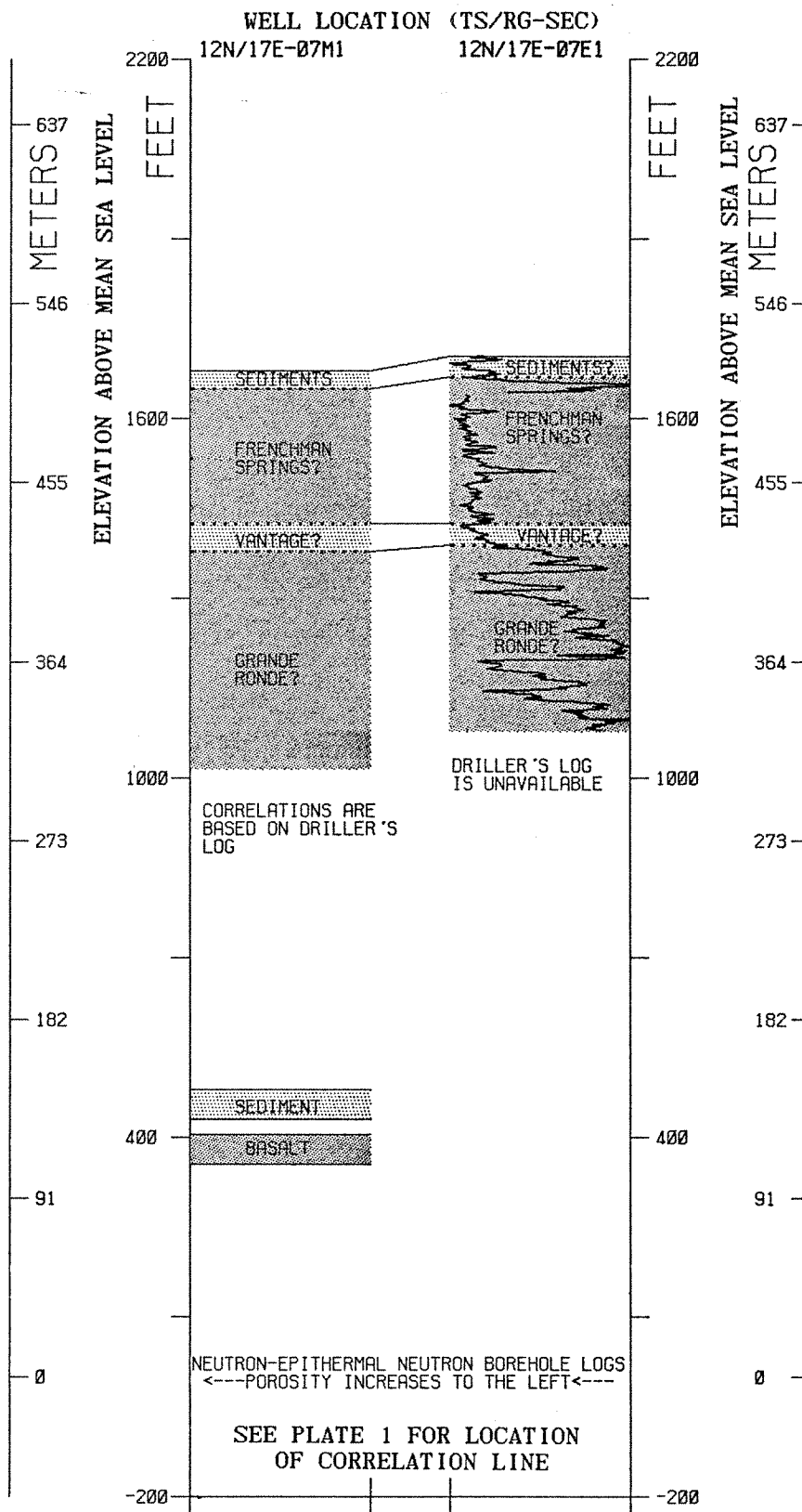


FIGURE 15 STRATIGRAPHIC CORRELATION DIAGRAM - LINE 12

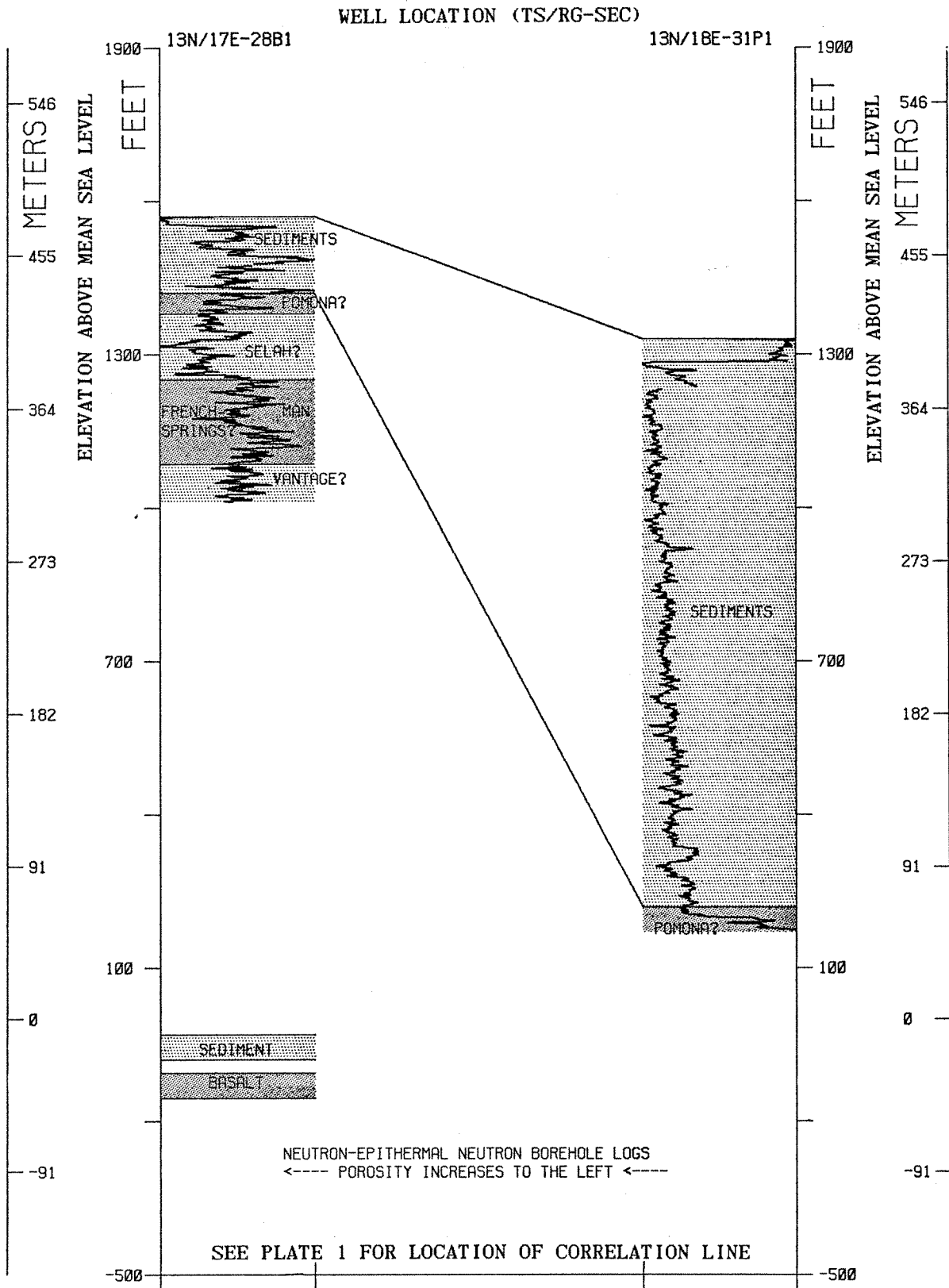


FIGURE 16 STRATIGRAPHIC CORRELATION DIAGRAM - LINE 13

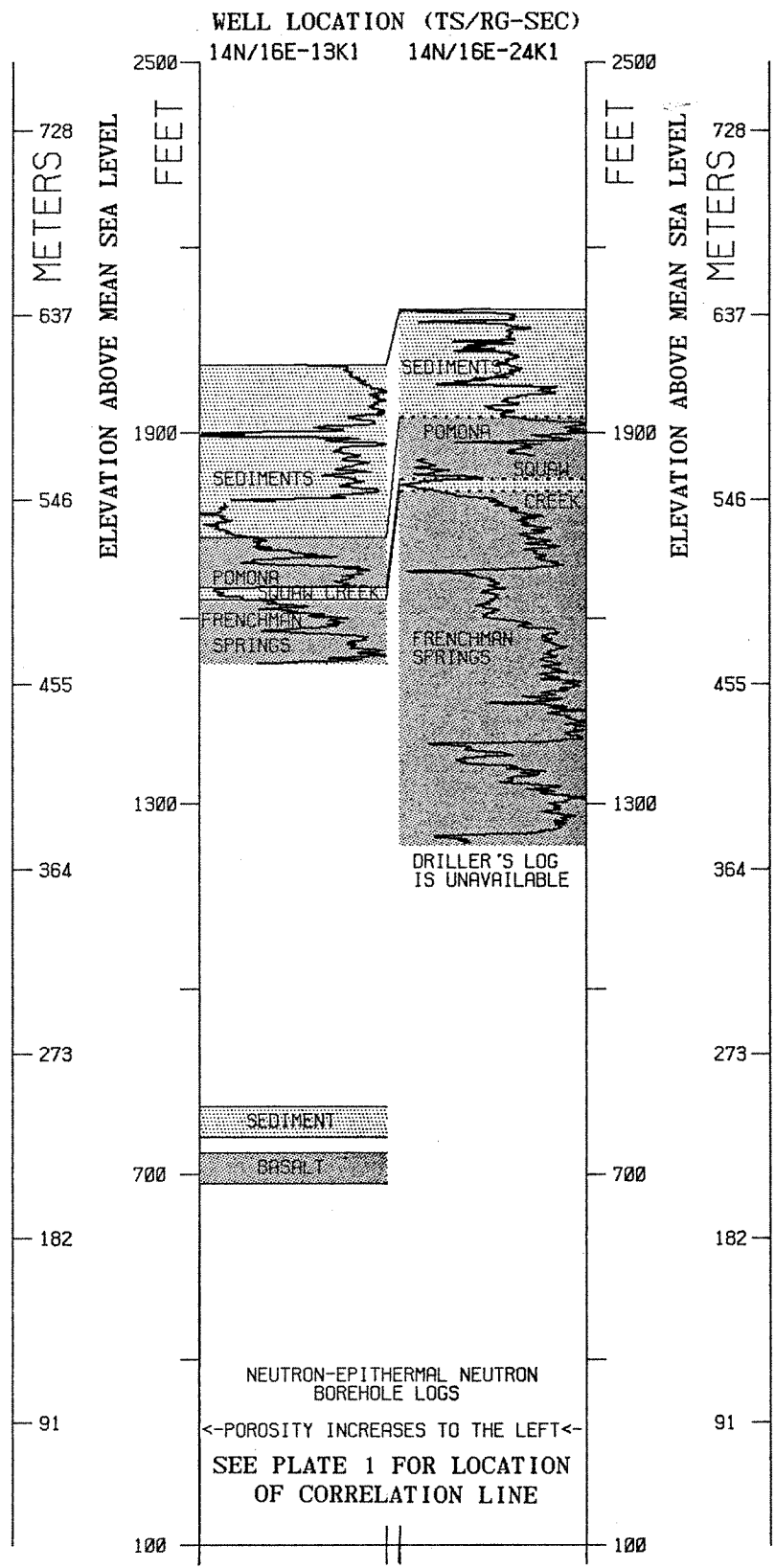


FIGURE 17 STRATIGRAPHIC CORRELATION DIAGRAM - LINE 14

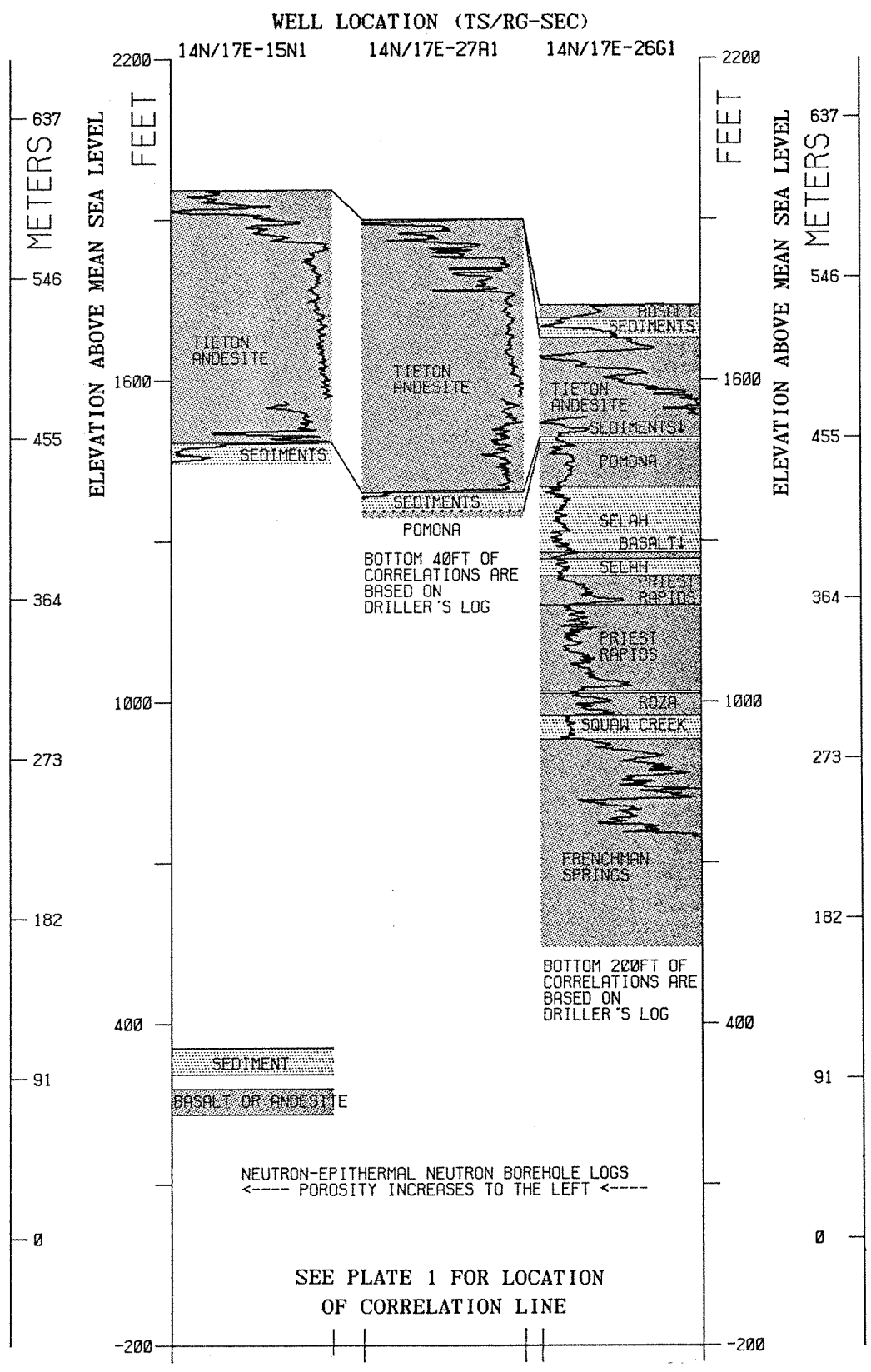


FIGURE 18 STRATIGRAPHIC CORRELATION DIAGRAM - LINE 15

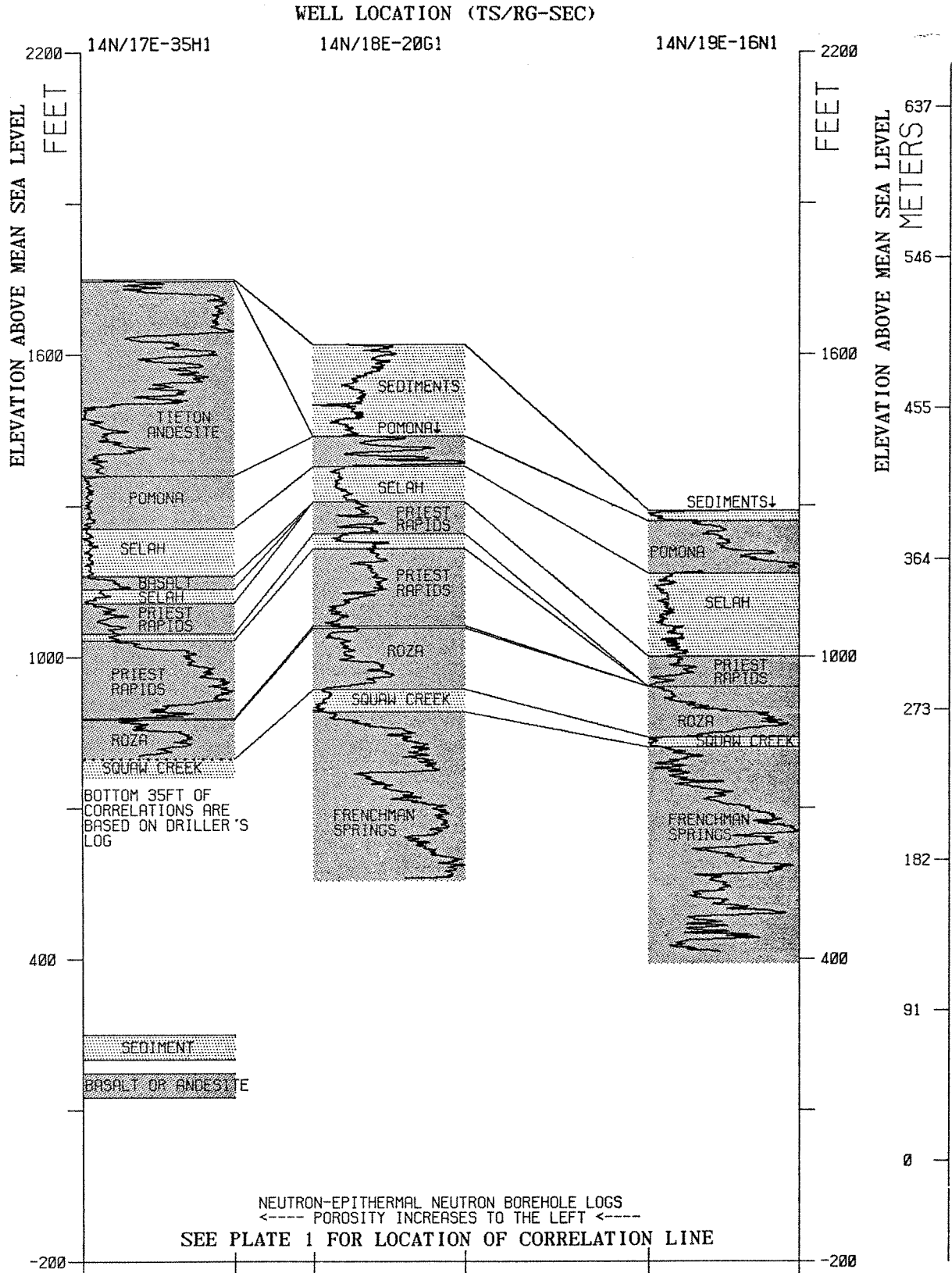


FIGURE 19 STRATIGRAPHIC CORRELATION DIAGRAM - LINE 16

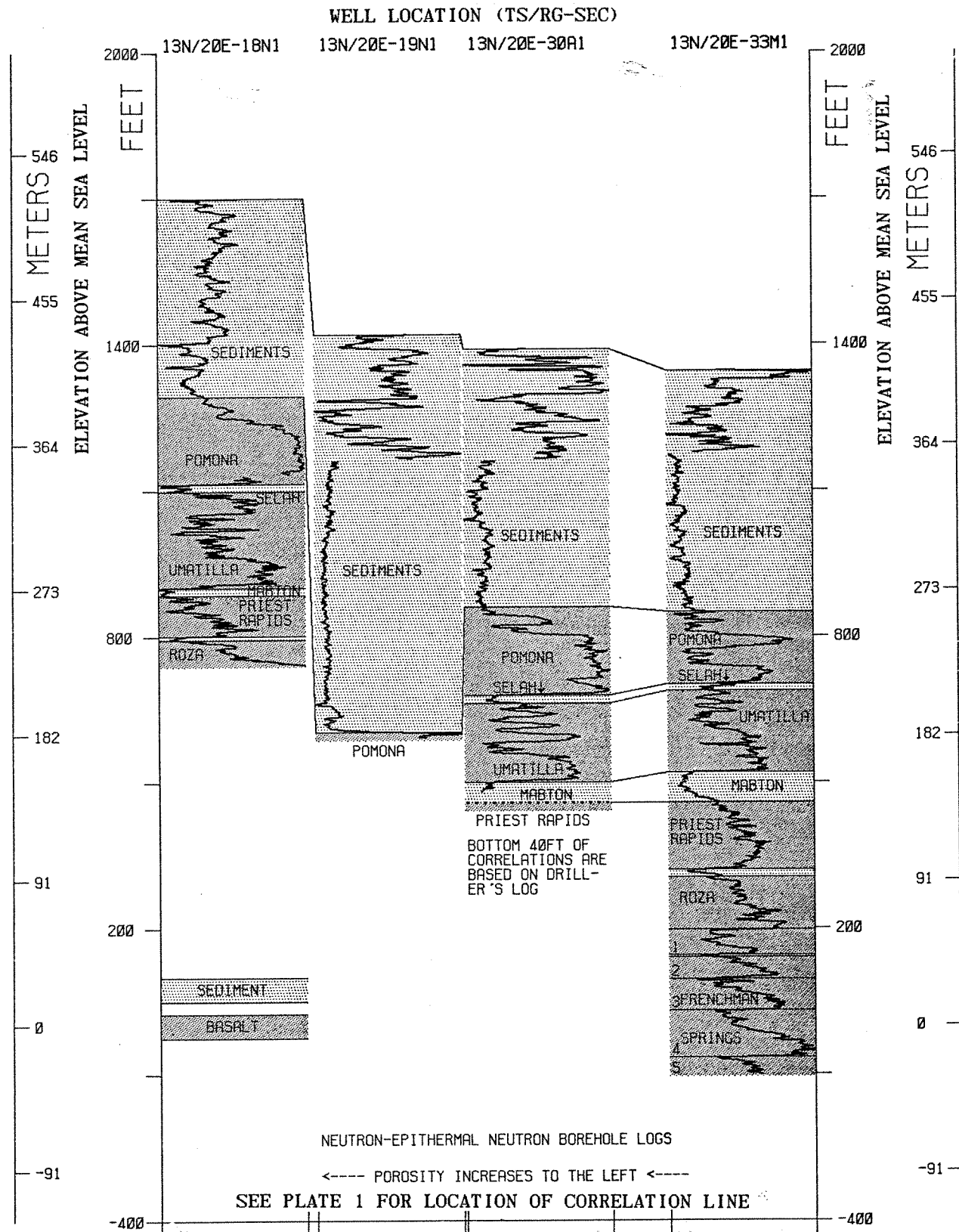


FIGURE 20 STRATIGRAPHIC CORRELATION DIAGRAM - LINE 17

Table 1. Elevations at the Tops of the Geologic Units  
in the Lower Yakima, Ahtanum, Moxee, and Black Rock Valleys<sup>1</sup>

Well Location	11N/20E-01M1	11N/20E-01R1	11N/20E-06A1	11N/20E-13R1	11N/21E-06L1	11N/21E-06Q1	11N/21E-16P1	11N/21E-20M1	11N/21E-22G2	11N/21E-34C1	11N/21E-36K1
Quaternary and Upper Ellensburg Formation	1170	1150	1060	1005	*	*	1275	1090	1275	1000	975
Elephant Mountain Member	880	750	445	465	1210	1230	945	525	1022	413	575
Rattlesnake Ridge Member	870	720		408	1165	1184	905		978	379	525
Pomona Member	487	400		145	830	855	615		668		
Selah Member	318	175		-119	617	625	405		495		
Umatilla Member	250	98		-165	560	580	335		468		
Mabton Member	5				*	*	108		236		
Priest Rapids Member (Upper)	-7				297	315	75		150		

Unnamed Interbed	-75	*	*	*
Priest Rapids Member (Lower)	-85	215	230	80
Interbed (Quincy? Member)	-252	*	*	*
Roza Member	-261	35	65	-85
Squaw Creek Member			-40	-195
Frenchman Springs Member, Flow 1			-92	-230
Frenchman Springs Member, Flow 2				-298
Frenchman Springs Member, Flow 3				-472
Frenchman Springs Member, Flow 4				-523 <sup>2</sup>
Frenchman Springs Member, Flow 5				
Frenchman Springs Member, Flow 6				
Vantage Member				
Grande Ronde Formation				

Table 1. Elevations at the Tops of the Geologic Units  
in the Lower Yakima, Ahtanum, Moxee, and Black Rock Valleys (cont.)

Well Location	11N/22E-26R1	11N/22E-28A1	11N/22E-29N1	11N/22E-30G1	12N/16E-12N1	12N/16E-15E1	12N/16E-18A1	12N/17E-07E1	12N/17E-07M1	12N/19E-27H1	12N/19E-28J1
Quaternary and Upper Ellensburg Formation	1280	*	1130	1160	1880	1886	2140	1704	1680	1120	920
Elephant Mountain Member	1265	1297	940	1070	*	*	*	*	*	*	
Rattlesnake Ridge Member	1215	1247	890	995	*	*	*	*	*	*	
Pomona Member	1075	1122	660	745	*	*	*	*	*	745	
Selah Member	*	*	*	*	*	*	*	*	*	561	
Umatilla Member	965	947	480	565	*	*	*	*	*	524	
Mabton Member	735	697	255		*	*	*	*	*	342	
Priest Rapids Member (Upper)	680	652	195		*	*	*	*	*	318	

Unnamed Interbed	*	*	*	*	*	*	*	*	**
Priest Rapids Member (Lower)	592	567	70	*	*	*	*	*	**
Interbed (Quincy? Member)	440	422	*	*	*	*	*	*	86
Roza Member	433	417	-95	*	*	*	*	*	76
Squaw Creek Member	295	272	-195	*	*	*	*	*	
Frenchman Springs Member, Flow 1	280	247	-225	1810	1851	2105	1669	1649	
Frenchman Springs Member, Flow 2	178								
Frenchman Springs Member, Flow 3	38								
Frenchman Springs Member, Flow 4	-8								
Frenchman Springs Member, Flow 5	-98								
Frenchman Springs Member, Flow 6	-157								
Vantage Member				1530	1756	1980	1424	1425	
Grande Ronde Formation				1460	1716	1935	1389	1378	

Table 1. Elevations at the Tops of the Geologic Units  
in the Lower Yakima, Ahtanum, Moxee, and Black Rock Valleys (cont.)

Well Location	12N/20E-13Q1	12N/20E-16H1	12N/20E-27N1	12N/20E-34N1	12N/20E-34N2	12N/20E-36P1	12N/21E-17L1	12N/21E-20D1	12N/21E-20P1	12N/22E-21R1	12N/22E-29B1
Quaternary and Upper Ellensburg Formation	1320	1360	1260	1160	1180	1240	1500	1440	1460	1780	1790
Elephant Mountain Member	733	68	889	1000	994	1163	1250	1104	855	*	*
Rattlesnake Ridge Member	700	49	862	970	961	1120	1230	1090	814	*	*
Pomona Member	495	32	505	610	630	766	1050	768	555	*	*
Selah Member	380	-10	268	350	360	527	*			*	*
Umatilla Member	328		188	300	304	502	950			1574	1657
Mabton Member	205		-12		97	*	810			1415	1488
Priest Rapids Member (Upper)	190				91	250	790			1405	1470

Unnamed Interbed	*	35	*	*	1313	1435
Priest Rapids Member (Lower)	125	29	177	720	1304	1420
Interbed (Quincy? Member)		-130	*	540	1154	1232
Roza Member		-142	2	538	1140	1220
Squaw Creek Member				442	1009	1095
Frenchman Springs Member, Flow 1				417	999	1075
Frenchman Springs Member, Flow 2				275	922	990
Frenchman Springs Member, Flow 3				212		815
Frenchman Springs Member, Flow 4				130		775
Frenchman Springs Member, Flow 5				45		675
Frenchman Springs Member, Flow 6						560
Vantage Member						
Grande Ronde Formation						

Table 1. Elevations at the Tops of the Geologic Units  
in the Lower Yakima, Ahtanum, Moxee, and Black Rock Valleys (cont.)

Well Location	12N/23E-16J1	12N/23E-19A1	13N/17E-28B1	13N/18E-31P1	13N/20E-18N1	13N/20E-19N1	13N/20E-30A1	13N/20E-33M1
Quaternary and Upper Ellensburg Formation	1400	1560	1570	1330	1700	1420	1390	1345
Elephant Mountain Member	*	*	*	*	*	603	*	*
Rattlesnake Ridge Member	*	*	*	*	*		*	*
Pomona Member	1340	1440	1420	219	1294		860	850
Selah Member	1245	1385	1380		1114		678	701
Umatilla Member	1232	1380	*		1090		662	687
Mabton Member	1092	1235	*		901		500	520
Priest Rapids Member (Upper)	1010	1205	*		885		458	458

Unnamed Interbed	*	*	*	*	*
Priest Rapids Member (Lower)	*	*	*	*	*
Interbed (Quincy? Member)	935	*	*	802	320
Roza Member	920	1125	*	794	305
Squaw Creek Member	775	970	*		*
Frenchman Springs Member, Flow 1	765	957	1250		197
Frenchman Springs Member, Flow 2	682	855			140 <sup>3</sup>
Frenchman Springs Member, Flow 3	545				95
Frenchman Springs Member, Flow 4	506				30
Frenchman Springs Member, Flow 5	410				-65
Frenchman Springs Member, Flow 6	304				
Vantage Member			1085		
Grande Ronde Formation					

Table 1. Elevations at the Tops of the Geologic Units  
in the Lower Yakima, Ahtanum, Moxee, and Black Rock Valleys (cont.)

---

Notes:

\* geologic unit is absent

\*\* elevation unknown because individual geologic units were not separated

<sup>1</sup> elevations are reported in feet above mean sea level

<sup>2</sup> 7.9m thick interbed located from -497 to -523ft

<sup>3</sup> 1.5m thick interbed located from 140 to 145ft

Table 2. Elevations at the Tops of the Geologic Units  
in the Cowiche and Naches Valleys<sup>1</sup>

Well Location	14N/16E-13K1	14N/16E-24K1	14N/17E-15N1	14N/17E-26G1	14N/17E-27A1	14N/17E-35H1	14N/18E-20G1	14N/19E-16N1
Quaternary and Upper Ellensburg Formation	2010	2100	*	*	*	1750	1620	1290
Tieton Andesite	*	*	1955	1740	1900	1746	*	*
Sediments	*	*	1485	1494	1390	*	*	*
Pomona Member	1730	1925		1483	1355	1360	1438	1268
Selah Member	*	*		1400		1255	1378	1165
Huntzinger(?) Member	*	*		1278		1160	*	*
Sediments	*	*		1265		1135	*	*
Priest Rapids Member (Upper)	*	*		1234		1106	1308	*

Unnamed Interbed	*	*	*	1046	1244	*
Priest Rapids Member (Lower)	*	*	1180	1033	1215	*
Interbed (Quincy? Member)	*	*	1020	879	1061	*
Roza Member	*	*	1015	876	1057	940
Squaw Creek Member	1650	1825	975	798	935	840
Frenchman Springs Member	1630	1805	930		890	820

Notes:

\* geologic unit is absent

<sup>1</sup> elevations are reported in feet above mean sea level

Table 3. Thicknesses of the Geologic Units  
in the Lower Yakima, Ahtanum, Moxee, and Black Rock Valleys<sup>1</sup>

Well Location	11N/20E-01M1	11N/20E-01R1	11N/20E-06A1	11N/20E-13R1	11N/21E-06L1	11N/21E-06Q1	11N/21E-16P1	11N/21E-20M1	11N/21E-22G2	11N/21E-34C1	11N/21E-36K1
Quaternary and Upper Ellensburg Formation	88.4	121.9	187.4	164.6	*	*	100.6	172.2	77.1	178.9	121.9
Elephant Mountain Member	3.0	9.1	2.1	17.4	13.7	14.0	12.2	16.8	13.4	10.4	15.2
Rattlesnake Ridge Member	116.7	97.5		80.2	102.1	100.3	88.4		94.5	46.3	82.3
Pomona Member	51.5	68.6		80.5	64.9	70.1	64.0		52.7		
Selah Member	20.7	23.5		14.0	17.4	13.7	21.3		8.2		
Umatilla Member	74.7	29.9		9.4	80.2	80.8 <sup>2</sup>	69.2		70.7		
Mabton Member	3.7				*	*	10.1		26.2		
Priest Rapids Member (Upper)	20.7				25.0	25.9	61.6 <sup>3</sup>		21.2		

Unnamed Interbed	3.0	*	*	*
Priest Rapids Member (Lower)	50.9	54.9	50.3	50.3
Interbed (Quincy? Member)	2.7	*	*	*
Roza Member	21.3	6.7	32.0	33.5
Squaw Creek Member			15.8	10.7
Frenchman Springs Member, Flow 1			11.6	20.7
Frenchman Springs Member, Flow 2				53.0
Frenchman Springs Member, Flow 3				7.6
Frenchman Springs Member, Flow 4				3.7
Frenchman Springs Member, Flow 5				
Frenchman Springs Member, Flow 6				
Vantage Member				
Grande Ronde Formation				

Table 3. Thicknesses of the Geologic Units  
in the Lower Yakima, Ahtanum, Moxee, and Black Rock Valleys (cont.)

Well Location	11N/22E-26R1	11N/22E-28A1	11N/22E-29N1	11N/22E-30G1	12N/16E-12N1	12N/16E-15E1	12N/16E-18A1	12N/17E-07E1	12N/17E-07M1	12N/19E-27H1	12N/19E-28J1
Quaternary and Upper Ellensburg Formation	4.6	*	57.9	27.4	21.3	10.7	10.7	10.7	9.4	114.3	91.4
Elephant Mountain Member	15.2	15.2	15.2	22.9	*	*	*	*	*	*	
Rattlesnake Ridge Member	42.7	38.1	70.1	76.2	*	*	*	*	*	*	
Pomona Member	33.5	53.3	54.9	54.9	*	*	*	*	*	56.1	
Selah Member	*	*	*	*	*	*	*	*	*	11.3	
Umatilla Member	70.1	76.2	68.6	7.6	*	*	*	*	*	55.5	
Mabton Member	16.8	13.7	18.3		*	*	*	*	*	7.3	
Priest Rapids Member (Upper)	26.8	25.9	38.1		*	*	*	*	*	70.7 <sup>3</sup>	

Unnamed Interbed	*	*	*	*	*	*	*	*	**
Priest Rapids Member (Lower)	46.3	44.2	50.3	*	*	*	*	*	**
Interbed (Quincy? Member)	2.1	1.5	*	*	*	*	*	*	3.0
Roza Member	42.1	44.2	30.5	*	*	*	*	*	27.1
Squaw Creek Member	4.6	7.6	9.1	*	*	*	*	*	
Frenchman Springs Member, Flow 1	31.1	33.5 <sup>3</sup>	25.9	85.3 <sup>3</sup>	29.0 <sup>3</sup>	38.1 <sup>3</sup>	74.7 <sup>3</sup>	68.3 <sup>3</sup>	
Frenchman Springs Member, Flow 2	42.7								
Frenchman Springs Member, Flow 3	14.0								
Frenchman Springs Member, Flow 4	27.4								
Frenchman Springs Member, Flow 5	18.0								
Frenchman Springs Member, Flow 6	26.8								
Vantage Member				21.3	12.2	13.7	10.7	14.3	
Grande Ronde Formation				146.3 <sup>4</sup>	125.0	45.7	95.4	111.2	

Table 3. Thicknesses of the Geologic Units  
in the Lower Yakima, Ahtanum, Moxee, and Black Rock Valleys (cont.)

Well Location	12N/20E-13Q1	12N/20E-16H1	12N/20E-27N1	12N/20E-34N1	12N/20E-34N2	12N/20E-36P1	12N/21E-17L1	12N/21E-20D1	12N/21E-20P1	12N/22E-21R1	12N/22E-29B1
Quaternary and Upper Ellensburg Formation	178.9	393.8	113.1	48.8	56.7	23.5	76.2	102.4	184.4	62.8	40.5
Elephant Mountain Member	10.1	5.8	8.2	9.1	10.1	13.1	6.1	4.3	12.5	*	*
Rattlesnake Ridge Member	62.5	5.2	108.8	109.7	100.9	107.9	54.9	98.1	78.9	*	*
Pomona Member	35.1	12.8	72.2	79.2	82.3	72.8	30.5	57.9 <sup>5</sup>	38.1	*	*
Selah Member	15.8	1.8	24.4	15.2	17.1	7.6	*			*	*
Umatilla Member	37.5		61.0	12.2	63.1	76.8	42.7			48.5	51.5
Mabton Member	4.6		8.5		1.8	*	6.1			3.0	5.5
Priest Rapids Member (Upper)	19.8				17.1	22.2	21.3			28.0	10.7

Unnamed Interbed	*	1.8	*	*	2.7	4.6
Priest Rapids Member (Lower)	10.7	48.5	53.3	54.9	45.7	57.3
Interbed (Quincy? Member)		3.7	*	0.6	4.3	3.7
Roza Member		25.3	28.0	29.3	39.9	38.1
Squaw Creek Member				7.6	3.0	6.1
Frenchman Springs Member, Flow 1				43.3	23.5	25.9
Frenchman Springs Member, Flow 2				19.2	14.0	53.3
Frenchman Springs Member, Flow 3				25.0		12.2
Frenchman Springs Member, Flow 4				25.9		30.5
Frenchman Springs Member, Flow 5				32.0		35.1
Frenchman Springs Member, Flow 6						54.9
Vantage Member						
Grande Ronde Formation						

Table 3. Thicknesses of the Geologic Units  
in the Lower Yakima, Ahtanum, Moxee, and Black Rock Valleys (cont.)

Well Location	12N/23E-16J1	12N/23E-19A1	13N/17E-28B1	13N/18E-31P1	13N/20E-18N1	13N/20E-19N1	13N/20E-30A1	13N/20E-33M1
Quaternary and Upper Ellensburg Formation	18.3	36.6	45.7	338.6	123.7 <sup>6</sup>	249.0	161.5	150.9
Elephant Mountain Member	*	*	*	*	*	5.5	*	*
Rattlesnake Ridge Member	*	*	*	*	*		*	*
Pomona Member	29.0	16.8	12.2	14.9	54.9		55.5	45.4
Selah Member	4.0	1.5	39.6		7.3		4.9	4.3
Umatilla Member	42.7	44.2	*		57.6		49.4	50.9
Mabton Member	25.0	9.1	*		4.9		12.8	18.9
Priest Rapids Member (Upper)	22.9	24.4	*		25.3		5.5	42.1

Unnamed Interbed	*	*	*	*	*
Priest Rapids Member (Lower)	*	*	*	*	*
Interbed (Quincy? Member)	4.6	*	*	2.4	4.6
Roza Member	44.2	47.2	*	17.4	32.9
Squaw Creek Member	3.0	4.0	*		*
Frenchman Springs Member, Flow 1	25.3	31.1	50.3 <sup>3</sup>		15.8
Frenchman Springs Member, Flow 2	41.8	14.6			13.7
Frenchman Springs Member, Flow 3	11.9				19.8
Frenchman Springs Member, Flow 4	29.3				29.0
Frenchman Springs Member, Flow 5	32.2				12.2
Frenchman Springs Member, Flow 6	13.4				
Vantage Member			22.9		
Grande Ronde Formation					

Table 3. Thicknesses of the Geologic Units  
in the Lower Yakima, Ahtanum, Moxee, and Black Rock Valleys (cont.)

---

Notes:

\* geologic unit is absent

\*\* thickness unknown because individual geologic units were not separated

<sup>1</sup> thicknesses are reported in meters. For most wells, the last thickness reported is not a true thickness because of incomplete penetration of the geologic unit.

<sup>2</sup> contains two lenses of shale

<sup>3</sup> reported thickness is actually the total thickness of more than one flow and/or interbed

<sup>4</sup> includes 6.1m of shale from 1288 to 1308ft

<sup>5</sup> may include Umatilla flow

<sup>6</sup> includes 2.1m of basalt

Table 4. Thicknesses of the Geologic Units  
in the Cowiche and Naches Valleys<sup>1</sup>

Well Location	14N/16E-13K1	14N/16E-24K1	14N/17E-15N1	14N/17E-26G1	14N/17E-27A1	14N/17E-35H1	14N/18E-20G1	14N/19E-16N1
Quaternary and Upper Ellensburg Formation	85.3	53.3	*	*	*	1.2	55.5	6.7
Tieton Andesite	*	*	143.2	75.0 <sup>2</sup>	155.4	117.6	*	*
Sediments	*	*	12.2	3.4	10.7	*	*	*
Pomona Member	24.4	30.5		25.3	4.0	32.0	18.3	31.4
Selah Member	*	*		37.2		29.0	21.3	50.3
Huntzinger(?) Member	*	*		4.0		7.6	*	*
Sediments	*	*		9.4		8.8	*	*
Priest Rapids Member (Upper)	*	*		16.5		18.3	19.5	*

Unnamed Interbed	*	*	*	4.0	8.8	*
Priest Rapids Member (Lower)	*	*	48.8	46.9	46.9	*
Interbed (Quincy? Member)	*	*	1.5	0.9	1.2	*
Roza Member	*	*	12.2	23.8	37.2	30.5
Squaw Creek Member	6.1	6.1	13.7	11.3	13.7	6.1
Frenchman Springs Member	32.0	175.3	118.3		102.1	131.1

Notes:

\* geologic unit is absent

<sup>1</sup> thicknesses are reported in meters. For most wells, the last thickness is not a true thickness because of incomplete penetration of the geologic unit.

<sup>2</sup> includes 11.3m of sediments

caliper logs were also utilized for these correlations. The borehole geophysical log suite that is commonly collected by Washington State University includes the neutron-epithermal neutron, neutron-gamma, natural gamma, gamma-gamma, fluid temperature, fluid resistivity, wall rock resistivity, spontaneous potential, flowmeter, and caliper logs. Borehole geophysical log suites for the wells shown in Figures 4 through 20 are available at the Geological Engineering Section.

An overview of the geologic units of the region is given below. Interested readers are referred to Swanson (1966), Swanson (1967), Schmincke (1967a, 1967b, 1967c), Diery and McKee (1969), Bentley (1977), Campbell (1976, 1977a, 1977b), Swanson and Wright (1978), Swanson and others (1979a, 1979b, 1979c), Myers and others (1979), Tanaka and others (1979), Gephart and others (1979), and Bentley and others (1980) for more detailed information.

### Grande Ronde Formation

The Grande Ronde Formation has been informally divided into four magnetostratigraphic units, of which three units ( $N_1$ ,  $R_2$ , and  $N_2$ , where N is normal and R is reversed magnetic polarity) have been mapped in the region (Swanson and others, 1979b). The total thickness of the Grande Ronde Formation in the Yakima region probably does not exceed 1,000m and may vary as much as 400m because of an irregular pre-basalt topography (Bentley and others, 1980). Individual flows average 20 to 30m in thickness (Bentley and others, 1980).

None of the wells for which correlation diagrams are given in this report have completely penetrated the formation. The Grande Ronde Formation was tentatively identified along correlation lines of the Ahtanum Valley (Figures 14 and 15) where a thickness of over 146m was penetrated. Surface exposures of the Grande Ronde Formation are found along the western margin of the region and the anticlinal ridges (Swanson and others, 1979b).

Interbeds within the Grande Ronde Formation are common and are generally less than 15m thick, with interbed thickness and abundance decreasing in an easterly direction (Bentley and others, 1980). The interbeds are composed of volcanoclastic sandstone, siltstone, claystone, and pumiceous volcanic breccia (Bentley and others, 1980). Although some interbeds may be extensive, most are laterally discontinuous and unreliable as stratigraphic markers (Bentley and others, 1980). Sources of sediment include contemporaneous volcanism in the Cascade region, alluvial deposition of plutonic-metamorphic sediments from the north, and local erosion (Schmincke, 1967a; Bentley and others, 1980).

### Vantage Member of the Ellensburg Formation

The Vantage Member of the Ellensburg Formation lies between the Grande Ronde and Wanapum Basalt formations throughout most of the region. This member is composed of volcanoclastic sandstones, siltstones, claystones, and minor amounts of conglomerate and diatomite (Diery and McKee, 1969; Bentley and others, 1980). The reported thickness of this member ranges from 0 to 30m (Diery and McKee, 1969; Bentley, 1977; Bentley and others, 1980).

The Vantage Member has been tentatively identified along correlation lines of the Ahtanum Valley (Figures 14 and 15). This interbed ranges in thickness from 10 to over 23m at these locations. The identification of this member in the correlation diagrams is based on its stratigraphic position between the Grande Ronde Formation and the Frenchman Springs Member. The accuracy of the identification of these two basalt flows in the Ahtanum Valley

is uncertain, and therefore the identification of the Vantage Member in the Ahtanum Valley is tentative.

### Wanapum Formation

In the Yakima region, the Wanapum Basalt Formation is composed of three members: the Frenchman Springs, Roza, and Priest Rapids. Interbedded between these flows are the Squaw Creek and Quincy(?) members and several unnamed interbeds of the Ellensburg Formation.

#### Frenchman Springs Member

The Frenchman Springs Member, the thickest (over 150m) and most widespread Wanapum Member, is composed of up to six flows at Union Gap but thins to two flows to the west (Bentley and others, 1980). The Frenchman Springs Member has been subdivided into four flow units in the Yakima region (Bentley, 1977; Bentley and others, 1980). These units are, from oldest to youngest, the Gingko flows, the Sand Hollow flow, the Kelly Hollow flow, and the Union Gap flows. These flows are differentiated by the abundance of phenocrysts and their stratigraphic position (Bentley and others, 1980).

In utilizing borehole geophysical logs for stratigraphic correlation in this report, the base of the Frenchman Springs Member was recognized by the presence of the Vantage (interbed) Member. Hence, Grande Ronde flows may be mistaken as Frenchman Springs flows in the absence of the Vantage Member. Conversely, the opposite may occur if a thick interbed is encountered within the Frenchman Springs Member.

Six flows have been tentatively identified in several wells in the lower Yakima and Black Rock valleys (Figures 9, 12, and 13) where their combined thickness is greater than 150m. Several thin (up to 8m thick in well 11N/21E-22G2, in Figure 8), discontinuous sedimentary interbeds lie between the Frenchman Springs flows. Bentley and others (1980) noted that thin interbeds (0-4m) were found above and below the Kelly Hollow flow along the northern side of Toppenish Ridge and in upper Satus basin. Individual flows are not separated in correlation diagrams of the Ahtanum, Cowiche, and Naches valleys (Figures 14 through 18) because of their overall poor definition on the borehole geophysical logs. The combined thickness of the Frenchman Springs flows at these locations ranges from 29 to over 131m.

#### Squaw Creek Member of the Ellensburg Formation

The Squaw Creek Member of the Ellensburg Formation lies between the Frenchman Springs and Roza members throughout most of the Yakima region. The thickness of the Squaw Creek Member ranges from 0 to nearly 16m. The composition of the Squaw Creek Member varies from a diatomite or jasperoid to sandstone or conglomerate (Schmincke, 1967a; Diery and McKee, 1969; Bentley and others, 1980). This member can be used as a stratigraphic marker when utilizing borehole geophysical logs for stratigraphic correlation because of its high natural gamma response. A typical response is shown in Figure 21 and may be caused by a high concentration of potassium-rich clays.

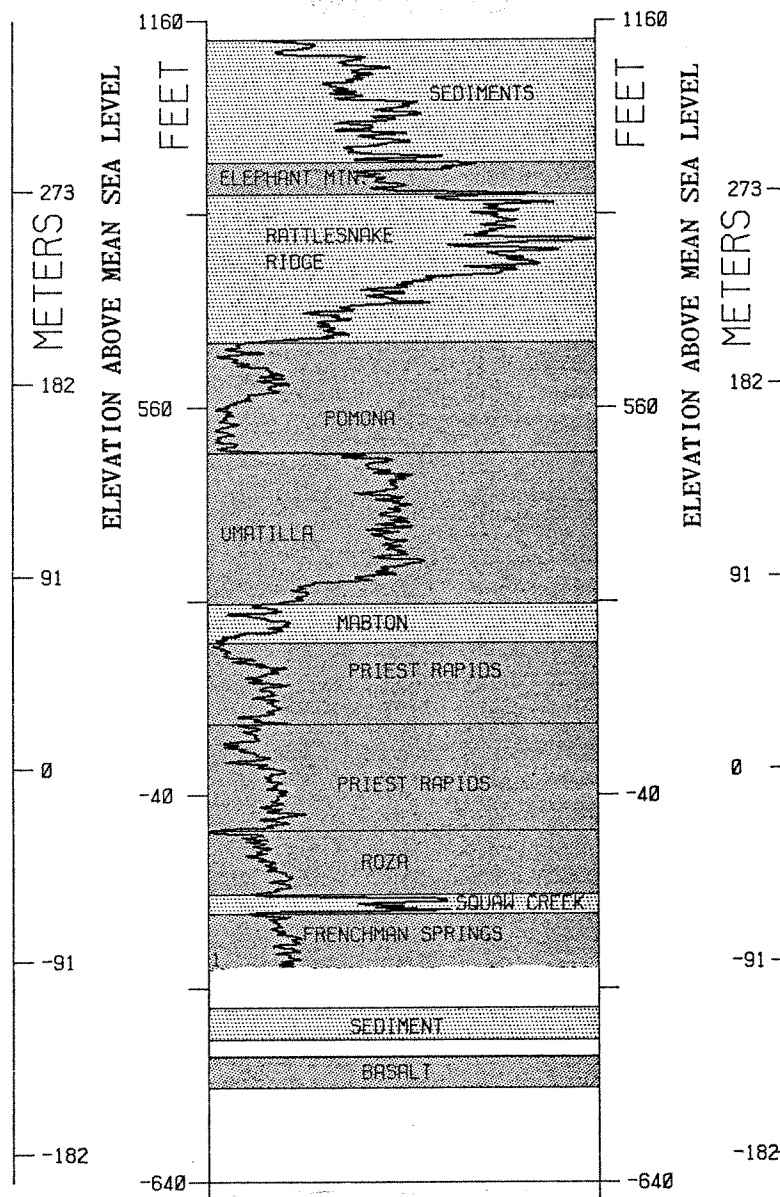


FIGURE 21 TYPICAL NATURAL GAMMA RESPONSE OF THE UMATILLA AND SQUAW CREEK MEMBERS

### Roza Member

The Roza Member occurs as a single flow in the Yakima region. The thickness of this member ranges from about 30 to nearly 50m along correlation lines of the lower Yakima, Black Rock, and Moxee valleys (Figures 4 through 13 and 20) and from over 12 to nearly 40m along correlation lines of the Naches Valley (Figures 18 and 19). The Roza Member is absent along correlation lines in the Ahtanum and Cowiche valleys (Figures 14 through 16).

### Quincy Member(?) of the Ellensburg Formation

A thin interbed, normally less than 3m thick, often separates the Roza Member from the overlying basalt flow in the Yakima region. In discussing these sediments, Swanson and others (1979a) abandoned the name "Quincy" in favor of the term "Squaw Creek Member" because of the invasive nature of the underlying Roza flow at many locations. The name Quincy Member(?) is used in this report because of the widespread occurrence of this interbed.

### Priest Rapids Member of the Wanapum Formation

Two basalt flows belonging to the Priest Rapids Member, referred to as the upper and lower flows in this report, occur in the subsurface of most of the region. The upper and lower flows correspond to the Lolo and Rosalia chemical types, respectively (Bentley and others, 1980). The thickness of the upper flow ranges from 10 to almost 40m, and the thickness of the lower flow ranges from 44 to almost 60m. A thin (up to 9m thick), unnamed interbed occurs rarely between these two flows. In several locations along correlation lines in the Black Rock and Cowiche valleys (Figures 13 and 19) only one flow was found. This flow has been correlated with the upper flow because of a similarity in the thickness of the flow throughout the region.

### Mabton Member of the Ellensburg Formation

The Mabton Member of the Ellensburg Formation overlies the Priest Rapids Member throughout most of the Yakima region. The thickness of the Mabton Member varies from 0 to over 25m. It is composed of volcanoclastic deposits and airfall tuff (Bentley and others, 1980).

### Saddle Mountains Formation

Four members of the Saddle Mountains Formation are found in the Yakima region: the Umatilla, Huntzinger (Asotin?), Pomona, and Elephant Mountain. Interbedded between these flows are sediments of the Ellensburg Formation that may be greater than 100m thick.

### Umatilla Member of the Saddle Mountains Formation

The Umatilla Member consists of a single basalt flow in the Yakima region. The thickness of this member ranges from 30 to 60m along correlation lines in the Black Rock and Moxee valleys (Figures 11 through 13 and 20) and from 55 to over 80m along correlation lines in the lower Yakima Valley (Figures 4 through 10). The Umatilla Member is absent along correlation lines of the Ahtanum, Cowiche, and Naches valleys (Figures 14 through 19).

The Umatilla Member serves as a stratigraphic marker when utilizing borehole geophysical logs for stratigraphic correlation because of its high natural gamma response (Crosby and others, 1972). A typical response is shown in Figure 21.

#### Huntzinger Valley Flow (Asotin Member?) of the Saddle Mountains Formation

The Huntzinger valley flow (Asotin Member?) occurs as a minor "valley filling" basalt flow in the Moxee and Black Rock valleys (Bentley, 1977; Campbell, 1977a) and along Yakima Ridge (Swanson and others, 1979b). The thinness and isolated occurrences of this flow make it difficult to identify by geophysical borehole logs.

A thin basalt flow lying beneath the Pomona Member in the Naches Valley (see wells 14N/17E-35H1 and 14N/17E-26G1, in Figures 18 and 19) may correlate to the Huntzinger flow. This flow has not been identified in any of the remaining correlation diagrams that were prepared for this report, although drillers' logs suggest that it may be present in wells located in the lower Yakima Valley (12N/20E-36P1 and 11N/21E-06L1).

#### Selah Member of the Ellensburg Formation

The Selah Member of the Ellensburg Formation lies between the Pomona Member and the underlying basalt flow, which is normally the Umatilla Member. The Selah Member is composed of volcanoclastic deposits and vitric tuffs (Schmincke, 1967b). Its thickness ranges from 0 to almost 25m along correlation lines in the lower Yakima Valley (Figures 4 through 10), from 0 to 15m along correlation lines in the Black Rock and Moxee valleys (Figures 11 through 13 and 20), from over 21 to under 38m along correlation lines in the Naches Valley (Figures 18 and 19), and from 0 to 39m along correlation lines in the Ahtanum Valley (Figures 14 through 16). Along the correlation lines in the Ahtanum and Naches valleys, the Selah Member may include older (Mabton?) sediments, because the Umatilla Member is absent in these areas.

#### Pomona Member of the Saddle Mountains Formation

The Pomona Member of the Saddle Mountains Formation consists of a single basalt flow in the Yakima region. The thickness of this member ranges from less than 40 to over 80m along correlation lines in the lower Yakima Valley (Figures 4 through 10), from 45 to 55m along correlation lines in the Moxee Valley (Figures 11, 12, and 20), from 0 to almost 30m along the correlation line in the Black Rock Valley (Figure 13), from over 18 to 32m along correlation lines in the Cowiche and Naches valleys (Figures 17 through 19), and from 0 to over 21m along correlation lines in the Ahtanum Valley (Figures 14 through 16). Bentley and others (1980) report a thickness of 50 to 60m, thinning westward to 30m, on the Yakima Indian Reservation.

The Pomona Member extends farther to the west than does the underlying Umatilla Member in the Yakima region (Schmincke, 1967c). This flow often displays the colonnade, entablature, and upper colonnade intraflow structures in the Yakima region (Schmincke, 1967c; Bentley and others, 1980).

### Rattlesnake Ridge Member of the Ellensburg Formation

The Rattlesnake Ridge Member lies between the Elephant Mountain and Ponoma members. In the Yakima region, this interbed is composed of siltstones, claystones, sandstones, tuffs, and conglomerates (Schmincke, 1967c; Campbell, 1977b; Bentley and others, 1980). The thickness of this member ranges from 40 to over 100m along correlation lines in the lower Yakima Valley (Figures 4 through 10). Bentley and others (1980) report a thickness of up to 200m in the Toppenish basin. Thicknesses of up to 100m occur along correlation lines in the Moxee Valley (Figures 11, 12, and 20).

The Rattlesnake Ridge Member loses its identity and is grouped with younger sediments when the Elephant Mountain Member is absent. This situation occurs along correlation lines in the Black Rock, Ahtanum, Cowiche, and Naches valleys (Figures 13 through 19).

### Elephant Mountain Member of the Saddle Mountains Formation

The Elephant Mountain Member of the Saddle Mountains Formation usually occurs as one flow in the Yakima region, with a second flow, locally known as the Ward Gap flow, exposed at Snipes Mountain (Campbell, 1977b) and at Ward Gap (Schmincke, 1967c). The thickness of this member ranges from 3 to 20m along correlation lines in the lower Yakima Valley (Figures 4 through 10) and from 0 to over 12m along correlation lines in the Moxee Valley (Figures 11, 12, and 20). The Elephant Mountain Member is absent along correlation lines in the Black Rock, Ahtanum, Cowiche, and Naches valleys (Figures 13 through 19).

### Upper Ellensburg Formation and Quaternary Sediments

Overlying the Elephant Mountain Member are Ellensburg and younger Quaternary sediments. The Ellensburg sediments include the conglomerate of Snipes Mountain, other conglomerates, sandstones, laharcic deposits, siltstones, and tuff (Campbell, 1976, 1977a, 1977b; Bentley and others, 1980). The Quaternary sediments include basaltic gravels, Touchet deposits of silt with lenses of clay and sand, loess, landslide debris, and alluvial clays, silts, sands, and gravels (Campbell, 1976, 1977a, 1977b; Waitt, 1979; Bentley and others, 1980). This informal grouping includes older sediments in the western portion of the Yakima region because of the progressive westward absence of the younger basalt flows. The upper Ellensburg Formation and Quaternary sediments are labeled "sediments" on the stratigraphic correlation diagrams (Figures 4 through 20).

Along correlation lines in the lower Yakima Valley (Figures 4 through 10), the thicknesses of these sediments range from 0 to nearly 180m, and greater thicknesses would be found towards the center of the valley. The thicknesses of these sediments range from over 18 to over 60m along the correlation line in the Black Rock Valley (Figure 13), from over 76 to over 390m along correlation lines in the Moxee Valley (Figures 11, 12, and 20), from over 9 to over 335m along correlation lines in the Ahtanum Valley (Figures 14 through 16), and from less than 1 to over 85m along correlation lines in the Cowiche and Naches valleys (Figures 17 through 19).

## Tieton Andesite

The Tieton Andesite flow(s) extends into the Naches Valley and reaches thicknesses of up to 155m along the correlation lines (Figures 18 and 19). This flow erupted a short distance to the west of this region in the Tieton River Canyon area (Swanson, 1966). The Tieton Andesite flow(s) is characterized by a high natural gamma response, which may prove useful for future stratigraphic correlations to the west of the Yakima region.

### Geologic Structure

The Yakima region is dominated by a series of southeastward-trending, narrow anticlinal ridges and broad, synclinal basins. These structures, from north to south, are the Cleman Mountain-Umtanum Ridge uplift, the Cowiche-Naches basins, the Cowiche Mountain-Yakima Ridge uplift, the Ahtanum-Moxee-Black Rock basins, the Ahtanum Ridge-Rattlesnake Hills uplift, the Toppenish-lower Yakima basins, and the Toppenish Ridge uplift. The Cle Elum-Wallula deformed belt or lineament, a northwesterly-trending zone of deformation, lies along the eastern and northern edges of the study area. Geologic structures of the Yakima region are shown in Plate 1, and a brief description of these structures is given below. Interested readers are referred to Campbell (1975), Bentley (1977), Campbell and Bentley (1979), Bentley and Farooqui (1979), Myers and others (1979), and Bentley and others (1980) for more detailed reports.

The anticlinal ridges are complex and change in structure laterally. The Cowiche Mountain-Yakima Ridge uplift is a box-fold anticline with sharp hinge lines along both flanks (Bentley, 1977; Myers and others, 1979). The Rattlesnake Hills "northern anticline" is an asymmetrical anticline with the northern flank displaying a greater dip than the southern flank (Myers and others, 1979). This structure is described as a box-fold anticline west of Union Gap along the Ahtanum Ridge (Bentley and others, 1980). The Toppenish Ridge anticlines are described as being asymmetric or box-fold also (Bentley and others, 1980).

Most of the known faulting within the region is associated with the anticlinal structures. Monoclinial folds and thrust faults and, less commonly, normal faults parallel the anticlinal axes (Swanson and others, 1979c; Myers and others, 1979; Bentley and Farooqui, 1979). The ridges often contain wide (100-200m), steeply dipping zones of shatter breccia (Bentley and Farooqui, 1979). Northwestly- to northeasterly-trending folds and strike-slip faults transect the anticlinal structures (Bentley and Farooqui, 1979; Myers and others, 1979; Swanson and others, 1979c). Deformation in the Yakima region began as early as Grande Ronde time and continued into the Quaternary (Bentley, 1977; Bentley and Farooqui, 1979; Campbell and Bentley, 1979; Bentley and others, 1980).

The stratigraphic correlation diagrams (Figures 4 through 20) reflect the presence of these geologic structures. Noteworthy examples include Figures 12 and 13. These figures show the Pomona Member thinning and pinching out towards the Hog Ranch Fault Axis, which separates the Moxee and Black Rock valleys. Another example is Figure 11, in which well 12N/20E-16H1, located near the thrust fault along the northern side of Elephant Mountain, shows a thicker than normal deposit of sediments overlying the Elephant Mountain Member. The Elephant Mountain and Pomona members have been mapped a short distance to the south of well 12N/20E-16H1 on Elephant Mountain. The basalt correlations in this well suggest that approximately 2000ft of vertical

movement occurred along the faults and folds associated with the Elephant Mountain structure.

It should be noted that geophysical borehole logs are not available for well 12N/20E-16H1 and that the driller's log was used for the stratigraphic correlation. Chemical analysis of rock chips collected during the drilling operation suggests that the stratigraphic correlation for well 12N/20E-16H1 is accurate (Bill Myers, personal communication, 1982).

### Ground-Water Hydrology of the Yakima Region

The occurrence of ground water is controlled primarily by the lithology, stratigraphy, and geologic structure of a region. Climate and cultural activities, past and present, also influence the ground-water system of a region. A great deal of information pertaining to these factors and their relationship to the ground-water system of the Columbia Plateau has been collected during the last two decades; however, the ground-water system is still poorly defined because of its complexity. Most of the information has been obtained from research associated with the Basalt Waste Isolation Project, the Columbia Basin and Yakima River Irrigation projects, and regional ground-water resource assessment and management studies. Columbia Plateau surface-water and ground-water studies are summarized by Gephart and others (1979). Ground-water studies in the Yakima region include Smith (1901), Waring (1913), Sceva and others (1949), Foxworthy (1962), Kinnison and Sceva (1963), Eddy (1971), U. S. Geological Survey (1974), Cearlock and others (1975), Corps of Engineers (1978), Gephart and others (1979), Tanaka and others (1979), and Bolke and Skrivan (1981). The following review of the ground-water hydrology relies heavily upon these previous studies.

### Ground-Water Flow Model in the Yakima Region

Conceptual models often utilize the terms local, intermediate, and regional to define the components and boundaries of a ground-water flow system. Boundaries are vaguely defined and based largely on scale and flow direction because of the interaction of the components. Normally, several local systems are thought to act within one topographic basin, while an intermediate system may act in one or more basins. A regional ground-water system often incorporates several intermediate systems. The ground-water flow path length and flow volume increase from local to regional systems.

In the hierarchy of ground-water flow systems, the Yakima region is considered to contain many local and several intermediate systems that act in concert with the regional system and/or systems of the Columbia Plateau (Kinnison and Sceva, 1963; Gephart and others, 1979). Plate 2 shows the approximate ground-water static levels that outline the intermediate ground-water basins of the Yakima region. The ground-water level contours, in general, mirror the topographic relief, with the divides of the ground-water basins coinciding with the topographic divides. The general direction of ground-water flow in the Yakima region is from the crests of the anticlinal structures towards the axes of the synclinal valleys and then down-gradient in the direction of the Yakima River (Kinnison and Sceva, 1963; Gephart and others, 1979; Tanaka and others, 1979). To what depth these ground-water basins and flow relationships hold true is unknown.

## Ground-Water Occurrence in the Yakima Region

Studies to quantify the ground-water resources of the Yakima region have normally identified three aquifers based on lithologic differences (U. S. Geological Survey, 1974; Cearlock and others, 1975). In the Toppenish basin, the aquifers have been referred to as the "young valley filling sediments," "old valley filling sediments," and "basalts" (U. S. Geological Survey, 1974). In the Moxee and Ahtanum valleys, the terms "gravels," "Ellensburg," and "basalts" have been used (Cearlock and others, 1975). Foxworthy (1962) recognized three sedimentary aquifers and a basalt aquifer in the Ahtanum Valley. The regional aquifers will be referred to as the "sedimentary" and "basalt" aquifers in the following discussion. It should be noted that these two aquifers are composed of a large number of water-bearing, lithologic units that possess differing hydraulic properties.

### The Sedimentary Aquifer

The ground water in the upper Ellensburg and Quaternary sediments, which comprise the sedimentary aquifer, is recharged by direct infiltration from precipitation, irrigation, and the influent reaches of the rivers, streams, and canals of the region. This aquifer is also recharged by upward flow from the basalt aquifer. It has been estimated that between 1910 and 1931 irrigation caused the ground-water static level of the sedimentary aquifer of the Toppenish basin to increase some 15m and that approximately 1.3 million acre-feet of water entered the aquifer as storage during this time (U. S. Geological Survey, 1974). The annual variation in the ground-water static level caused by irrigation and canal seepage is as great as 15ft near Wapato (Bolke and Skrivan, 1981). The sedimentary aquifer discharges directly to the effluent reaches of the streams and rivers of the region and to the basalt aquifer by downward flow.

The lithologic heterogeneity of the sedimentary aquifer results in a wide range of horizontal and vertical transmissivities. The gravel and sand-rich sediments are much more permeable than the clay and silt-rich sediments. As a consequence, ground water in the sedimentary aquifer occurs under perched, unconfined (water table) and confined conditions.

Reported values of transmissivity range from 0.1 to 600gpd/ft, with more common values being less than 100gpd/ft. Reported values of transmissivity, specific storage, and pumping yields are summarized in Table 5.

### The Basalt Aquifer

Ground water in the basalt aquifer is recharged directly by infiltration along the anticlinal ridges and along the influent reaches of the rivers and streams of the region where the basalt is at the surface. The basalt aquifer is also recharged by downward flow from the sedimentary aquifer. The basalt aquifer discharges to the overlying sedimentary aquifer and to the effluent streams and rivers of the region when the basalt is at the ground surface. Direct recharge and discharge from the Yakima River to the basalt aquifer is significant in the upper Yakima River basin (Kinnison and Sceva, 1963; Gephart and others, 1979).

The transmissivity of the basalt aquifer can vary by several orders of magnitude both horizontally and vertically. As noted earlier, the typical basalt flow has zones of much higher effective porosity at both the top and the bottom as compared with the central portion of the flow. Horizontal

Table 5. Transmissivities, Specific Capacities, and Pumping Yields of the Yakima Region Sedimentary Aquifer

Aquifer Description	Geographic Location	Transmissivity (gpd/ft x 10 <sup>3</sup> )	Specific Capacity (gpm/ft)	Pumping Yield (gpm)	Source
Young valley fill (Quaternary?)	Toppenish Basin	4 to 116 <sup>1</sup> Avg. of 20	2 to 58 Avg. of 10	5 to 1000 Avg. of 30	U.S. Geological Survey (1974)
Old valley fill (Ellensburg?)	Toppenish Basin	6 to 600 Avg. of 60	3 to 300 Avg. of 30	as much as 1500	U.S. Geological Survey (1974)
Ellensburg Formation	Moxee Valley	9.7 <sup>2</sup>	4.9 <sup>1</sup>	---	Cearlock and others (1975)
Ellensburg Formation	Ahtanum Valley	1.9 to 15.0 <sup>2</sup>	0.9 to 7.5 <sup>1</sup>	---	Cearlock and others (1975)
Sand and gravel	Ahtanum Valley	30 to 90	28 to 73	62 to 69	Foxworthy (1962), a summary of four pump tests
Gravels	Selah area	<0.7	<0.35	---	Eddy (1971)
Ellensburg Formation	Selah area	>0.1	>0.06	---	Eddy (1971)

<sup>1</sup>calculated by assuming transmissivity (gpd/ft) = specific capacity (gpm/ft) x 2000 (after Theis and others, 1963)

<sup>2</sup>transmissivity values utilized in a ground-water model of the Moxee-Ahtanum valleys (Cearlock and others, 1975)

transmissivity within the basalt aquifer is influenced greatly by the presence of these high porosity zones (Waring, 1913). Cooling joints and tectonic fractures also contribute to horizontal transmissivity. These high porosity zones may be areally extensive but often exhibit large variations in productivity, primarily because of changes in aquifer thickness and secondary mineralization or clay infilling (Crosby and Mellott, 1973; Brown, 1979b). Vertical transmissivity within the basalt aquifer is controlled largely by the presence of cooling joints and tectonic fractures. The central portion of a basalt flow may act as an aquitard in the absence of these features.

The sedimentary interbeds--the Selah, Mabton, Quincy(?), Squaw Creek, and Vantage members--also influence the horizontal and vertical transmissivities of the basalt aquifer. Both horizontal and vertical transmissivities should increase where the interbeds are composed of porous sands and gravels. Conversely, the transmissivities should decrease where there are less porous clayey or tuffaceous sediments.

The Vantage Member in the Pullman and Central Basin areas, the Mabton Member in the Horse Heaven Hills area, and the underlying basalt flow(s) in all three areas may act as an aquitard on a regional basis (Brown, 1980). It is not known if such aquitards exist on a regional scale in the Yakima area. The presence of local aquitards, as will be shown later, is very common in the basalt aquifer of the Yakima region and results in intra-borehole flow of ground water between aquifers. There seems to be a high degree of vertical conductivity on a regional scale in at least the younger basalt flows of the Yakima region. Ground-water levels in the basalt aquifer have shown a general decline in the Toppenish basin because of irrigation withdrawals (U. S. Geological Survey, 1974) which would suggest that the horizontal, high porosity zones are hydraulically connected on a regional scale.

Reported transmissivity values in the basalt aquifer range from less than 2000 to 800,000gpd/ft and average less than 40,000gpd/ft. Specific capacity ranges from less than 1 to 400gpm/ft and averages less than 20gpm/ft. Transmissivities, specific capacities, and pumping yields for the Columbia Plateau basalt aquifer are summarized in Table 6. These same values for wells in the Yakima region are summarized in Table 7.

## Geothermal Resources of the Yakima Region

### Introduction

On a global scale, heat flows from the deeper zones of the earth towards the surface. Estimates of the average heat flow of the earth range from 50 to 63mW/m<sup>2</sup> (Goguel, 1976; Lachenbruch and Sass, 1977). Average temperature gradients range from 25 to 30°C/km (Goguel, 1976; Freeze and Cherry, 1979). Lachenbruch and Sass (1977) provide the following equations which define the flow of heat in terms of the processes that generate, transport, and store heat in the subsurface of the earth:

$$-\nabla \cdot \bar{q} = -A + \rho'c'v \cdot \nabla T + \rho c \frac{\partial T}{\partial t} \quad (1)$$

$$-\nabla \cdot \bar{q} \equiv \nabla \cdot (k\nabla T) \quad (2)$$

Table 6. Transmissivities, Specific Capacities, and Pumping Yields of the Basalt Aquifer of the Columbia Plateau

Aquifer Description	Geographic Location	Transmissivity (gpd/ft x 10 <sup>3</sup> )	Specific Capacity (gpm/ft)	Pumping Yield (gpm)	Source
Basalt	Toppenish Basin	<2 to 800 <sup>1</sup> Avg. of 32	1 to 400 Avg. to 16	45 to 2200	U.S. Geological Survey (1974)
Basalt	Ahtanum Valley	16.8 to 35.9 <sup>2</sup>	8.4 and 18.0 <sup>1</sup>	---	Cearlock and others (1975)
Basalt	Moxee Valley	6.0 to 26.2 <sup>2</sup>	3.0 to 13.3 <sup>1</sup>	---	Cearlock and others (1975)
Basalt	Odessa area	Avg. of 29.9 <sup>1</sup>	1 to 360 <sup>3</sup>	---	Luzier and Burt (1974)
Basalt	Grant and Lincoln counties, exclusive of the Odessa area	Avg. of 12 <sup>1</sup>	1 to 120 <sup>3</sup>	---	Luzier and Burt (1974)
Basalt	Adams and Franklin counties, exclusive of the Odessa area	Avg. of 15 <sup>1</sup>	1 to 270 <sup>3</sup>	---	Luzier and Burt (1974)
Basalt	Spokane County	Avg. of 29.9 <sup>1</sup>	1 to 80 <sup>3</sup>	---	Luzier and Burt (1974)
Basalt	Whitman County	Avg. of 15.0 <sup>1</sup>	1 to 1440 <sup>3</sup>	---	Luzier and Burt (1974)
Basalt	Pullman-Moscow area	0.6 to 210 <sup>2</sup>	0.3 to 105 <sup>1</sup>	---	Barker (1979)

Table 6. Transmissivities, Specific Capacities, and Pumping Yields of the Basalt Aquifer of the Columbia Plateau (cont.)

Aquifer Description	Geographic Location	Transmissivity (gpd/ft x 10 <sup>3</sup> )	Specific Capacity (gpm/ft)	Pumping Yield (gpm)	Source
Basalt	Odessa-Lind area	2 to >299 <sup>2</sup>	1.0 to 149.6 <sup>1</sup>	---	Luzier and Skrivan (1975)
Basalt	Walla Walla area	---	---	30 to 3000	MacNish and others (1973)
Basalt	Goldendale area	---	---	500 to 2000	Brown (1979b)
Basalt	Eastern Klickitat County	---	---	as much as 2000 to 3000	Brown (1979b)
Basalt	Camas Prairie-Glenwood area	---	---	as much as 180 <sup>4</sup>	Cline (1976)
Wanapum and Grande Ronde Basalts	Adams, Lincoln, and Grant counties	Avg. of 10 to 300 <sup>1</sup> Avg. as much as 600	Avg. of 5 to 150 <sup>1</sup>	---	Tanaka and others (1979)
Wanapum and Saddle Mountains Basalts	Yakima County	Avg. of 10 to 30 <sup>1</sup> Avg. as much as 300	Avg. of 5 to 15 <sup>1</sup>	---	Tanaka and others (1979)

<sup>1</sup>calculated by assuming transmissivity (gpd/ft) = specific capacity (gpm/ft) x 2000 (after Theis and others, 1963)

<sup>2</sup>minimum and maximum transmissivity values utilized in regional ground-water models

<sup>3</sup>median specific capacity for 342 wells in Grant, Lincoln, Adams, Franklin, Spokane, and Whitman counties equaled 12 gpm/ft (Luzier and Burt, 1974)

<sup>4</sup>pumping yields limited by shallow depths of the wells of the area (Cline, 1976)

Table 7. Transmissivities, Specific Capacities, and Pumping Yields of Wells that Penetrate the Basalts in the Yakima Region

Location and Well Designation	Transmissivity <sup>1</sup> (gpd/ft x 10 <sup>3</sup> )	Specific Capacity <sup>1</sup> (gpm/ft)	Pumping Yield (gpm)	Source
8/22-11J (Flower)	9.4	4.7	1302	State of Wash. water well rept.
10/23-17B (Stout)	11.5	5.8	2052	State of Wash. water well rept.
11/20-1M (Forrest)	7.1	3.6	800	State of Wash. water well rept.
11/20-13R (Soost)	30.5	15.3	2000	State of Wash. water well rept.
11/21-6Q (Dahl)	20.0	10.0	1100	State of Wash. water well rept.
11/21-17N (Prentis)	28.0	14.0	--	Tanaka and others (1979)
11/21-22G (Sandlin)	2.0	1.0	--	Tanaka and others (1979)
11/21-35 (Carpenter)	28.0	14.0	--	Tanaka and others (1979)
12/16-12N (Shelton)	69.6	34.8	940	State of Wash. water well rept.
12/17-7M (Bates)	15.1	7.5	460	State of Wash. water well rept.
12/18-32H	216.9	108.5	--	U.S. Geological Survey (1974)
12/18-33A	32.2	16.1	--	U.S. Geological Survey (1974)
12/19-16P (Gangle)	15.2	7.6	600	State of Wash. water well rept.
12/19-27H (Stepniewski)	0.7	0.4	50	State of Wash. water well rept.
12/20-36P (Cheyne)	4.8	2.4	550	State of Wash. water well rept.
12/22-21R (Marley)	46.8	23.4	1450	State of Wash. water well rept.
12/22-29B (Changala)	14.7	7.4	700	State of Wash. water well rept.
13/18-31P (Hull)	8.8	4.4	614	State of Wash. water well rept.
14/17-15N (Majnarich)	0.6	0.3	35	State of Wash. water well rept.
14/17-26G (Allen)	2.8	1.4	258	State of Wash. water well rept.

<sup>1</sup>calculated by assuming that transmissivity (gpd/ft) = specific capacity (gpm/ft) x 2000 (after Theis and others, 1963)

where:  $\bar{q}$  = conductive flux vector (e.g., milliwatt/meter<sup>2</sup>)  
 A = heat generation  
 $\rho, \rho'$  = density of the static and moving material, respectively  
 $c, c'$  = heat capacity of the static and moving material, respectively  
 T = temperature  
 t = time  
 v = seepage velocity  
 k = thermal conductivity  
 x, y, z = Cartesian coordinate directions  
 $\nabla = i \frac{\partial}{\partial x} + j \frac{\partial}{\partial y} + k \frac{\partial}{\partial z}$

Geothermal studies often utilize quasi-one-dimensional models which neglect three-dimensional effects and define quantities in terms of the depth (z) below the surface of the earth (Lachenbruch and Sass, 1977). The sign convention of q is also reversed. Equations (1) and (2) reduce to the following under these assumptions:

$$\frac{\partial q}{\partial z} = -A + \rho' c' v_z \frac{\partial T}{\partial z} + \rho c \frac{\partial T}{\partial t} \quad (3)$$

$$q \equiv k \frac{\partial T}{\partial z} \quad (4)$$

where: q = vertical conductive flux, or "heat flow"  
 $v_c$  = vertical seepage velocity  
 $\frac{\partial T}{\partial z}$  = geothermal gradient

Heat flow (equation 4) is determined by measuring the thermal conductivity of the lithologic units (k) and the geothermal gradient ( $\partial T/\partial z$ ). Heat flow values are often used to compare the differing thermal regimes of large geographical regions (e.g., Blackwell, 1971; Blackwell, 1974; Lachenbruch and Sass, 1977; Blackwell, 1978; Sass and Lachenbruch, 1979). Accurate heat flow values are difficult to obtain because of the problems in defining the horizontal and vertical variations of near-surface thermal conductivity.

The poor definition of thermal conductivity precludes the use of the heat flow value as a predictive tool in the low-temperature geothermal resource assessment of the Yakima region. The geothermal gradient, or rate of change

of temperature with depth, and the projected land-surface temperature are used in this report to describe the geothermal resources of the region.

Several factors influence the geothermal gradient that is measured in a ground-water aquifer. Climatic temperature variation often produces diurnal and seasonal changes in the geothermal gradient which are noticeable to depths of 10 to 20m. Below this transient zone, the geothermal gradient varies from one region to another because of differences in the heat flow, thermal conductivity, land-surface temperature, and the redistribution of the heat by ground-water flow.

Differences in land-surface temperature (LST) influence the geothermal gradient by affecting both the heat conduction and convection processes. Several factors, including topography and ground cover, contribute to the LST of an area. Topography affects the observed geothermal gradient in several ways. Atmospheric temperature gradients associated with elevation and differences in solar insolation caused by land slope azimuth and land slope dip produce differences in the LST. For example, the LST would be expected to be cooler at higher elevations as compared with the LST at lower elevations. Slopes with a southward aspect would be expected to be warmer than slopes with a northward aspect (in the northern hemisphere). Topographic effects and terrain corrections for geothermal gradients and heat flow data have been reviewed recently by Blackwell and others (1980). Ground cover, which acts to reduce the amount of solar radiation striking the ground, will also influence the LST. For example, a forested area would be expected to be cooler than a grassland.

The redistribution of heat by ground-water flow, or "forced convection," is significant when studying the near-surface distribution of geothermal gradients (Stallman, 1963; Parsons, 1970). Forced convection makes it difficult to interpret Columbia Plateau heat flow measurements in terms of regional crustal processes (Lachenbruch and Sass, 1977). Stallman (1963) developed the following equation which describes the change in the geothermal gradient caused by ground-water flow:

$$\nabla^2 T = \frac{c' \rho'}{k} \left[ \frac{\partial(v_x T)}{\partial x} + \frac{\partial(v_y T)}{\partial y} + \frac{\partial(v_z T)}{\partial z} \right] + \frac{c \rho}{k} \frac{\partial T}{\partial t} \quad (5)$$

where:  $v_x, v_y, v_z$  = components of ground-water seepage velocity in the x, y, and z directions

$$\nabla^2 T = \frac{\partial^2 T}{\partial x^2} + \frac{\partial^2 T}{\partial y^2} + \frac{\partial^2 T}{\partial z^2}$$

Figure 22 shows the influence of a simplified regional ground-water flow system on the observed geothermal gradient. The following statements apply to this simple model. Near-surface geothermal gradients would be expected to be greater in ground-water discharge areas as compared with recharge areas (Freeze and Cherry, 1979). Geothermal gradients would be expected to increase with depth in ground-water recharge areas and decrease with depth in discharge areas (Freeze and Cherry, 1979). Surface temperatures might be expected to be greater in ground-water discharge areas than in recharge areas (Parsons, 1970).

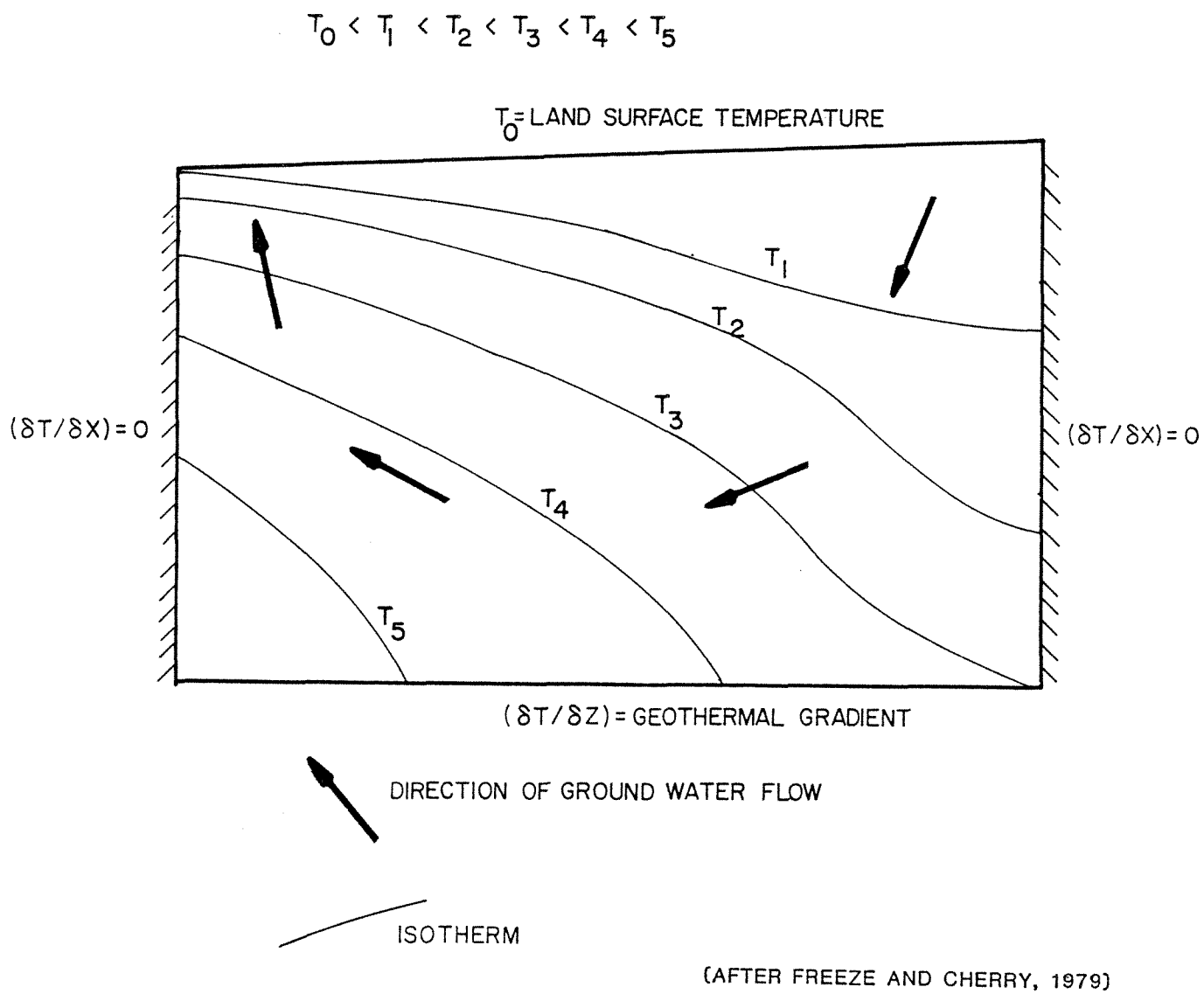


**FIGURE 22 RELATIONSHIP BETWEEN THE GROUND-WATER FLOW SYSTEM AND THE GEOTHERMAL GRADIENT**

The difference in the LST caused by topography is often enhanced by the effects of ground-water flow in areas where forced convection is significant. In the Yakima region, ground water is believed to flow from the areas of greater elevation (anticlinal ridges), which are regions of cooler LST, towards the lower elevations, which are regions of warmer LST. Ground-water temperatures and geothermal gradients would be influenced by such a flow system, but the ability to model the resulting temperature distribution is limited by the lack of quantitative ground-water flow data and models. As reviewed previously, the ground-water flow system in the Yakima region is complex, and a simple, one-component ground water recharge-discharge model and the corresponding geothermal gradient distribution would not apply over the large areas and depths being considered in this project.

#### Previous Geothermal Research in the Yakima Region

Geothermal research in the Yakima region began at least as early as the turn of the century. Smith (1901) noted the warm temperatures (approximately 22°C) of the ground water from flowing wells in the Moxee Valley and calculated geothermal gradients of 50 to 73°C/km for the region. Foxworthy (1962) reported an average geothermal gradient of 40.5°C/km in water wells greater than 15m deep in the Ahtanum Valley and suggested that the rock type had little effect on the gradient. Schuster (1980) noted that geothermal gradients of 50 to 70°C/km were commonly measured in water wells of the region and that relatively warm temperatures (20 to 27°C) were recorded in several shallow (up to 35m deep) wells.

Most of the geothermal gradients listed by Schuster (1980) and Korosec (1980) for the Yakima region are in the 35 to 45°C/km range. Depths to the 20°C isotherm in water wells of the Yakima region were reported to range from 9 to 471m, with the majority from 100 to 200m (Schuster, 1980).

Blackwell (1980) reported geothermal gradients of 30.0 to 37.2°C/km and corresponding heat flow values of 47 to 64mW/m<sup>2</sup> in boreholes located on the Hanford Reservation, east of the Yakima region. Robinette and others (1977) reported geothermal gradients ranging from over 23 to 79°C/km in areas of Grant, Benton, Franklin, and Adams counties, east of Yakima County. Schuster and others (1978) recorded geothermal gradients of 44.5 to 53.4°C/km and heat flow values of about 56 to 75mW/m<sup>2</sup> from the Indian Heaven area, southwest of the Yakima region.

Heat flow data are unavailable in the Yakima region because of the poor or "disturbed" quality of the geothermal gradients and the lack of thermal conductivity data. Several studies, including those by Diment and others (1975), Lachenbruch and Sass (1977), Blackwell (1978), and Sass and Lachenbruch (1979), have presented contoured heat flow maps for the western United States. The most recent of these studies has shown the Yakima region to have a heat flow of approximately 60mW/m<sup>2</sup>. Interested readers are referred to the previously noted studies for additional information concerning the significance of the heat flow of the region in terms of tectonics and crustal models.

The low-temperature geothermal potential of the Columbia Plateau and the Yakima region has been reviewed in reports by Blackwell (1974), Bloomquist (1979), Jhaveri and Miller (1980), Schuster (1980), and Korosec and others (1981). The Yakima region has been described as being favorable for the exploration and development of low-temperature ground water. Present commercial utilization in the Yakima region is limited to irrigation (soil warming) and as a source of warm water for a car wash (Bloomquist, 1979).

Domestic heat pumps have been installed in the Yakima region, but no attempt to identify and assess these installations has been made. Economic and engineering studies have or are being conducted currently to investigate the possibility of using the warm ground water as a heat source for public buildings (Jhaveri and Miller, 1980; Korosec and others, 1981).

### Temperature Data

Subsurface temperature data from the Yakima region have been collected primarily by three research groups or agencies. These groups are the Geological Engineering Section at Washington State University (WSU), the Washington State Department of Natural Resources and Southern Methodist University (DNR-SMU), and the U. S. Geological Survey (USGS). The USGS data and the pre-1979 DNR-SMU data were obtained from Korosec (1980). Post-1979 DNR-SMU data were compiled by the DNR and made available for this investigation. The temperature data have been collected primarily from domestic and irrigation water wells. Bottom-hole temperatures, depths, and locations of 184 wells in the Yakima region are given in the Appendix. Well locations are shown in Plate 3.

The accuracy of the temperature data varies with the collecting agency. The temperature data collected by DNR-SMU have an accuracy of approximately  $\pm 0.2^{\circ}\text{C}$  (Blackwell, 1980). The accuracy of the temperature data collected by the USGS is unknown.

The temperature probes utilized by WSU since 1974 were recalibrated in a water bath as part of this project. The results of previous calibrations were approximate because of the use of a nonstandard thermometer. The change in calibration averaged less than  $-1.0^{\circ}\text{C}$ , and the calibration error was nearly constant for each probe. The temperature probes were calibrated over a temperature range from less than 15 to  $50^{\circ}\text{C}$ .

The WSU borehole logging system records data continuously as "hard copy" on a chart recorder and also samples and records data on punched paper tape for later computer processing and plotting. The temperature data are sampled every foot and processed or "smoothed" with a three-point box average. The accuracy of the post-1974 temperature probes is estimated to be  $\pm 0.4^{\circ}\text{C}$ . The temperature probes used by WSU prior to 1974 are no longer available, and their accuracy is therefore uncertain. Previously published WSU temperature data have been corrected to reflect the changes in calibration and computer processing.

The WSU temperature probes move uphole at a rate of 4.6m/min and are not normally the first tool to be run in the well. A check on the WSU temperature probes was conducted to determine whether the recorded temperatures are lagged because of the rate of logging and whether the temperature distribution within the well was disturbed by the prior passage of other logging tools. The DNR Black Rock well #1 (12N/23E-16J1) was logged on successive days with DNR-SMU probe VPR1 and WSU temperature probe "A." The DNR-SMU temperature data were collected at 5m intervals after allowing time for the temperature probe to reach equilibrium. The temperature logs were in close agreement, even though the WSU probe was the fourth tool to be run in the hole that morning.

The quality of the temperature data in the Appendix ranges from excellent to poor or "disturbed." Drilling and pumping operations and intra-borehole flow often disturb the borehole temperature gradient so that it does not represent the actual geothermal gradient.

Several WSU and DNR-SMU bottom-hole temperatures (BHT's) are actually temperatures measured at a maximum logging depth which was not the bottom of

the well. When identified, these "intermediate depth temperatures" have been indicated as such in the Appendix. Obstructions in the well or an inadequate probe cable length prohibited logging to the total depth in these wells.

Actually, bottom-hole temperatures are rarely recorded from the total drilled depth of a water well. Rock and other debris normally collect at the well bottom, especially in wells previously pumped, and prohibit logging to the total depth. In addition, it is poor logging practice to let a probe come in contact with the well bottom, because the cable can become twisted and the probe can become lodged. It is possible that an error in the BHT of approximately  $+0.1^{\circ}\text{C}$  is introduced for each 3m off of the well bottom that the measurement is made, assuming that the flow is uphole and originates at the well bottom.

The quality of the USGS data is unknown, and USGS data listed as BHT's in the Appendix may, in fact, include "intermediate depth temperatures" and maximum temperatures measured in water flowing from wells during pumping tests or well development operations (Korosec, personal communication, 1982). However, the analysis of the BHT data, in a later section of this report, indicates that most of the USGS data are reliable and of good quality.

#### Calculation of Geothermal Gradients in the Yakima Region

Determination of geothermal gradients in water wells of the Yakima region and the Columbia Plateau is complicated by intra-borehole flow. The net result of the borehole flow is a distorted borehole temperature log, often assuming a step-like form, with the recorded temperature gradient being unrepresentative of the actual geothermal gradient (see Figure 23). The borehole flow effect may be less obvious at low velocities, with the borehole temperature log appearing as a "straight line" geothermal gradient.

Three options or methods have been available to past investigators in their attempts to determine accurate geothermal gradients in Columbia Plateau water wells. The first option, and the least desirable, is to disregard the data that are affected by borehole flow. The second method involves the measurement of geothermal gradients along "straight line" segments of the temperature-depth profile. This method is adequate in those wells which are not affected by borehole flow. Unfortunately, these wells are rare on the Columbia Plateau. In addition, it is not possible to assess the effect of very low velocity borehole flow in those wells that do exhibit "straight line" gradient segments. The WSU log suites occasionally include the borehole flowmeter log, but this tool is not sensitive enough to accurately detect borehole flows of less than approximately 0.03mps.

The third, and most common method, is based on the BHT and assumed land-surface temperature (LST), as shown in equation (6):

$$\text{geothermal gradient} = \frac{\text{BHT} - \text{LST}}{\text{BHD}} \quad (6)$$

where: BHT = bottom-hole temperature

LST = land surface temperature

BHD = bottom-hole depth

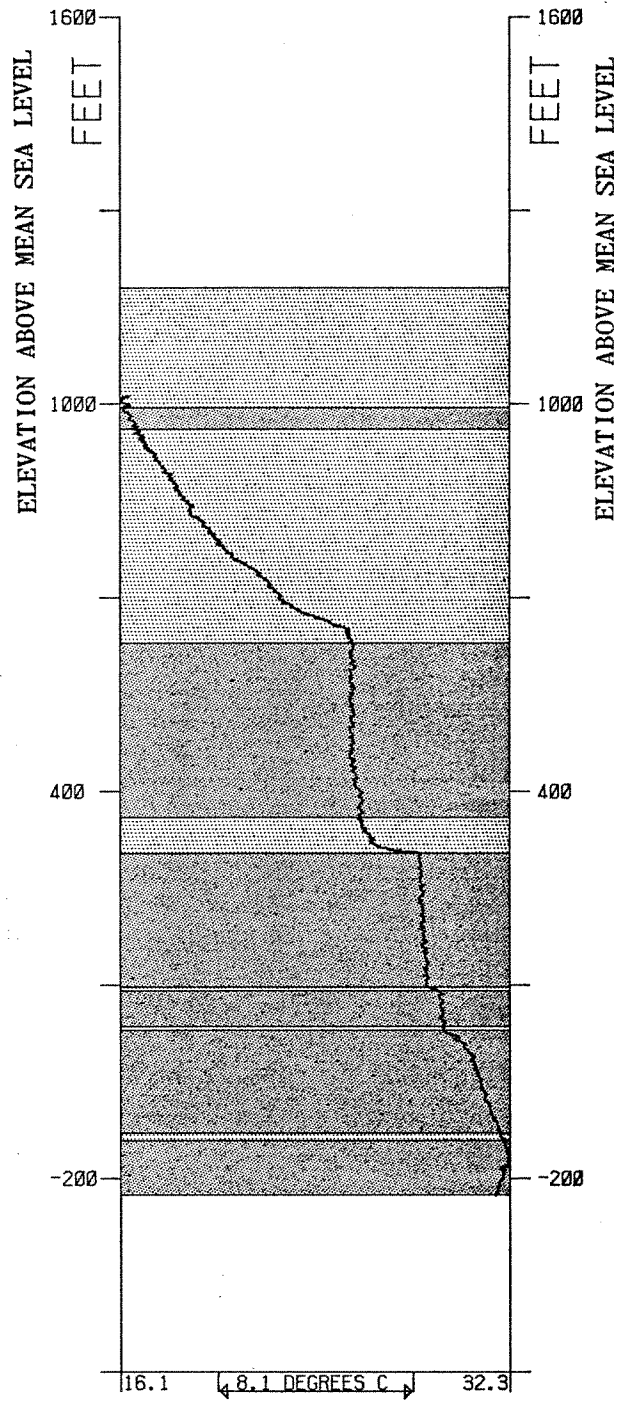


FIGURE 23 STEP-LIKE DISTORTION OF THE BOREHOLE TEMPERATURE LOG

Ground-water temperatures 10 to 20m below the land surface are often 1 to 2°C warmer than the local mean annual air temperatures (Stevens and others, 1975). This relationship has led past investigators to use the mean annual air temperature to approximate the LST in equation (6). Schuster (1980) and Korosec (1980) have assumed an LST of 12°C based upon a mean annual air temperature of 10 to 14°C over most of the Columbia Plateau.

For shallow wells, it is very important that an accurate LST be used in equation (6). The error in the geothermal gradient (as calculated by equation 6) varies according to equation (7) and is large for even small errors in the LST:

$$\text{error in the geothermal gradient} = \frac{\text{LST}_{(\text{assumed})} - \text{LST}_{(\text{actual})}}{\text{BHD}} \quad (7)$$

For example, a 1.0°C error in the assumed LST temperature results in an error of ±10°C/km in the geothermal gradient at 100m depth. This amounts to an error of approximately 25 to 30 percent for geothermal gradients typical of the Columbia Plateau. Table 8 summarizes the error involved with equation (6) caused by errors of 0.5, 1.0, and 2.0°C in the assumed LST. Although it is apparent that the error generated by assuming an incorrect LST decreases with increasing depth, this error is still significant at depths of 300m or greater, because the magnitude of the error is probably greater than the actual variation of the geothermal gradient (from one location to another) within the small areas being investigated.

Equation (6) was applied to wells in the Yakima region with very limited success, partially because variations in the LST cannot be accurately predicted. The geothermal gradients of neighboring wells calculated in such a manner often differed by more than 100 percent. More importantly, the calculated geothermal gradients and the assumed LST's failed to predict aquifer temperatures accurately or to explain the observed borehole temperature logs.

Robinette and others (1977) applied this method in the area just east of the Yakima region, selecting the LST from a contoured map of mean annual air temperature. It was noted that the calculated geothermal gradients did not fall into predictable groupings of higher or lower gradients, and their distribution was referred to as being random.

The large variation in calculated geothermal gradients from neighboring wells, both in this study and in the study by Robinette and others (1977), is caused not only by inaccurate LST's but also by unidentified "intermediate depth temperatures", BHT's affected by borehole flow, and other poor quality BHT's. A small part of the variation is caused by the fact that BHT's are rarely recorded at the total drilled depth and also by the differences that may exist between the many different temperature probes utilized for the collection of BHT data over the years.

The ability to accurately model or predict the LST of a region would, of course, greatly reduce the error involved in the calculation of shallow gradients. The LST model would have to incorporate not only the various microclimatic effects, but also, more importantly, the effect of the ground-water flow system. The effect of the ground-water flow system cannot be ignored because almost all of the temperature data have been obtained from ground-water aquifers. Microclimatic and ground-water flow system modeling is complex and well beyond the scope of this project. The combination of the LST

Table 8. Error in the Geothermal Gradient  
Resulting from Incorrect Land Surface Temperatures  
as a Function of Depth

Depth (m)	Error in Assumed Land Surface Temperature		
	0.5°C (±°C/km)	1.0°C (±°C/km)	2.0°C (±°C/km)
25	20.0	40.0	80.0
50	10.0	20.0	40.0
100	5.0	10.0	20.0
150	3.3	6.7	13.3
200	2.5	5.0	10.0
300	1.7	3.3	6.7

error, the difficulty involved in recognizing poor quality data, and the subjective bias towards the higher geothermal gradients resulting from the errors makes the method of equation (6) less than desirable for shallow, low-temperature geothermal resource assessment.

A different approach was developed for this project to decrease the error generated by the calculation of the geothermal gradient and to increase the size of the "usable" BHT data base. This method utilizes a least squares linear regression analysis of the relationship between the BHT and the "bottom-hole depth" (BHD) of two or more water wells. Ideally, the BHT's of wells belonging to a particular well data group (WDG) would all be affected, in a similar manner, by the factors that influence the geothermal gradients of the area in which the water wells are located. The equation relating the BHT's and BHD's in such an area would accurately define the geothermal gradient and the projected LST of an area. This equation should accurately predict the aquifer temperature for the depth interval considered in the regression analysis.

The BHT vs. BHD linear regression analysis has several advantages over the previously reviewed calculation methods of geothermal gradients. Uphole flow within the water well, which often severely distorts the borehole temperature gradient, would not be expected to alter the BHT. The BHT would also be expected to be disturbed the least, as compared with a borehole temperature log, by drilling and pumping operations. This is significant, since most of the temperature data from Columbia Plateau water wells are collected during the short time period between the termination of drilling operations and pump installation or during periods when a pump has been pulled from a well for maintenance.

Downhole flow within the borehole can affect the BHT, but, in many cases, the deepest portion of the water well appears to be isolated from the flow. A rapid temperature increase is often noted in the bottom of water wells isolated from downhole flow. A BHT affected by downhole flow can be identified on a plot of BHT vs. BHD in the presence of unaffected BHT's since the affected BHT will lie below the line defining the WDG predicted temperature curve. In a similar fashion, poor quality data can be identified because of their "lack of fit" to the rest of the BHT's belonging the WDG. Incorrectly identified BHT's that were actually recorded at some intermediate depth will plot above or below the line of the WDG predicted temperature curve depending on whether the borehole flow direction is up or down, respectively.

An additional advantage of the BHT vs. BHD linear regression analysis is that the error generated by assuming an incorrect LST in equation (6) is eliminated from the calculation of the geothermal gradient. Although the error introduced by assuming an inaccurate LST in equation (6) decreases with increasing BHD, the error will still exist even after additional BHT's are sampled within the region. The opposite is true in the case of the BHT vs. BHD analysis. Additional sampling of BHT's will result in decreased error in the BHT vs. BHD gradient calculation process.

Errors in the geothermal data calculated by the BHT vs. BHD linear regression analysis can result if most of the BHT's of a particular WDG are of poor quality and/or are affected by downhole flow. This problem can be identified by the scatter or "randomness" of the BHT-BHD data and by the poor fit of the regression equation to the data. This scatter of the BHT-BHD data results from the unlikely chance that the data are subject to a constant error from one location to another within the WDG.

Errors in the geothermal data calculated by the BHT vs. BHD linear regression analysis may also result from departures from the ideal situation

in which all the BHT's of a particular WDG are similarly affected by the factors controlling the geothermal regime of the region. The magnitude of the effect of such factors as the LST and ground-water flow can be assumed to decrease rapidly with depth and to be nearly constant over small geographic areas and depth intervals. The heat flow also should be nearly constant within the small geographic areas and depth intervals encompassed by a WDG of the Yakima region. The vertical and horizontal variations of thermal conductivity, even in small areas, cannot be easily predicted and may cause errors. In regions where there is a large contrast in thermal conductivity, the BHT vs. BHD plot may actually help define the variation in thermal conductivity.

The linear regression analysis also may introduce errors that result from an uneven distribution of data, and an "eyeball" fit of the line of the WDG predicted temperature curve may be more accurate in some cases. The linear regression analysis was utilized in this report in order to eliminate this investigator's bias towards the recognition of higher than normal geothermal gradients.

The errors involved with the BHT vs. BHD linear regression analysis can be assumed to decrease as the geographic size and the depth interval decreases and as the number of available BHT's increases. The geographic area encompassed by a WDG and the depth interval that yields an accurate definition of the geothermal regime will be limited by the magnitude of the rate of change of the geothermal gradient within the WDG.

#### Geothermal Gradients in the Yakima Region

Bottom-hole temperatures of water wells in the Yakima region were separated into 14 WDG's based on four criteria: geographic proximity of the BHT data, similar land slope azimuth and dip in the area, position of the WDG within the conceptualized regional ground-water flow system, and BHD's ranging from over 50 to less than 700m.

Geographic proximity was used as a standard on the assumption that the geothermal regime within small areas and depth intervals would be nearly constant. Land slope azimuth and dip were used in an attempt to segregate BHT's into WDG's that are similarly affected by LST and ground-water flow. Position within the conceptualized regional ground-water flow system occurred in most cases by meeting the first two criteria. The fourth criterion of BHD's less than 700m was normally met by necessity because irrigation wells in the region rarely are drilled beyond that depth. BHT's from BHD's of less than 50m were excluded from the analysis because of the transient nature of the geothermal gradient caused by seasonal and other near-surface effects. The extent to which a particular WDG fulfills the first three criteria was controlled largely by the availability or concentration of BHT data.

One additional WDG was created on the basis of a single criterion, a BHD greater than 700m. This WDG was formed in order to investigate the possibility that a single regression equation could accurately define the geothermal regime at depths greater than 700m in a large geographic region.

Plots of BHT's vs. BHD's for WDG 1 through WDG 14 are shown in Figures 24 through 37. The results of the least squares regression analyses are summarized in Table 9. Locations, geothermal gradients, projected LST's, and depths to the 20°C isotherm for the WDG's are shown in Plate 2. Geothermal gradients for the shallow (less than 700m deep) WDG range from 24.9 to 52.5°C/km. The projected LST's range from 10.6 to 14°C. The depth to the 20°C isotherm ranges from 142 to 346m.



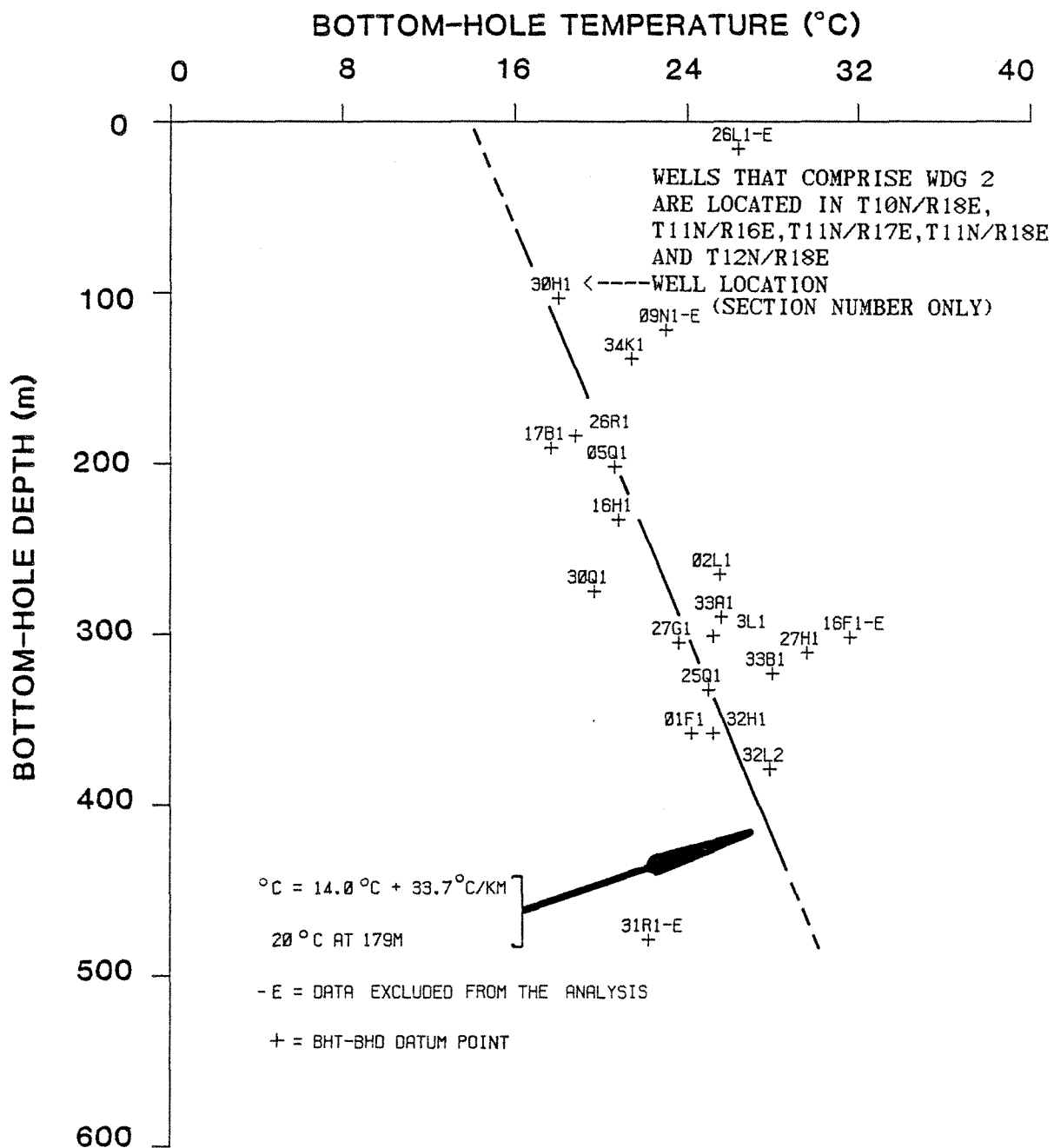


FIGURE 25 PLOT OF BOTTOM-HOLE TEMPERATURE VS. BOTTOM-HOLE DEPTH FOR WELL DATA GROUP 2

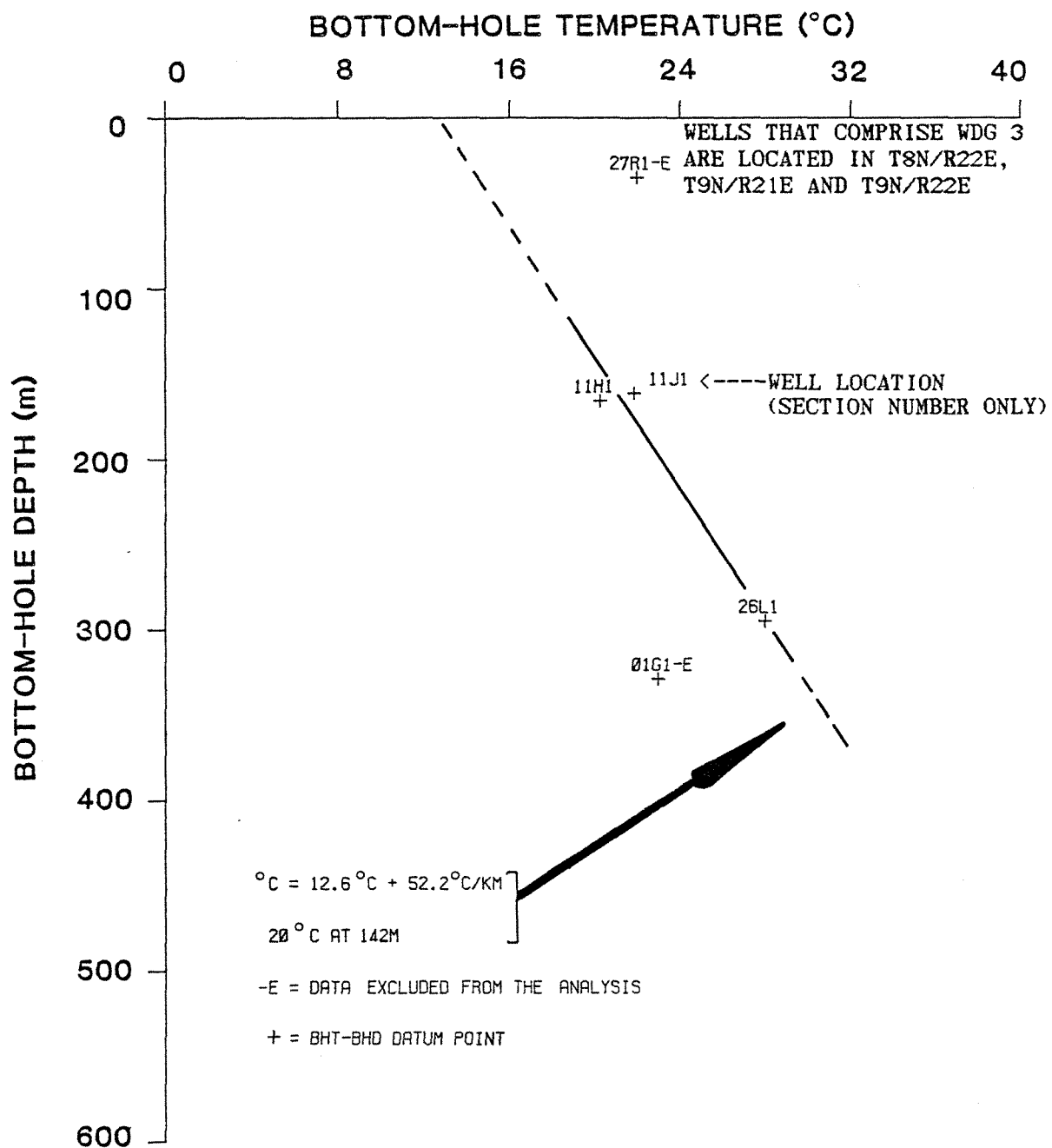


FIGURE 26 PLOT OF BOTTOM-HOLE TEMPERATURE VS. BOTTOM-HOLE DEPTH FOR WELL DATA GROUP 3

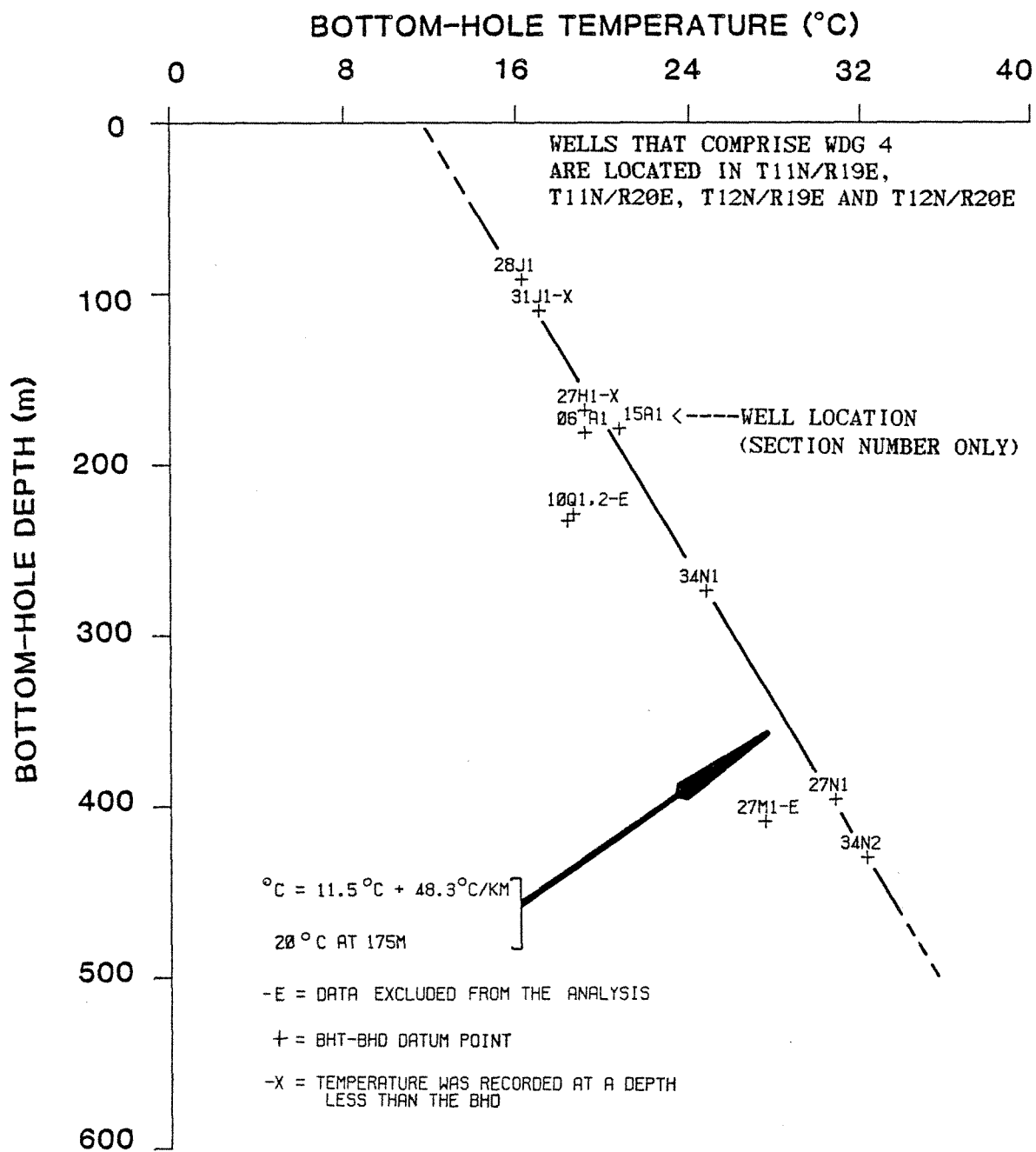
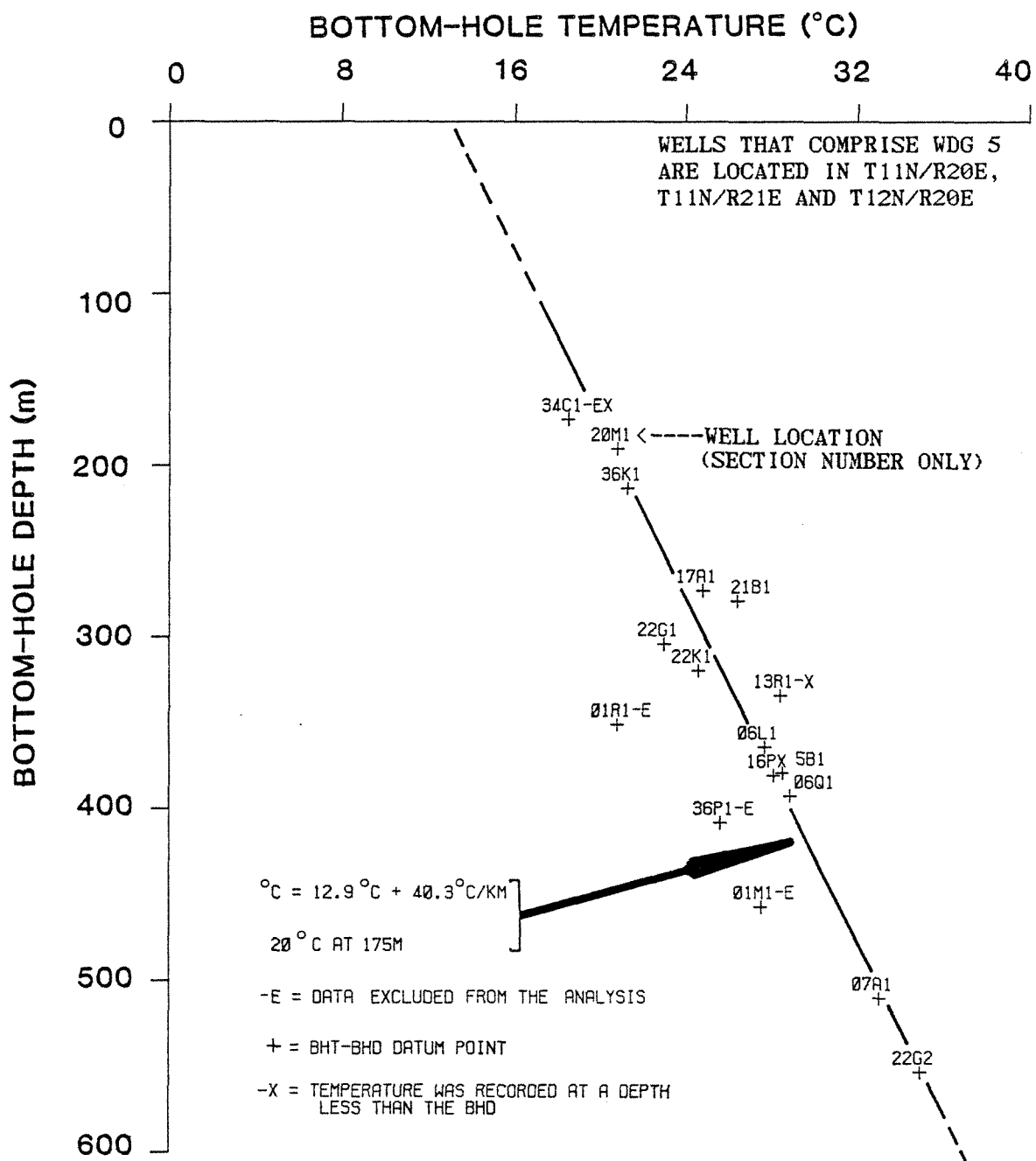


FIGURE 27

PLOT OF BOTTOM-HOLE TEMPERATURE VS.  
BOTTOM-HOLE DEPTH FOR WELL DATA GROUP 4



**FIGURE 28 PLOT OF BOTTOM-HOLE TEMPERATURE VS. BOTTOM-HOLE DEPTH FOR WELL DATA GROUP 5**

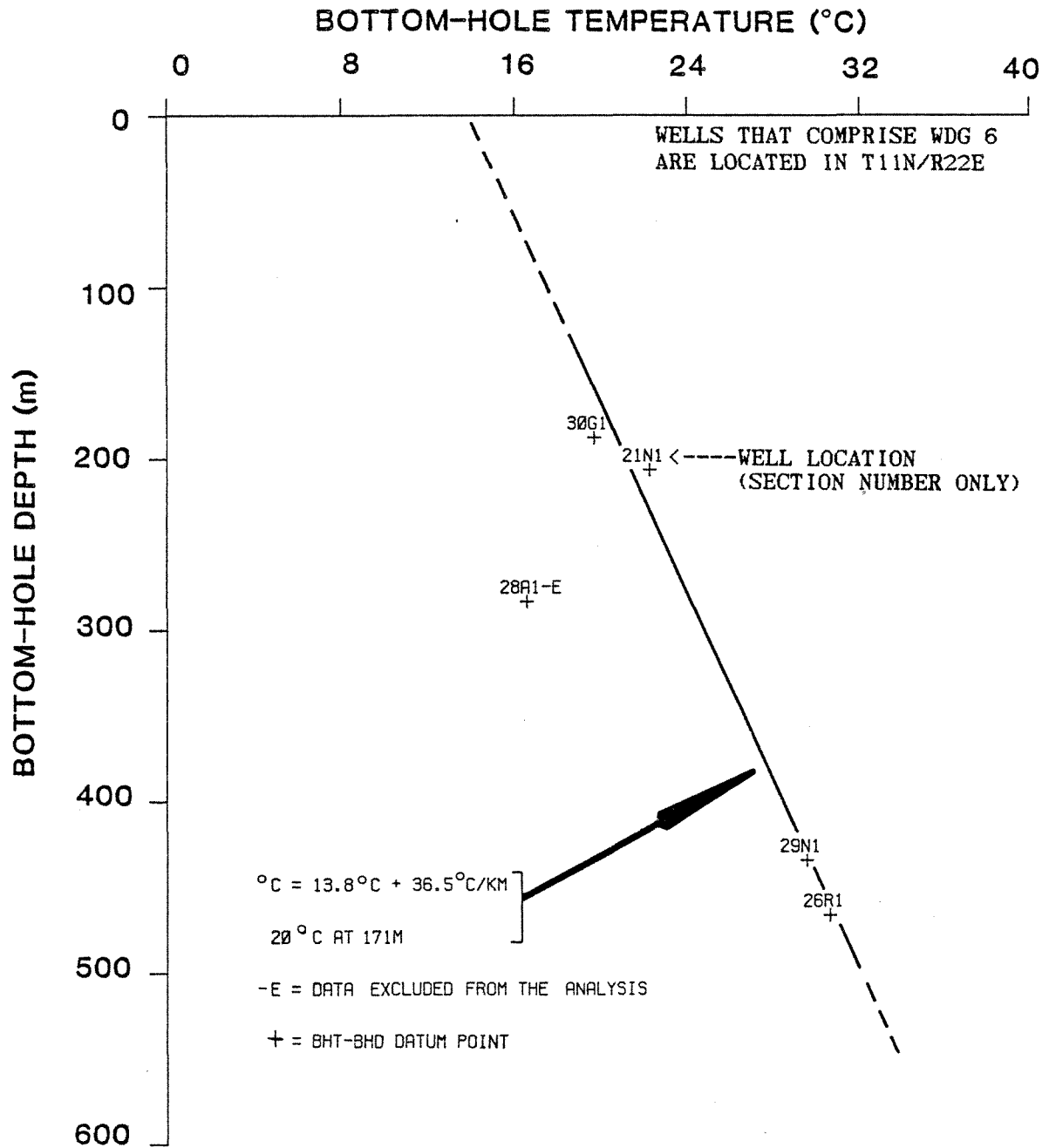
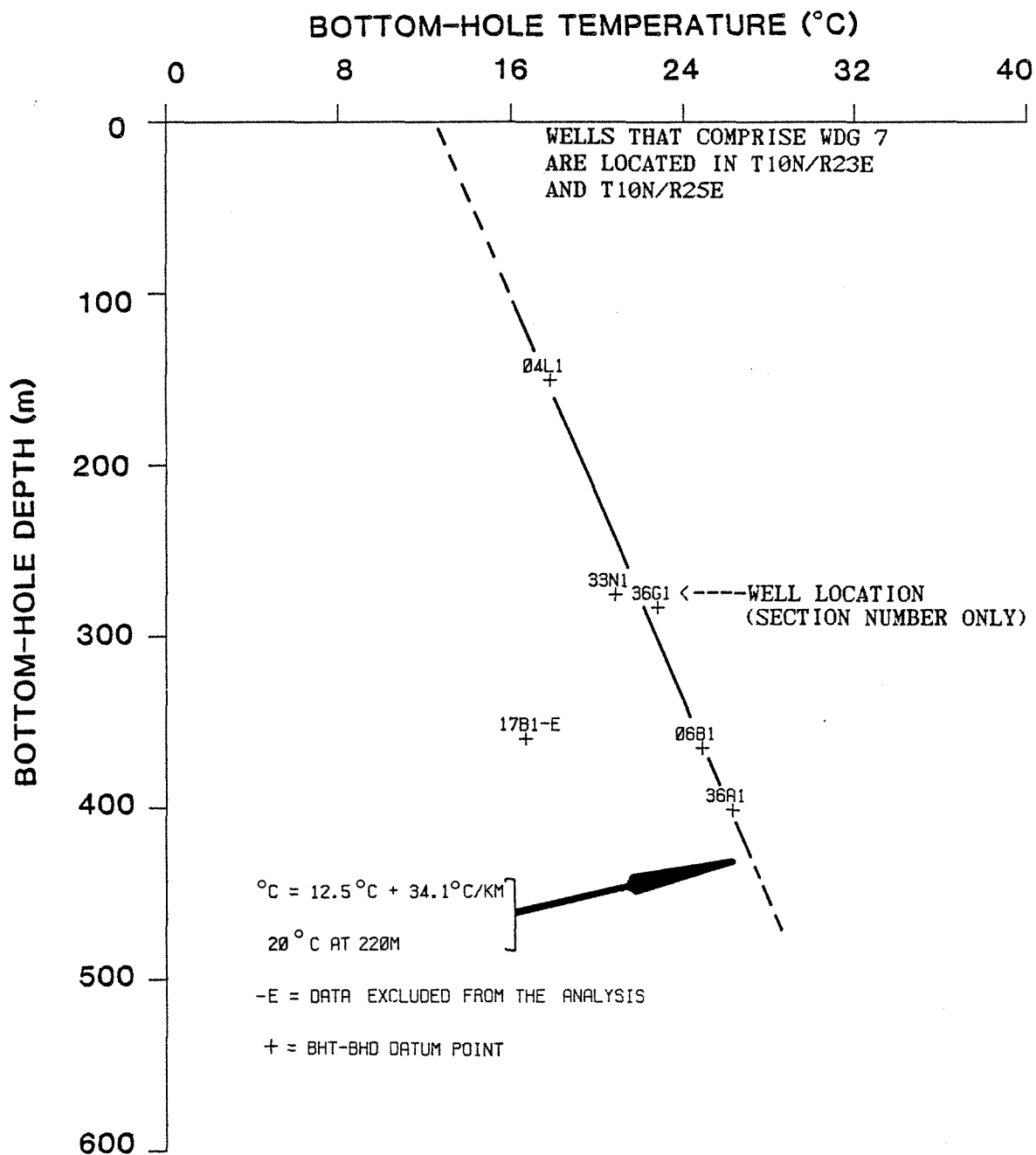


FIGURE 29 PLOT OF BOTTOM-HOLE TEMPERATURE VS. BOTTOM-HOLE DEPTH FOR WELL DATA GROUP 6



**FIGURE 30** PLOT OF BOTTOM-HOLE TEMPERATURE VS. BOTTOM-HOLE DEPTH FOR WELL DATA GROUP 7

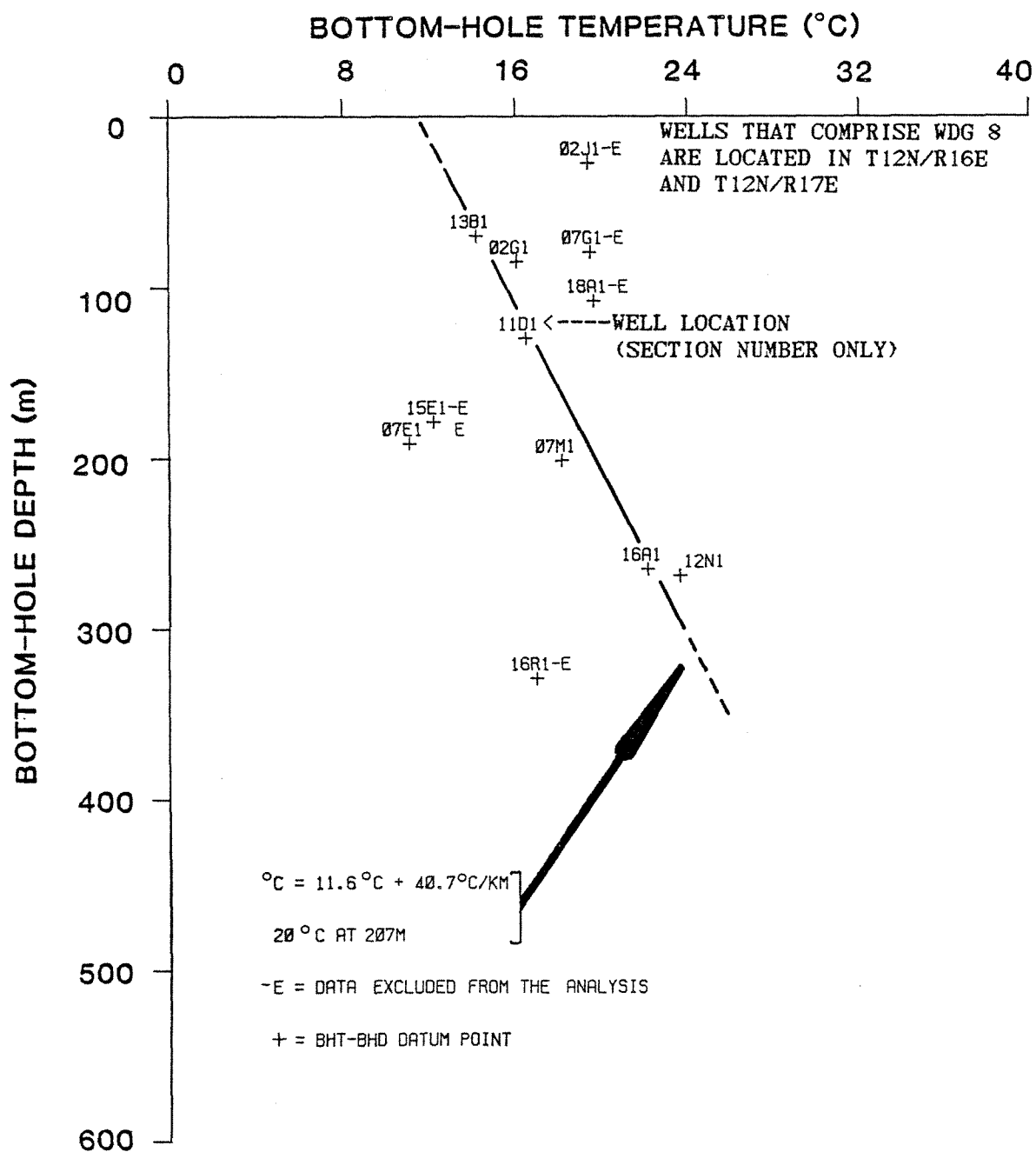
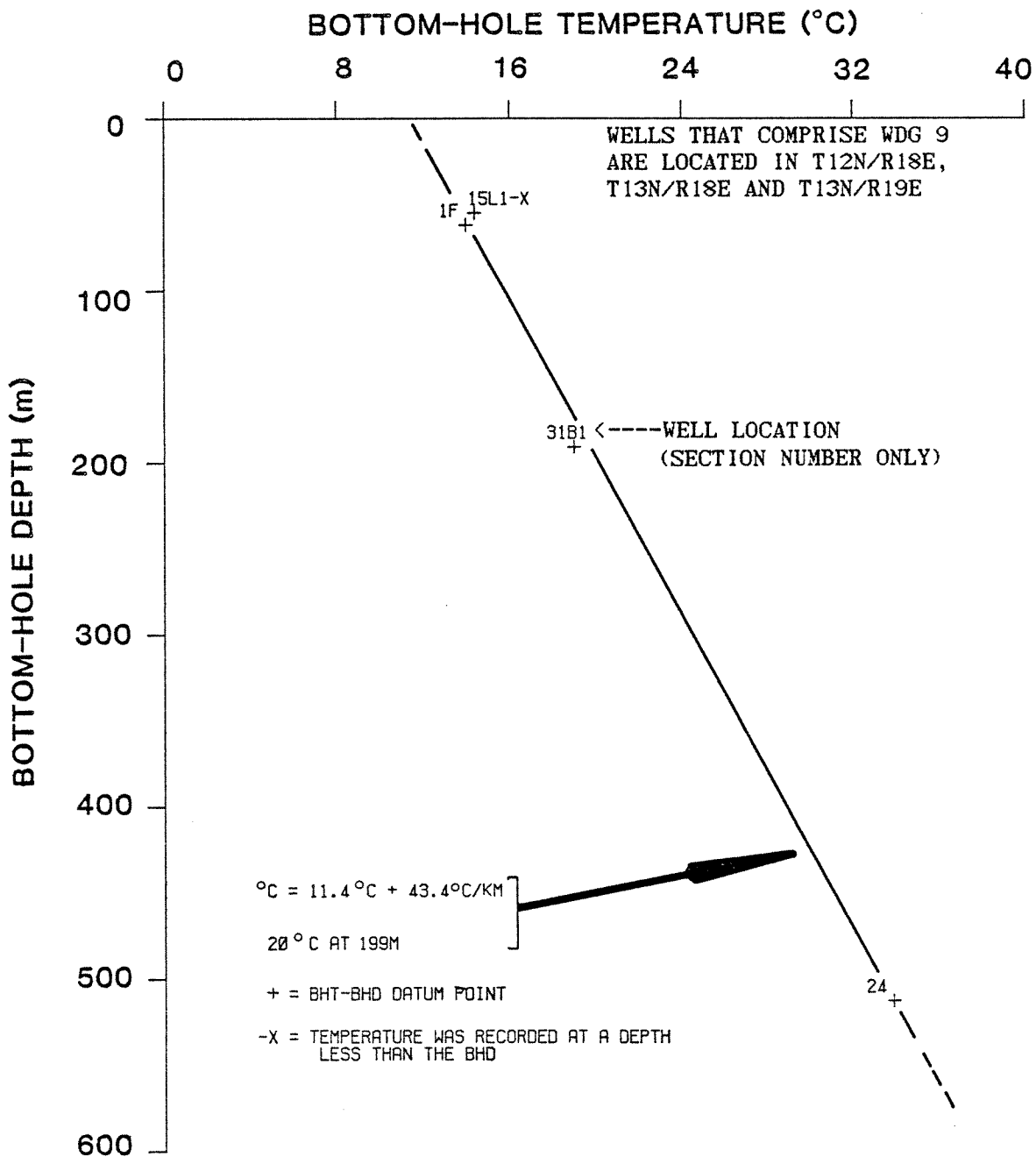
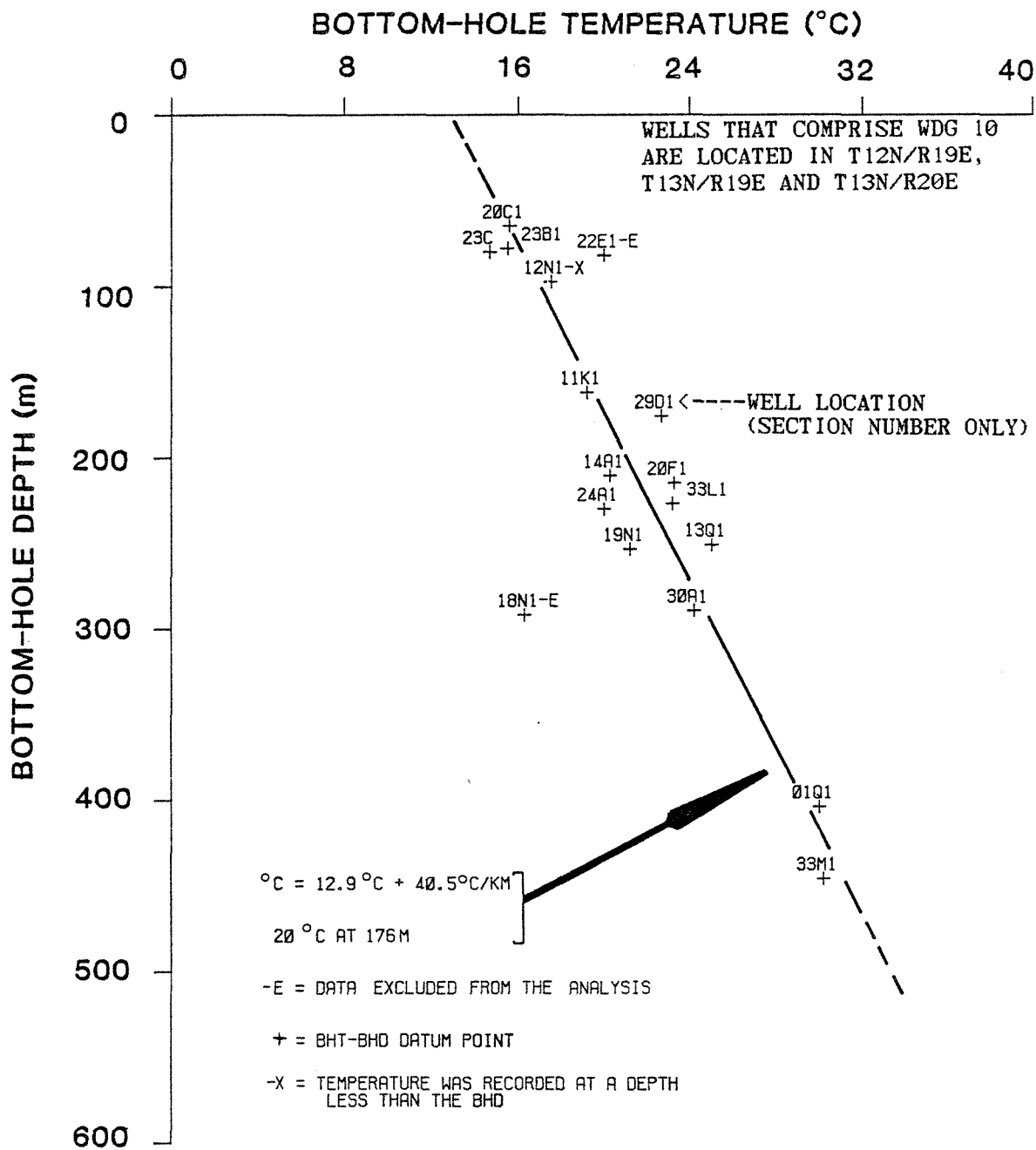


FIGURE 31 PLOT OF BOTTOM-HOLE TEMPERATURE VS. BOTTOM-HOLE DEPTH FOR WELL DATA GROUP 8



**FIGURE 32 PLOT OF BOTTOM-HOLE TEMPERATURE VS. BOTTOM-HOLE DEPTH FOR WELL DATA GROUP 9**



**FIGURE 33 PLOT OF BOTTOM-HOLE TEMPERATURE VS. BOTTOM-HOLE DEPTH FOR WELL DATA GROUP 10**

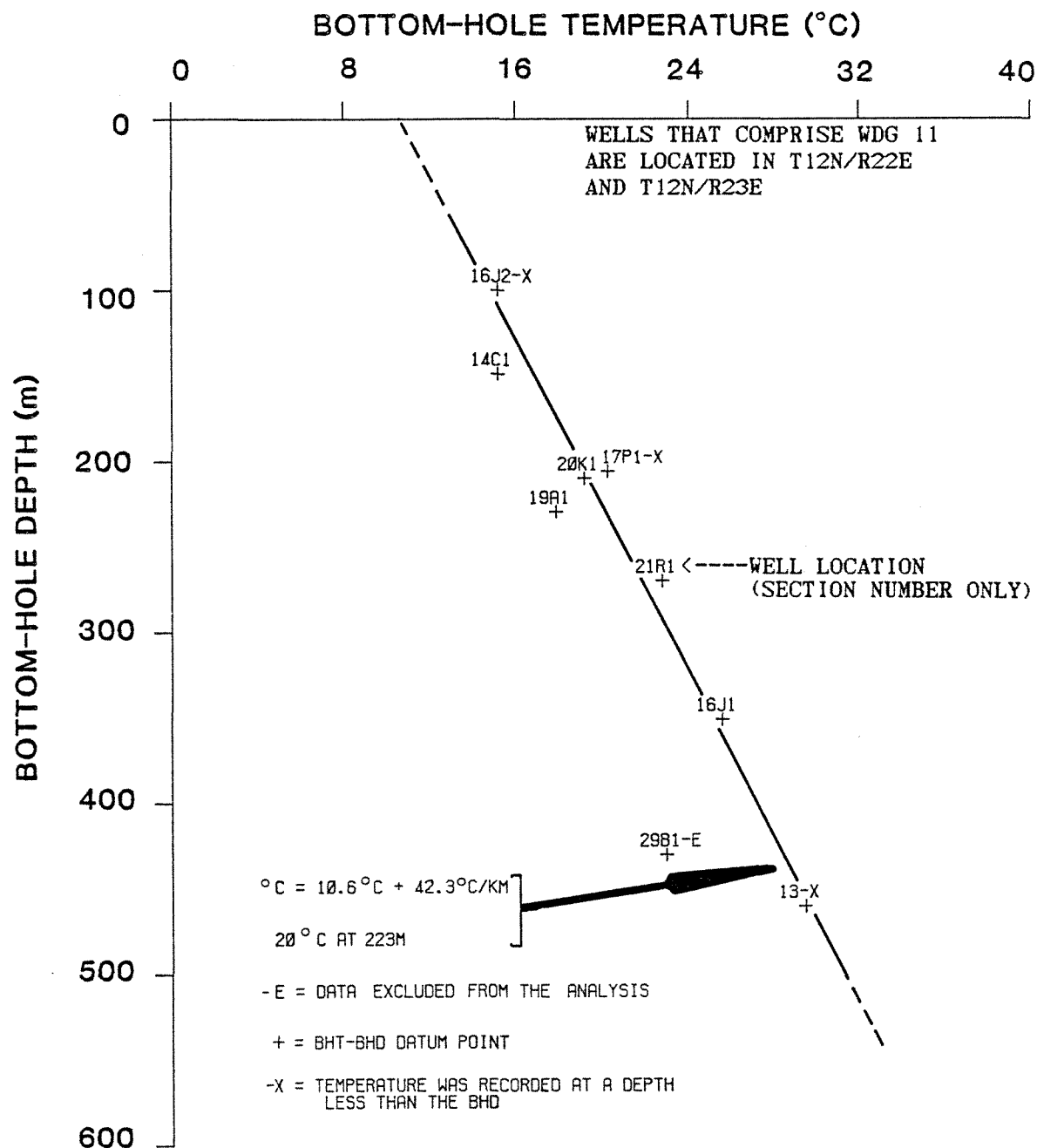


**FIGURE 34 PLOT OF BOTTOM-HOLE TEMPERATURE VS. BOTTOM-HOLE DEPTH FOR WELL DATA GROUP 11**

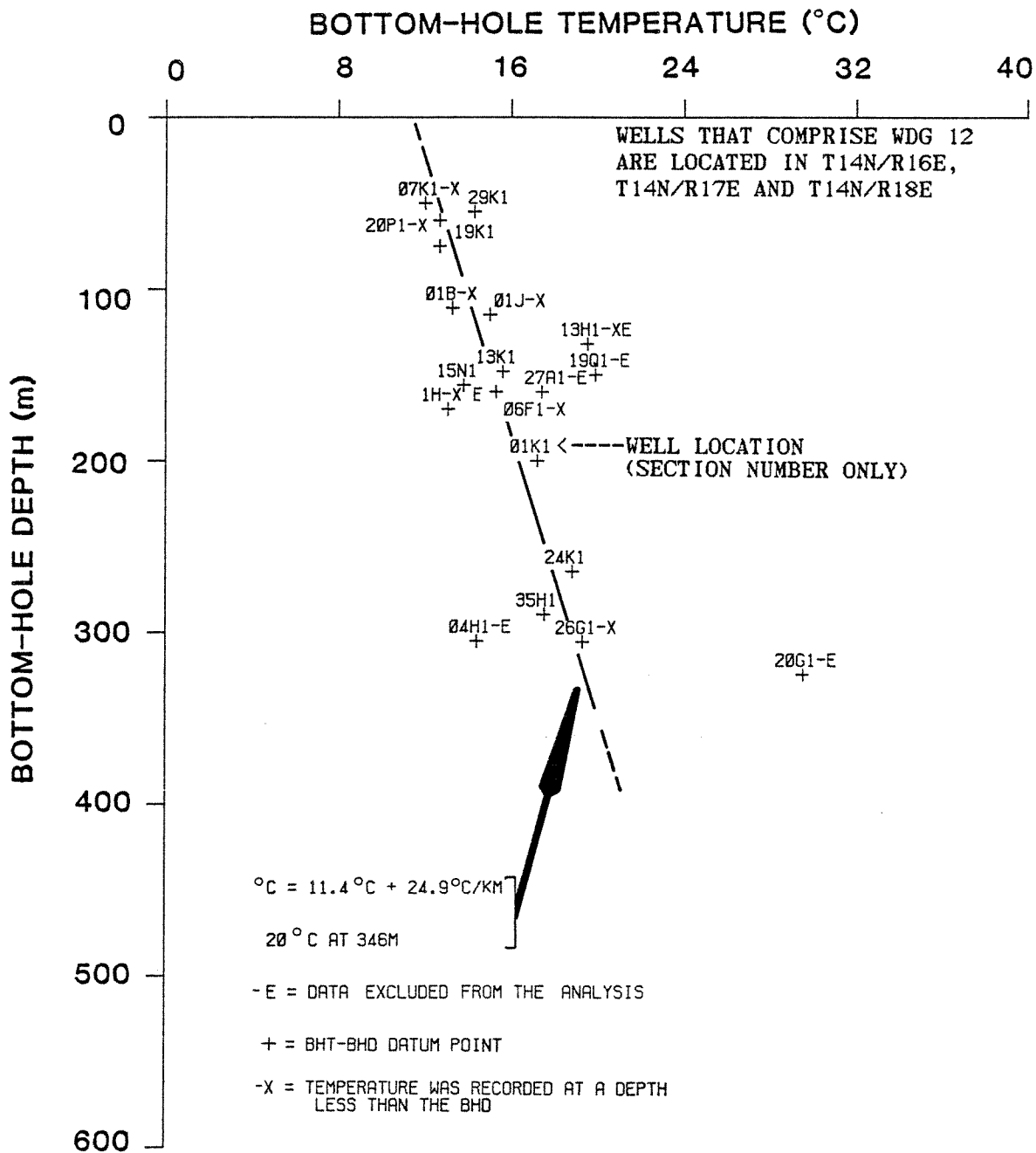


**FIGURE 35 PLOT OF BOTTOM-HOLE TEMPERATURE VS. BOTTOM-HOLE DEPTH FOR WELL DATA GROUP 12**

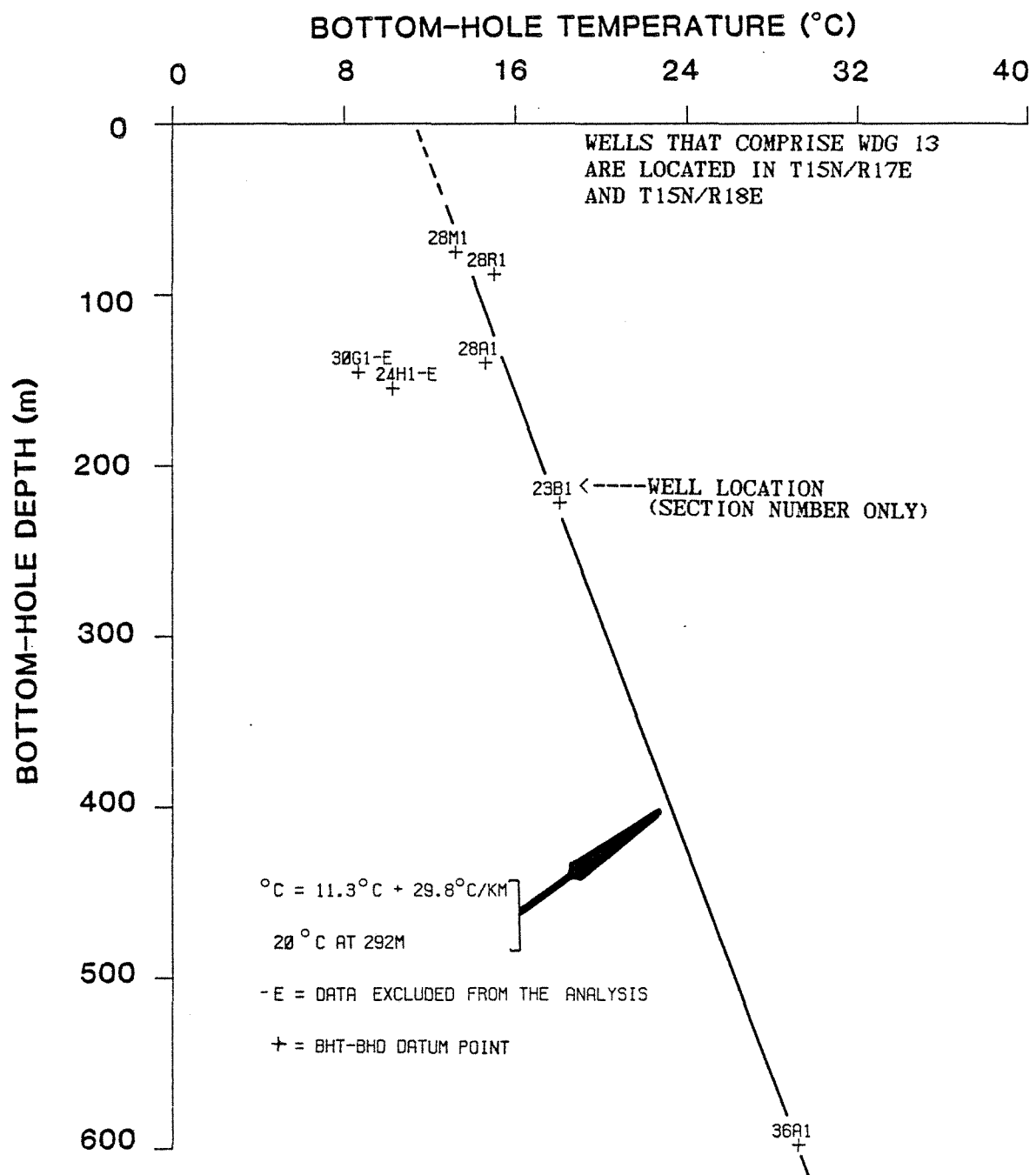


FIGURE 36 PLOT OF BOTTOM-HOLE TEMPERATURE VS. BOTTOM-HOLE DEPTH FOR WELL DATA GROUP 13

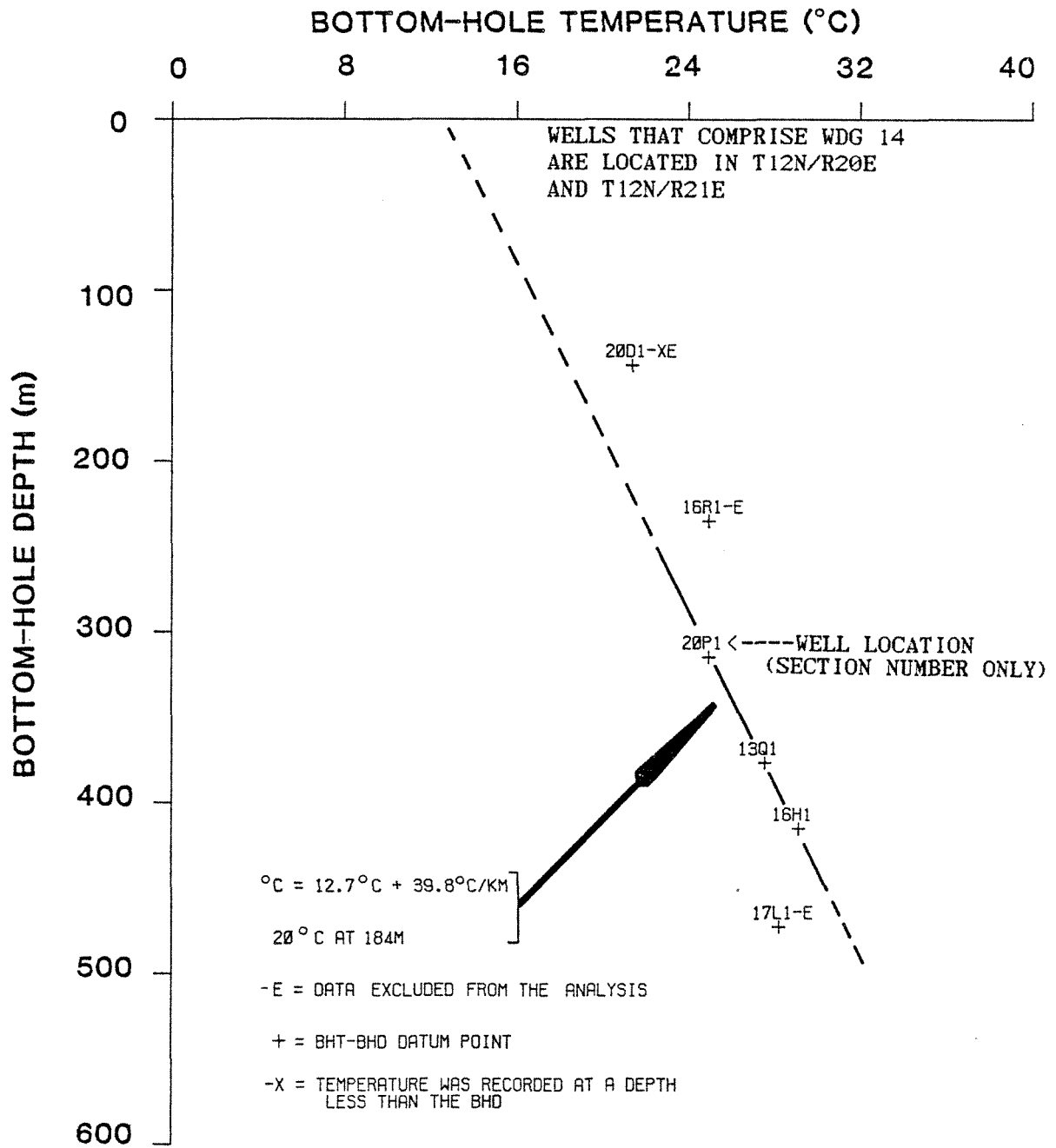


FIGURE 37 PLOT OF BOTTOM-HOLE TEMPERATURE VS. BOTTOM-HOLE DEPTH FOR WELL DATA GROUP 14

Table 9. Quality Designations, Geothermal Gradients, Land Surface Temperatures, and Depths to 20°C Isotherm of Well Data Groups

Well Data Group	Quality Designation <sup>1</sup>	Geothermal Gradient (°C/km)	Land Surface Temperature (°C)	Depth to 20°C Isotherm (m)
1	A	38.7	11.8	212
2	C	33.7	14.0	179
3	C	52.2	12.6	142
4	A	48.3	11.5	175
5	A	40.3	12.9	175
6	A	36.5	13.8	171
7	A	34.1	12.5	220
8	B	40.7	11.6	207
9	B	43.4	11.4	199
10	A	40.5	12.9	176
11	A	42.3	10.6	223
12	C	24.9	11.4	346
13	A	29.8	11.3	292
14	B	39.8	12.7	184

<sup>1</sup>a subjective assessment of the reliability of the predicted information, with "A" designating the highest quality

Figures 24 through 37 indicate an excellent correlation between the BHT's and BHD's of the water wells grouped within the 14 WDG's. The accuracy of the geothermal information provided by this analysis increases as the density of the BHT data increases and/or as the area of the WDG decreases. For example, the information from WDG 3 (Figure 26), where only three BHT's are available, should be considered less reliable than information from WDG 4 (Figure 27), where eight BHT's are available from a smaller region. Likewise, the information from WDG 11 (Figure 34) should be considered more reliable than information from WDG 2 (Figure 25) because the data of WDG 11 and the regression equation fit better or show less scatter. A subjective quality designation has been assigned to the different WDG's to provide this investigator's assessment of the reliability of the information. The letters "A," "B," and "C" have been assigned to the WDG's, with "A" designating the highest quality. Quality designations are given in Table 9.

To check the accuracy of the individual WDG's, an analysis of the relationship between the predicted geothermal data and the actual borehole temperature logs was conducted. Borehole temperature logs from water wells of WDG's 4, 5, 6, 8, 10, 11, 12, and 14 were plotted along with the WDG temperature curves predicted by the BHT vs. BHD regression analysis. The combination borehole temperature logs-WDG predicted temperature curves are shown in Figures 38 through 53. These plots indicate that, in most cases, the predicted geothermal data can be used not only to predict aquifer temperatures but also to determine borehole flow direction (uphole or downhole flow).

The direction of borehole flow, interpretation of the flowmeter log, and pump test temperatures, if available, are noted in each plot of the combination borehole temperature log-WDG predicted temperature curve (Figures 38 through 53). A borehole temperature log that lies to the right of the WDG predicted temperature curve indicates uphole flow, whereas the opposite would be observed in the case of downhole flow.

The flowmeter probes used by WSU normally will not detect a borehole flow velocity of less than approximately 0.03mps. This insensitivity leads to a flowmeter log interpretation, when available, of "no flow" for most of the wells for which temperature logs are shown in Figures 38 through 53. This occurs despite the fact that most of the temperature logs are obviously disturbed by borehole flow. A borehole flow velocity of 0.03mps would, of course, be expected to severely distort the borehole temperature gradient. Hence, the interpretation of "no flow" as noted in Figures 38 through 53 is meant to serve only as a guide to the actual borehole flow velocity.

The location of points of influx and efflux of water are indicated by a change in the borehole temperature gradient. Figures 38 through 53 indicate that the intra-borehole flow originates at or near a basalt flow contact in many of the wells that were investigated. In addition, it is apparent that the flow of water occurs not only in the open borehole but also within the annulus between the casing and borehole in many of the wells shown in Figures 38 through 53.

The direction of the intra-borehole flow and the aquifer from which the flow originates, as indicated by Figures 38 through 53, are noted in Plate 2. In those wells for which a flow direction could be determined, the intra-borehole flow that begins in the sedimentary aquifer is in a downward direction in almost every instance. Intra-borehole flow which begins in the basalt aquifer was found to move in both the upward and downward directions. The complexity of the regional ground-water flow system is reflected in the fact that opposite flow directions are found in neighboring wells and within a single well.

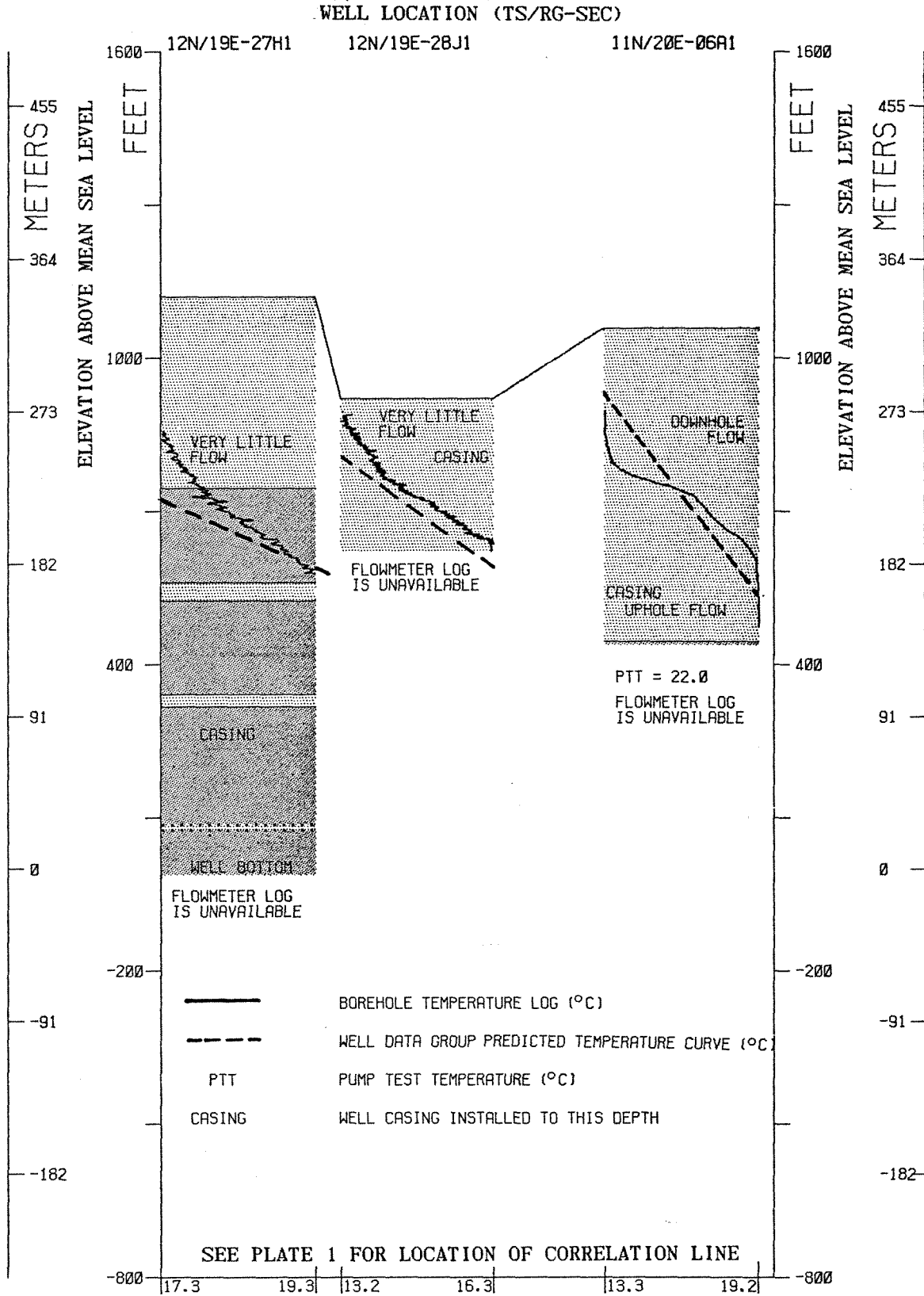


**FIGURE 38 BOREHOLE TEMPERATURE LOGS AND WELL DATA GROUP PREDICTED TEMPERATURE CURVES - LINE 1**







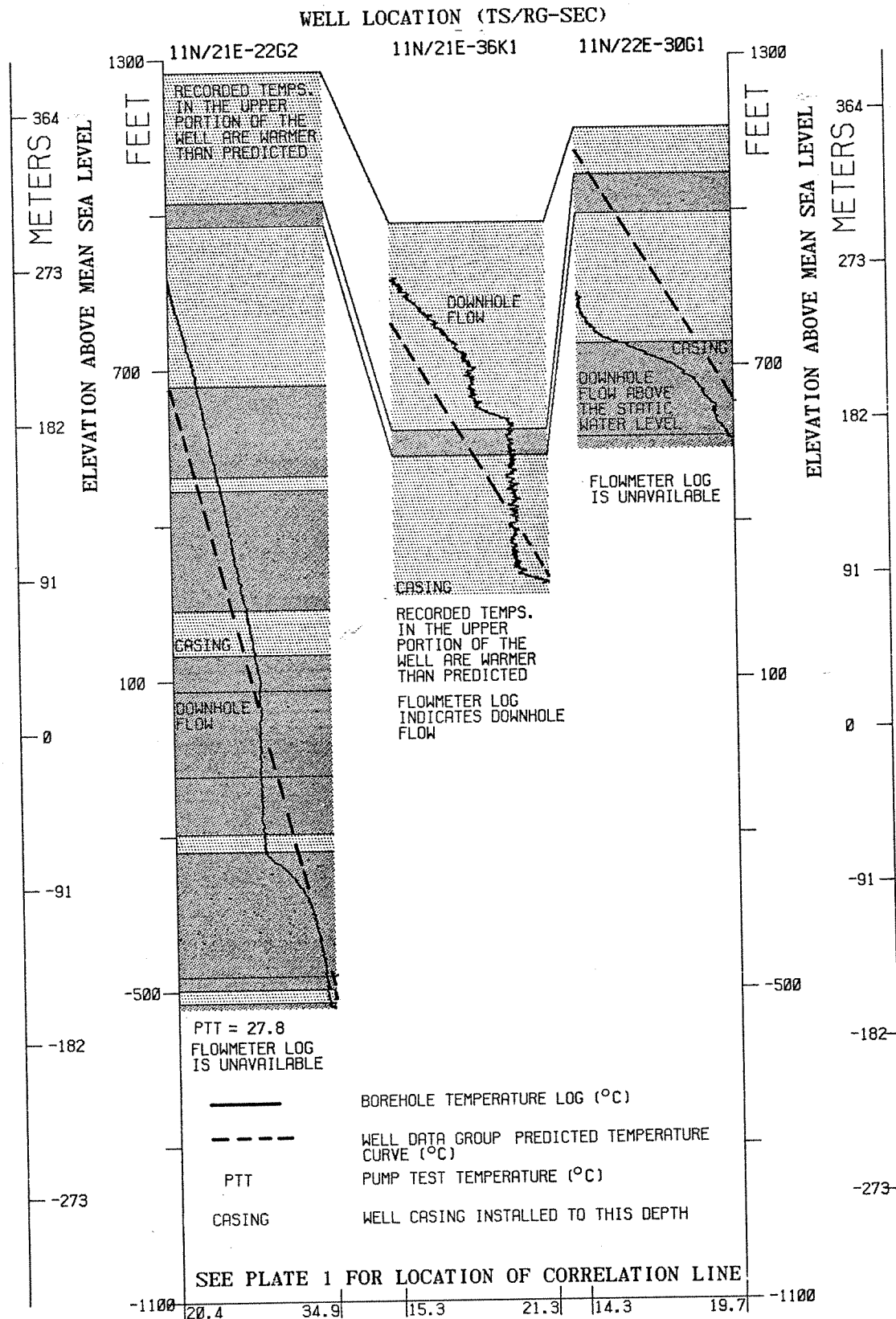


**FIGURE 42 BOREHOLE TEMPERATURE LOGS AND WELL DATA GROUP PREDICTED TEMPERATURE CURVES - LINE 5**

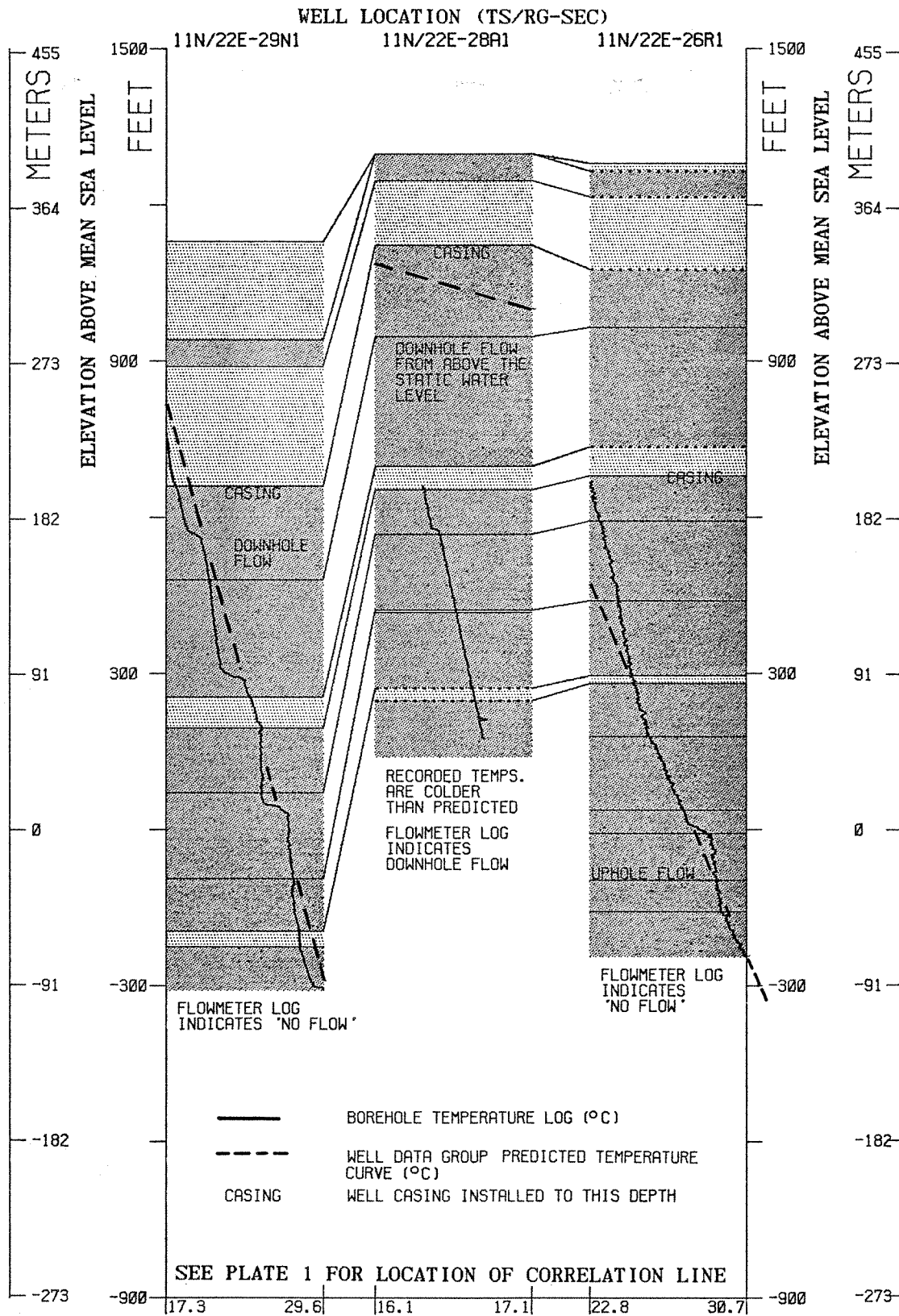


**FIGURE 43 BOREHOLE TEMPERATURE LOGS AND WELL DATA GROUP PREDICTED TEMPERATURE CURVES - LINE 6**





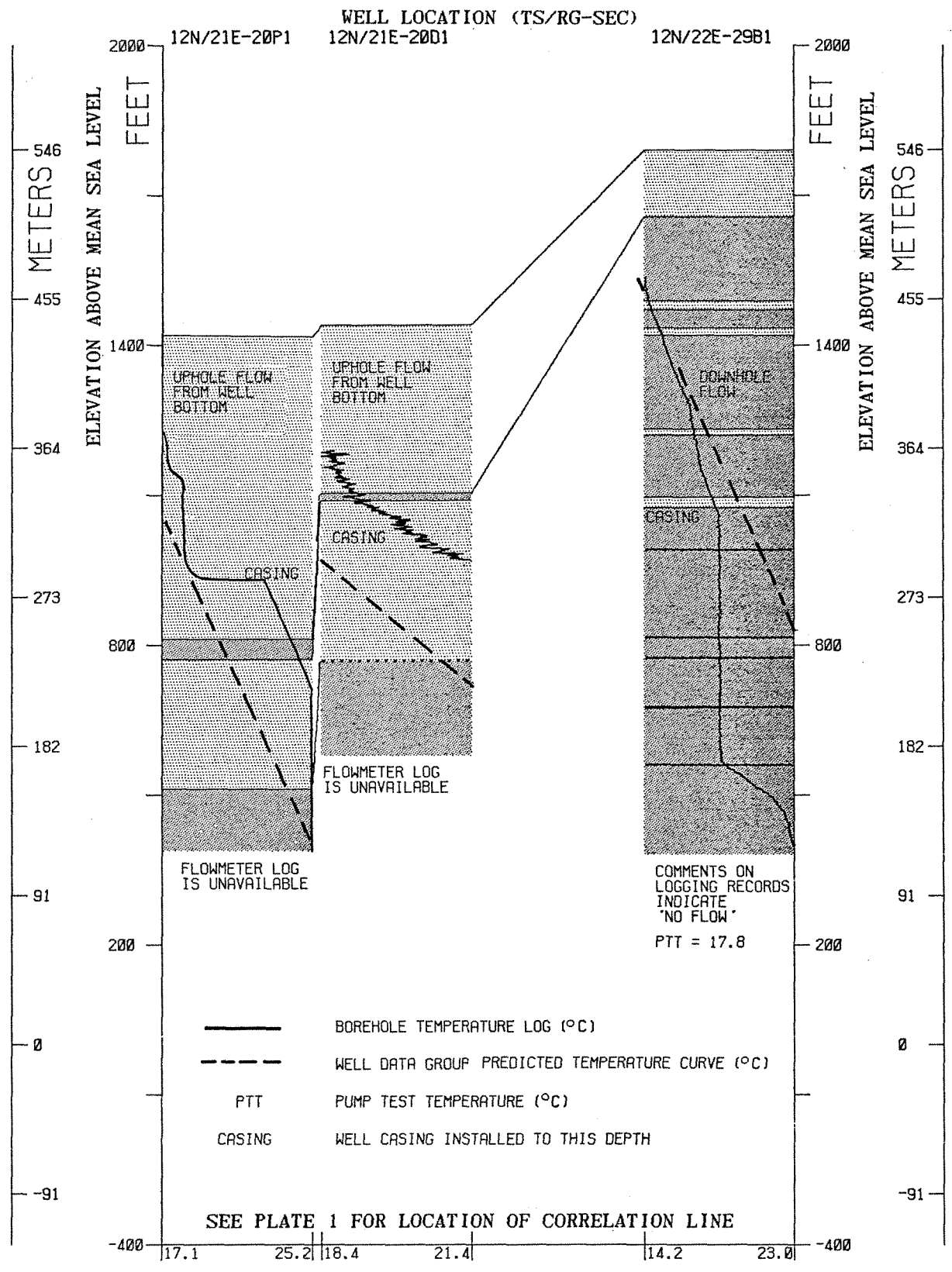


**FIGURE 46 BOREHOLE TEMPERATURE LOGS AND WELL DATA GROUP PREDICTED TEMPERATURE CURVES - LINE 9**

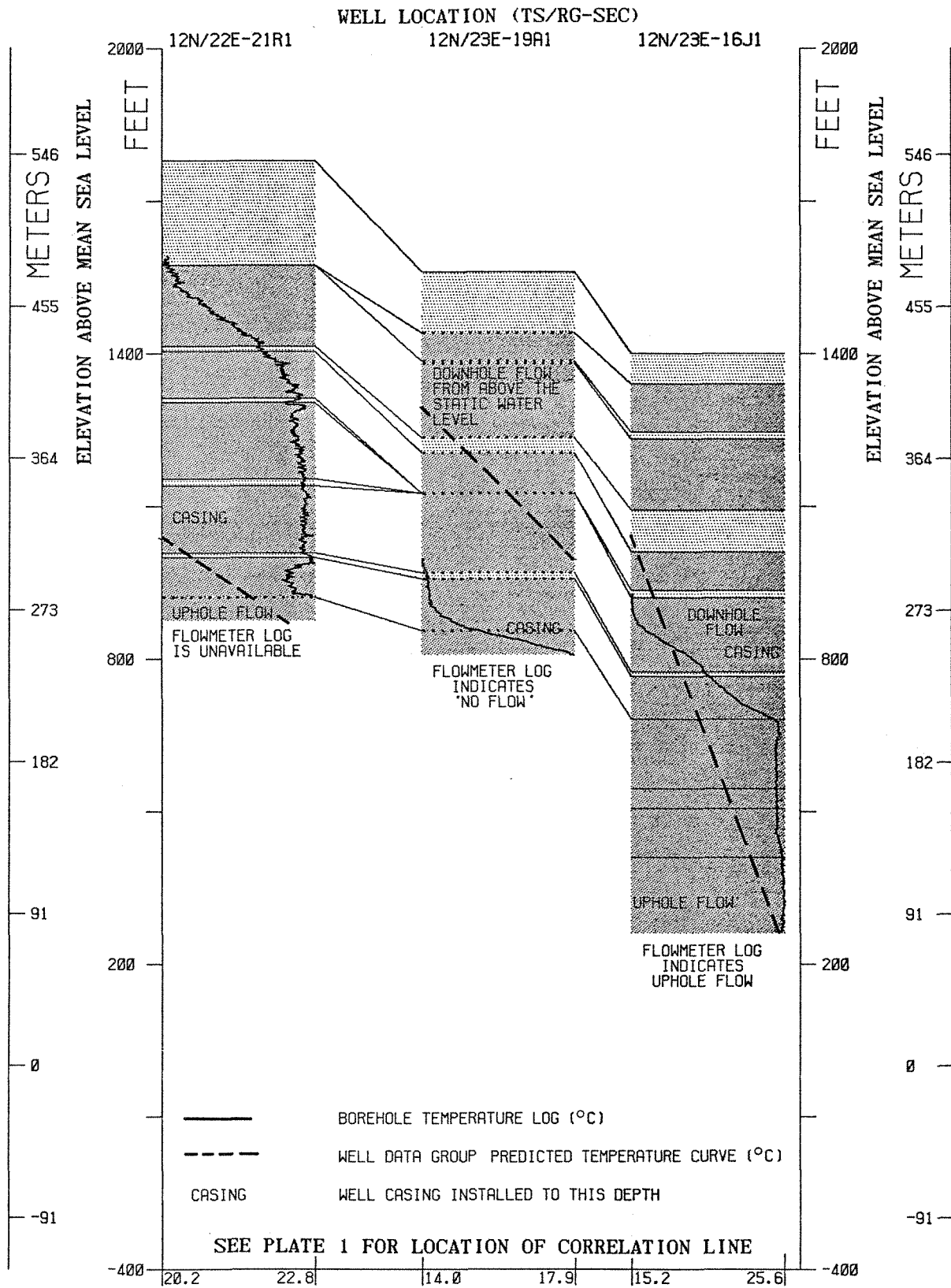


**FIGURE 47 BOREHOLE TEMPERATURE LOGS AND WELL DATA GROUP PREDICTED TEMPERATURE CURVES - LINE 10**

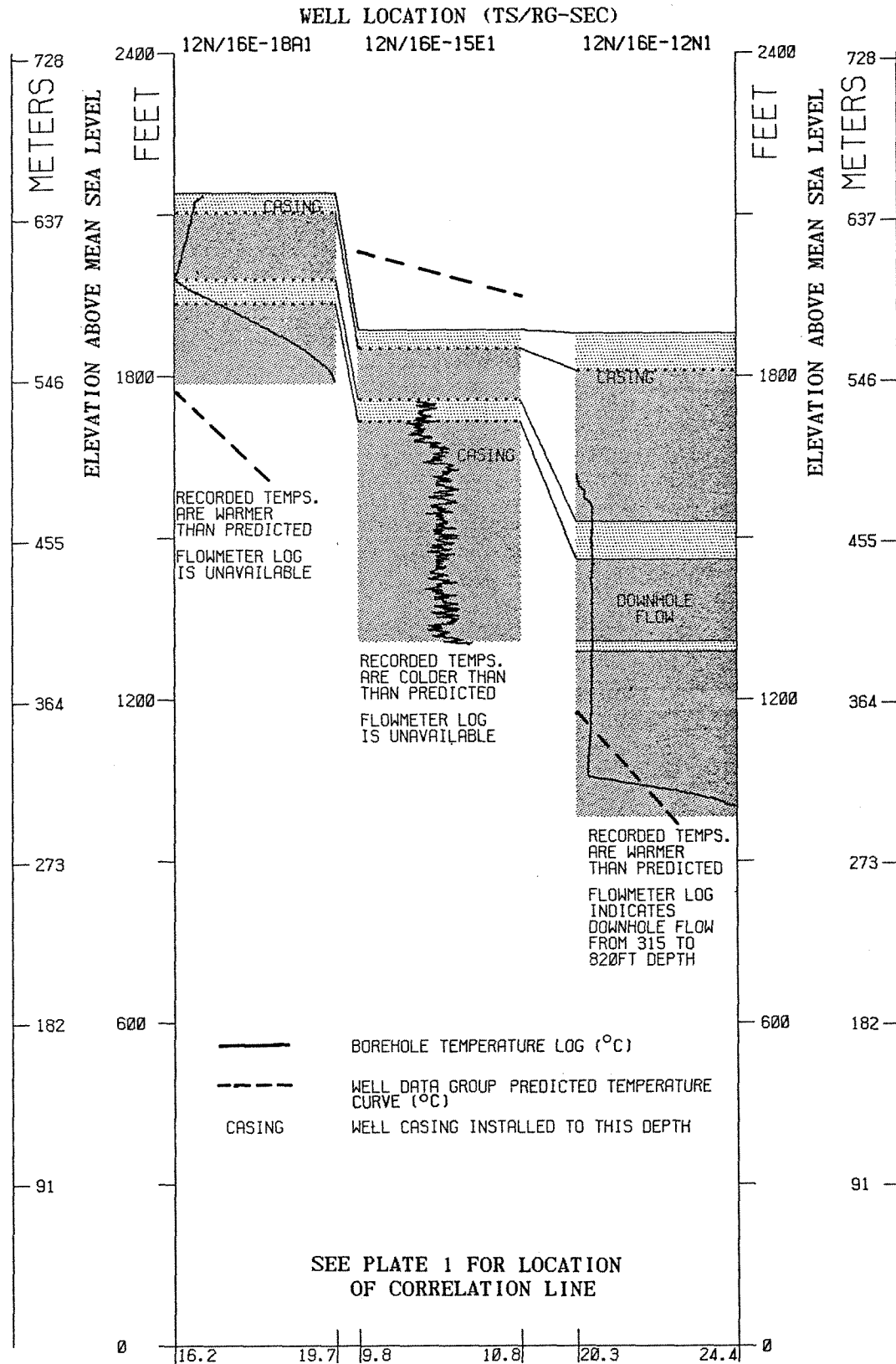
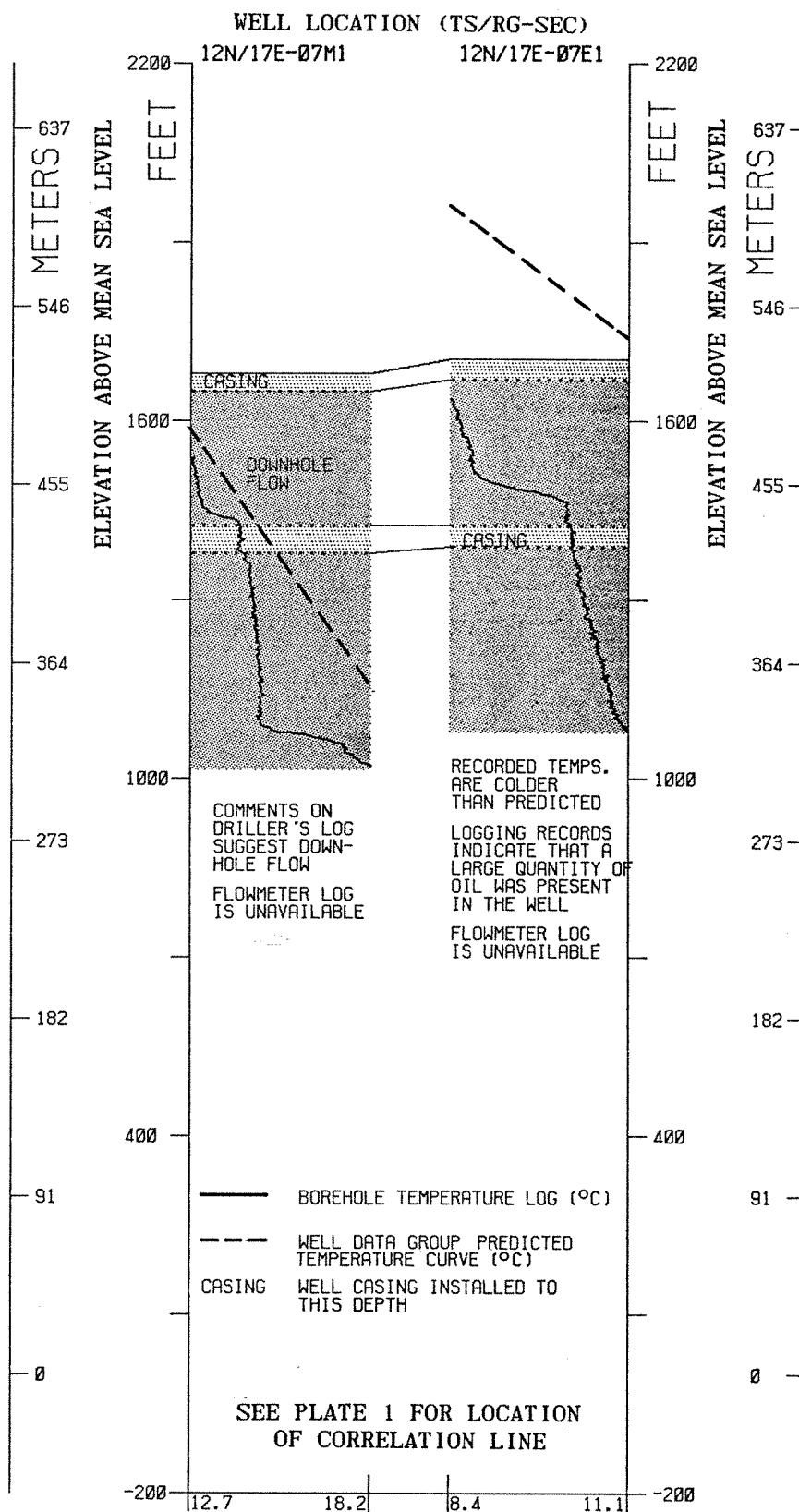


FIGURE 48 BOREHOLE TEMPERATURE LOGS AND WELL DATA GROUP PREDICTED TEMPERATURE CURVES - LINE 11



**FIGURE 49 BOREHOLE TEMPERATURE LOGS AND WELL DATA GROUP PREDICTED TEMPERATURE CURVES - LINE 12**

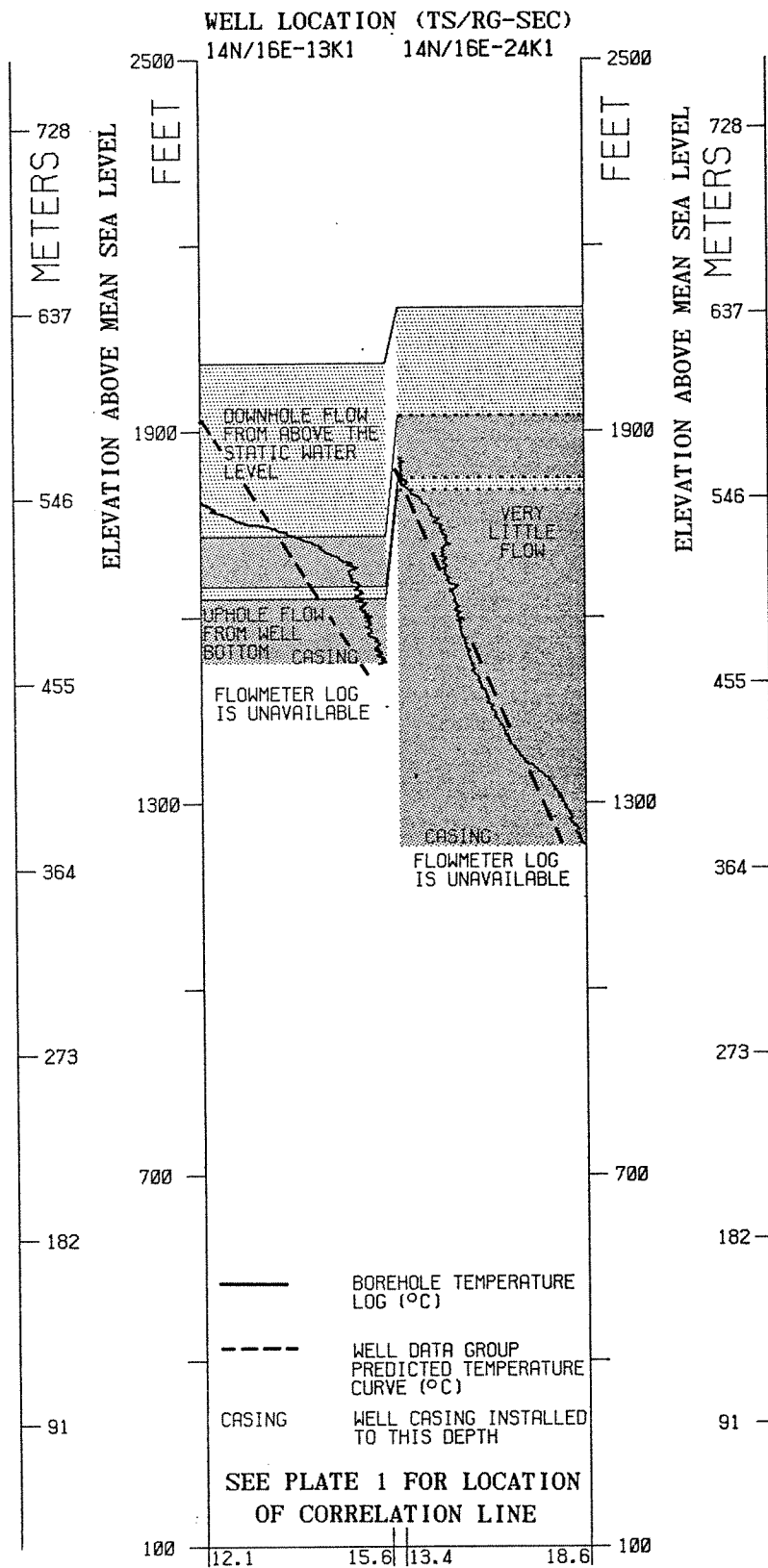
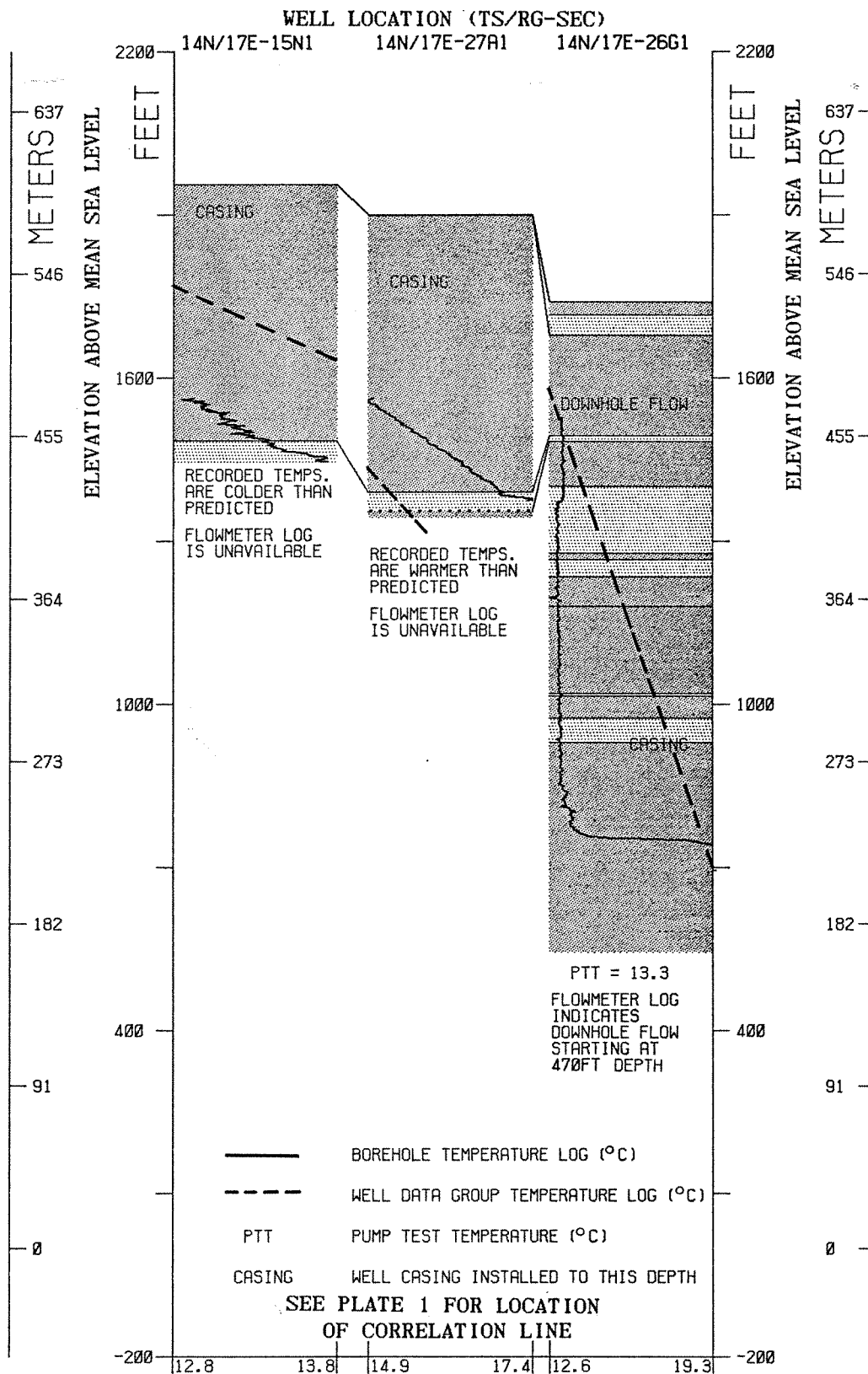
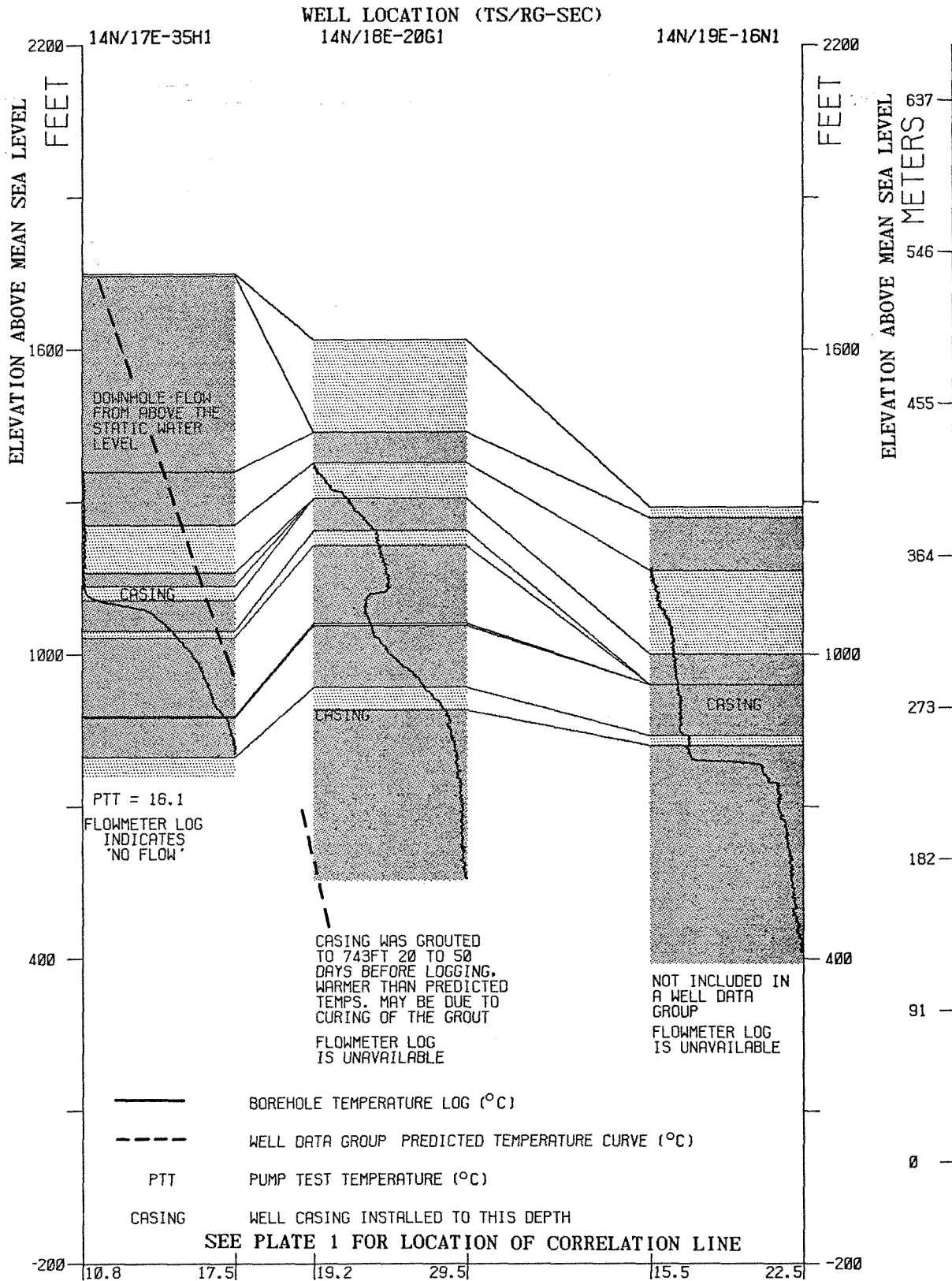


FIGURE 50 BOREHOLE TEMPERATURE LOGS AND WELL DATA GROUP PREDICTED TEMPERATURE CURVES - LINE 14



**FIGURE 51 BOREHOLE TEMPERATURE LOGS AND WELL DATA GROUP PREDICTED TEMPERATURE CURVES - LINE 15**



**FIGURE 52 BOREHOLE TEMPERATURE LOGS AND WELL DATA GROUP PREDICTED TEMPERATURE CURVES - LINE 16**

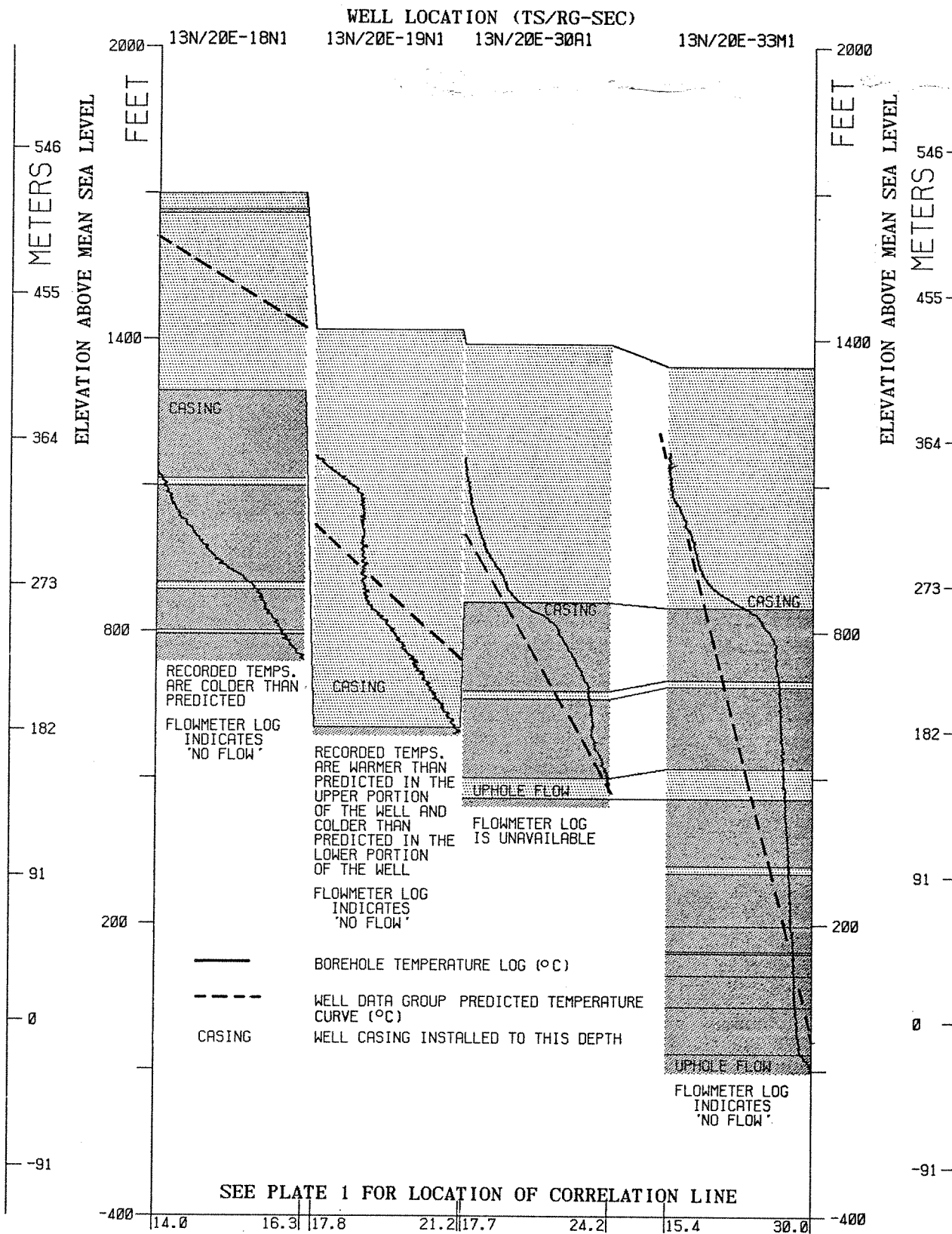


**FIGURE 53 BOREHOLE TEMPERATURE LOGS AND WELL DATA GROUP PREDICTED TEMPERATURE CURVES - LINE 17**

Pump test temperatures are data recorded during pumping or well development operations and may give an indication of expected production temperatures. Pump test temperatures were normally obtained from the Washington State well reports. The accuracy of the pump test temperatures is unknown.

The validity of the BHT vs. BHD linear regression analysis becomes obvious when the WDG predicted temperature curve is compared to the borehole temperature log from a water well with downhole flow. For example, the BHT of well 12N/22E-29B1 plots below the line defining the geothermal gradient of WDG 11 (Figure 34). The temperature log (Figure 46) from this well is severely distorted by downhole flow despite the fact that the flowmeter registered "no flow." Even so, the predicted geothermal gradient in combination with the projected LST accurately describes the borehole temperature gradient and aquifer temperature as recorded in the undisturbed upper portion of the well (see Figure 46). Without prior knowledge of the predicted geothermal gradient and the projected LST as calculated by the regression analysis of the BHT-BHD data from the neighboring wells of WDG 11, it would not be possible to determine either the borehole flow direction or the fact that the upper portion of this temperature log is undisturbed. The geothermal gradient calculated by assuming an LST of 12°C (equation 6) is 25.6°C/km. The geothermal gradient based on the BHT vs. BHD regression analysis is 42.3°C/km with a projected land-surface temperature of 10.6°C. The large difference in gradients is caused not only by the downhole flow which affected the BHT but also by the difference in the projected LST and assumed LST.

Many more examples of the excellent correlation between the undisturbed portion of the borehole temperature log and the WDG predicted temperature curve, as shown in Figures 38 through 53, could be cited. This is especially true of the WDG's given the "A" quality designation. Five out of the 7 WDG's investigated were rated as "A" quality.

WDG 12 was given a "C" quality rating, and the apparent mismatch of the borehole temperature logs and the WDG predicted temperature curves in 3 of the 7 wells studied reflects this lower quality (Figures 50 through 52). The fact that the WDG predicted temperature curve is related to the borehole temperature log in 4 of the 7 wells studied (Figures 50 through 52) suggests that the predicted geothermal data is accurate and that the temperature data from the 3 mismatched wells are of poor quality and unrepresentative of true geothermal gradient.

The geothermal gradients of the individual wells that comprise a WDG were calculated according to equation (6). Two different geothermal gradients were calculated for each well. The first, geothermal gradient G1, was determined by assuming that the LST is equal to the WDG projected LST. The second, geothermal gradient G2, was determined by assuming that the LST is 12°C. Mean geothermal gradients G1 and G2 of each WDG are given in Table 10. It should be noted that the BHT-BHD data that were excluded from the WDG regression analysis have also been excluded from the calculation of the mean geothermal gradients G1 and G2. The recognition and exclusion of this poor quality data would have been difficult if the regression analysis had not already been conducted.

As would be expected, the mean geothermal gradient G1 and the WDG geothermal gradient (as predicted by the regression analysis) are nearly the same. The difference between the WDG geothermal gradient and the mean geothermal gradient G1 is always smaller than the difference between the WDG geothermal gradient and the mean geothermal gradient G2.

Table 10. Well Data Group Geothermal Gradients, Mean Geothermal Gradients G1 and G2, Errors in Geothermal Gradient G2, and Corrected Mean Geothermal Gradient G2

Well Data Group	Well Data Group Geothermal Gradient ( $^{\circ}\text{C}/\text{km}$ ) <sup>1</sup>	Mean Geothermal Gradient G1 ( $^{\circ}\text{C}/\text{km}$ ) <sup>2</sup>	Mean Geothermal Gradient G2 ( $^{\circ}\text{C}/\text{km}$ ) <sup>3</sup>	Error in Geothermal Gradient G2 ( $^{\circ}\text{C}/\text{km}$ ) <sup>4</sup>	Corrected Mean Geothermal Gradient G2 ( $^{\circ}\text{C}/\text{km}$ ) <sup>5</sup>
1	38.7	38.8	37.9	0.8	38.7
2	33.7	35.0	43.4	-7.5	35.9
3	52.2	52.1	55.2	-2.9	52.3
4	48.3	48.6	45.8	2.2	48.0
5	40.3	40.8	43.7	-2.6	41.1
6	36.5	36.3	42.8	-5.6	37.2
7	34.1	34.0	35.9	-1.7	34.2
8	40.7	40.9	37.8	2.4	40.2
9	43.4	45.0	38.8	2.9	41.7
10	40.5	40.0	45.8	-4.2	41.6
11	42.3	40.7	33.8	5.7	39.5
12	24.9	24.9	19.4	3.9	23.3
13	29.8	30.3	25.0	3.1	28.1
14	39.8	39.7	41.6	-1.9	39.7

<sup>1</sup>geothermal gradient as predicted by the WDG regression analysis

$$\text{<sup>2</sup>mean geothermal gradient G1} = \frac{\text{BHT} - \text{WDG Projected LST}}{\text{BHD}} \text{ /number of wells}$$

$$\text{<sup>3</sup>mean geothermal gradient G2} = \frac{\text{BHT} - 12^{\circ}\text{C}}{\text{BHD}} \text{ /number of wells}$$

$$\text{<sup>4</sup>error in geothermal gradient G2} = \frac{12^{\circ}\text{C} - \text{WDG projected LST}}{\text{Mean WDG BHD}}$$

$$\text{<sup>5</sup>corrected mean geothermal gradient G2} = \text{mean geothermal gradient G2} + \text{error in geothermal gradient G2}$$

The error in the mean geothermal gradient G2 resulting from the difference between the WDG projected LST and the assumed LST of 12°C was calculated according to equation (7) and is given in Table 10. The BHD utilized in these calculations is the well data group mean BHD. The error in geothermal gradient G2 as calculated by equation (7) accounts for most of the difference between the WDG geothermal gradient and the mean geothermal gradient G2 of each of the fourteen WDG's (see Table 10).

The error in geothermal gradient G2 ranges from 5.7 to -7.5°C/km. These errors are significant because their magnitude is almost as great as the actual variation in the geothermal gradient of the region. The error in geothermal gradient G2 would have been greater if the poor quality BHT-BHD data had not been excluded from the calculation of the mean geothermal gradient G2.

#### Projected Land Surface Temperatures, Mean Elevations, Land Slope Azimuths, and Dip Angles of Well Data Groups

A simple analysis of any relationship between the predicted geothermal data and the mean elevation and land slope azimuth of a WDG was conducted in an attempt to relate the geothermal regime of a region to its topography. The mean elevation, land slope azimuth, and mean dip angle of a WDG were determined by sampling elevation data contained on magnetic digital terrain tapes available from the National Cartographic Center. Elevation data were sampled approximately every 254m on a square grid, or at a rate of about 15.5 points per square kilometer. Computer programs to read and sample the elevation data were written by Ken Seymour, a WSU staff member. The land slope azimuths and mean elevations of the WDG's are given in Table 11.

The mean dip angle for each of the WDG's was found to be about 2°. The relationship between the projected LST and the mean dip angle of the WDG was not studied further because of the uniformity in the dip angles.

A plot of the mean elevation vs. the projected LST of the WDG's is shown in Figure 54. A least squares linear regression analysis of these data yields the following equation:

$$^{\circ}\text{C} = 14.2^{\circ}\text{C} - 5.0^{\circ}\text{C}/\text{km} (\text{elevation}) \quad (8)$$

The correlation is poor and suggests that factors other than mean elevation influence the projected LST's. It is interesting to note that the air temperature-elevation gradient in this region is approximately -5.5°C/km (Donaldson, 1979), nearly the same as that predicted by the mean elevation vs. projected LST regression analysis.

A plot of the mean elevations vs. depths to the 20°C isotherm of the WDG's is shown in Figure 55. A least squares linear regression analysis of these data yields the following equation:

$$\text{Depth to the } 20^{\circ}\text{C isotherm} = 0.8 (\text{elevation}) - 110.0\text{m} \quad (9)$$

The correlation is fair and suggests that the depth to the 20°C isotherm increases as the land surface elevation increases.

Table 11. Mean Elevations and Azimuths of Well Data Groups

Well Data Group	Mean Elevation <sup>1</sup> of Well Data Group (m)	Azimuth <sup>2</sup> of Well Data Group (degrees)
1	319	28
2	300	149
3	220	18
4	308	194
5	368	207
6	372	192
7	366	214
8	536	62
9	338	143
10	413	211
11	538	142
12	520	104
13	513	138
14	445	320

$${}^1\text{mean elevation} = \frac{\Sigma \text{elevation at grid node}}{\text{number of points sampled}}$$

$${}^2\text{azimuth} = \tan^{-1} \phi = \frac{\Sigma \sin \phi}{\Sigma \cos \phi}$$

$\phi$  = azimuth from 0 to 360° at each grid node

$\overline{\phi}$  = azimuth of resultant vector

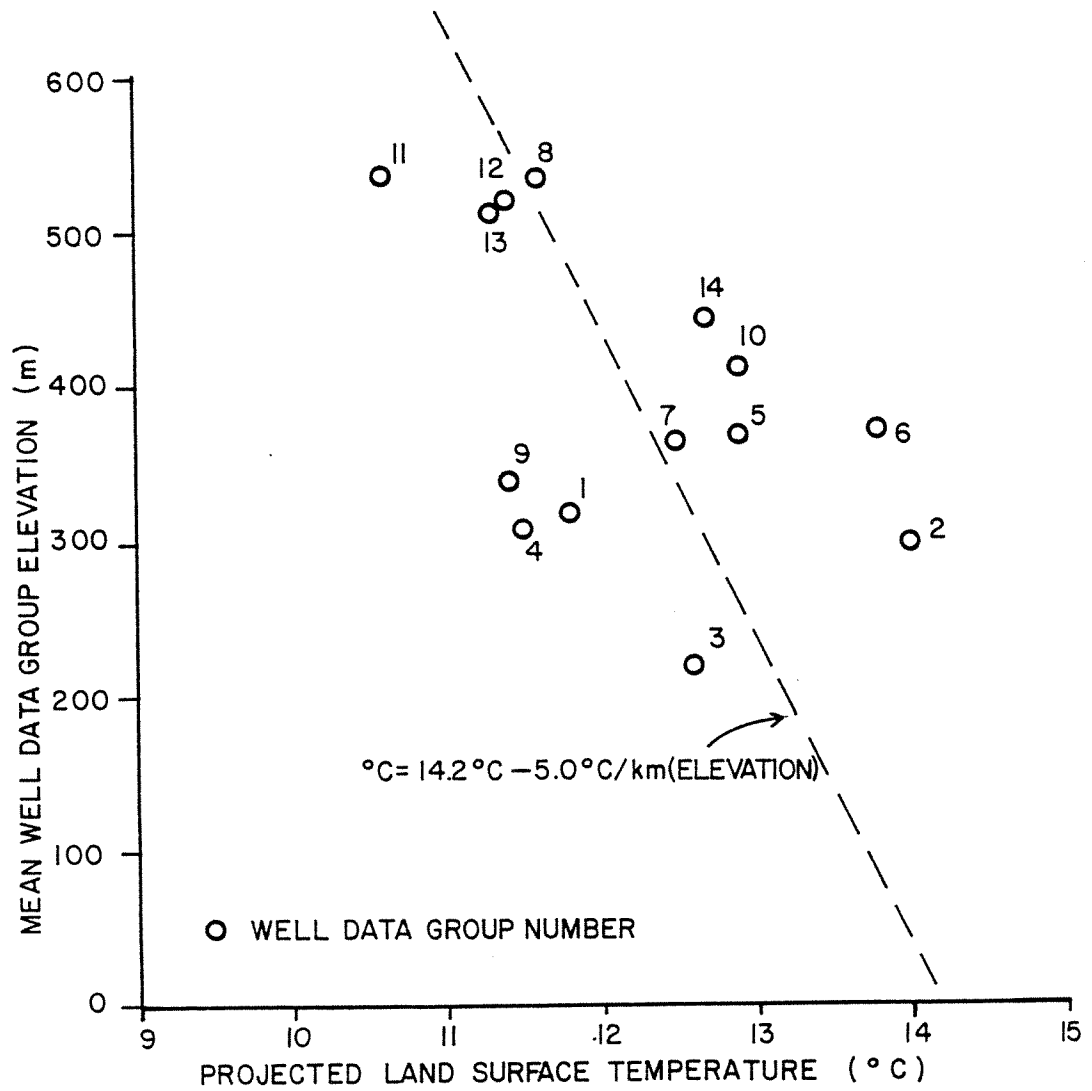


FIGURE 54 MEAN ELEVATION VS. PROJECTED LAND SURFACE TEMPERATURE OF THE WELL DATA GROUPS

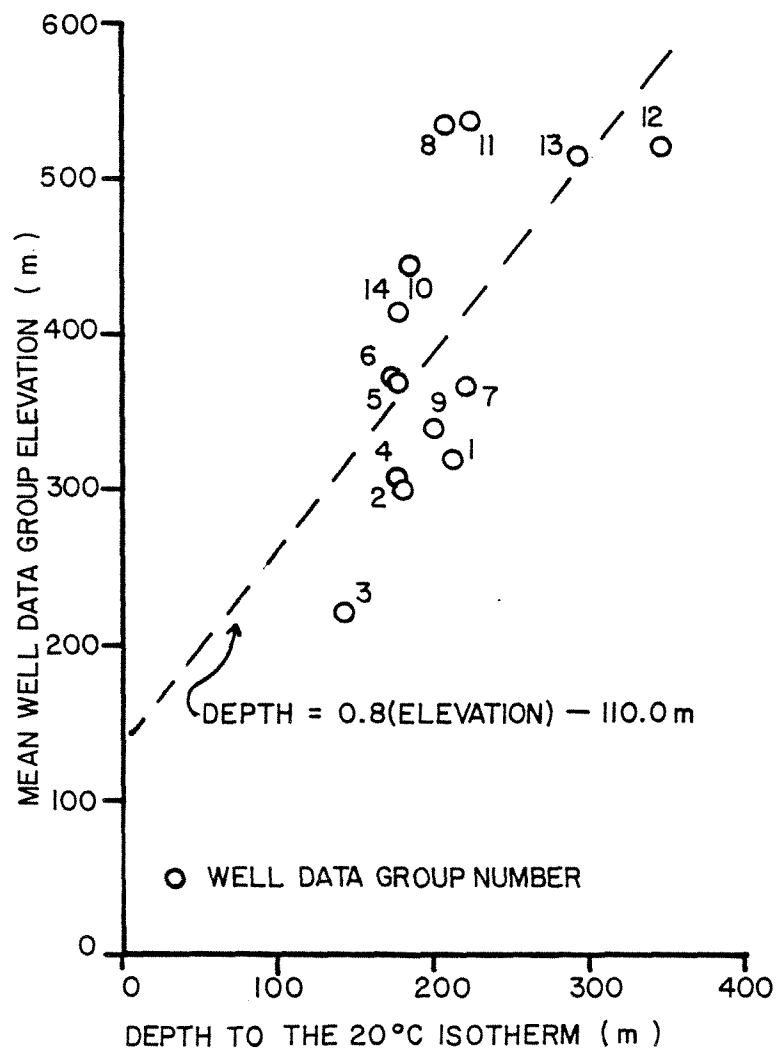


FIGURE 55 MEAN ELEVATION VS. DEPTH TO THE 20°C ISOTHERM OF THE WELL DATA GROUPS

The predicted geothermal gradients do not appear to be related to the mean elevations of the WDG's. In addition, the projected LST's, the depths to the 20°C isotherm, and predicted geothermal gradients do not appear to be related to the land slope azimuths of the WDG's. The apparent lack of correlation between the land slope azimuths and the predicted geothermal data of the WDG's may be caused, in part, by the simple method (linear) by which these relationships were examined. Other possible causes include the BHD's considered (i.e., greater than 50m) and the size of the geographic areas included in each WDG.

The apparent correlation between the mean elevations and the depths to the 20°C isotherm and between the mean elevations and the projected LST's of the WDG's may be explained by the ground-water flow system of the Yakima region. As noted earlier, the direction of ground-water flow in the region is from higher elevations towards lower elevations. The difference in the overall ground-water flow direction in the recharge portion (higher elevations) and discharge portion (lower elevations) and the increase in the residence time of the water in the flow system towards the lower elevations may be the cause of elevated temperatures at the lower elevations.

#### Deep vs. Shallow Geothermal Gradients

Bottom-hole temperatures from the Columbia Plateau recorded at depths greater than 700m are rare. A BHT vs. BHD plot for a WDG containing 14 wells with BHD's greater than 700m is shown in Figure 56. The BHT's used in the WDG analysis range from 41°C at 742m to 110°C at 2889m. The deep wells are located in a large triangular-shaped region of approximately 2000 square miles. These wells, which comprise the "deep" WDG, along with the locations of the "shallow" (less than 700m BHD) WDG's, are shown in Plate 4.

The BHT vs. BHD linear regression analysis for the deep WDG resulted in a predicted geothermal gradient of 31.3°C/km and a projected LST of 21.8°C. The depth to the 100°C isotherm is approximately 2513m. Figure 56 indicates an excellent correlation between the BHT and BHD data of the WDG. This result was not expected, considering the distance, a maximum of 130km, separating the well locations. The fact that there is an excellent correlation suggests that both heat flow and thermal conductivity remain nearly constant throughout this region and depth interval. It also suggests that the effect of the regional ground-water flow system upon the geothermal gradient is nearly constant and/or negligible at BHD's greater than 700m. The high projected LST (21.8°) of the deep WDG may result from a curvature in the geothermal gradient as the depth below the surface of the earth increases.

The BHT and BHD data used in WDG's 1 through 14, the shallow WDG's, are plotted in Figure 57. The linear regression analysis of the entire shallow BHT vs. BHD data set results in a predicted geothermal gradient of 43.0°C/km, a projected LST of 11.3°C, and a depth to the 20°C isotherm of 202m. These values should provide a reasonable estimate of the average geothermal gradient, the projected LST, and the depth to the 20°C isotherm within the areas encompassed by the shallow WDG's.

Direct comparisons between the shallow and deep predicted geothermal gradients should be made with caution because all of the deep wells but one (11N/22E-30G2) are located in an area to the east of the Yakima region. It does appear that the deep geothermal gradient of south-central Washington is less than the shallow geothermal gradient of the Yakima region.

The minimum depth limit of 700m of the deep WGD coincides with a decrease in the number of BHT's recorded at BHD's greater than 700m, and this limit is

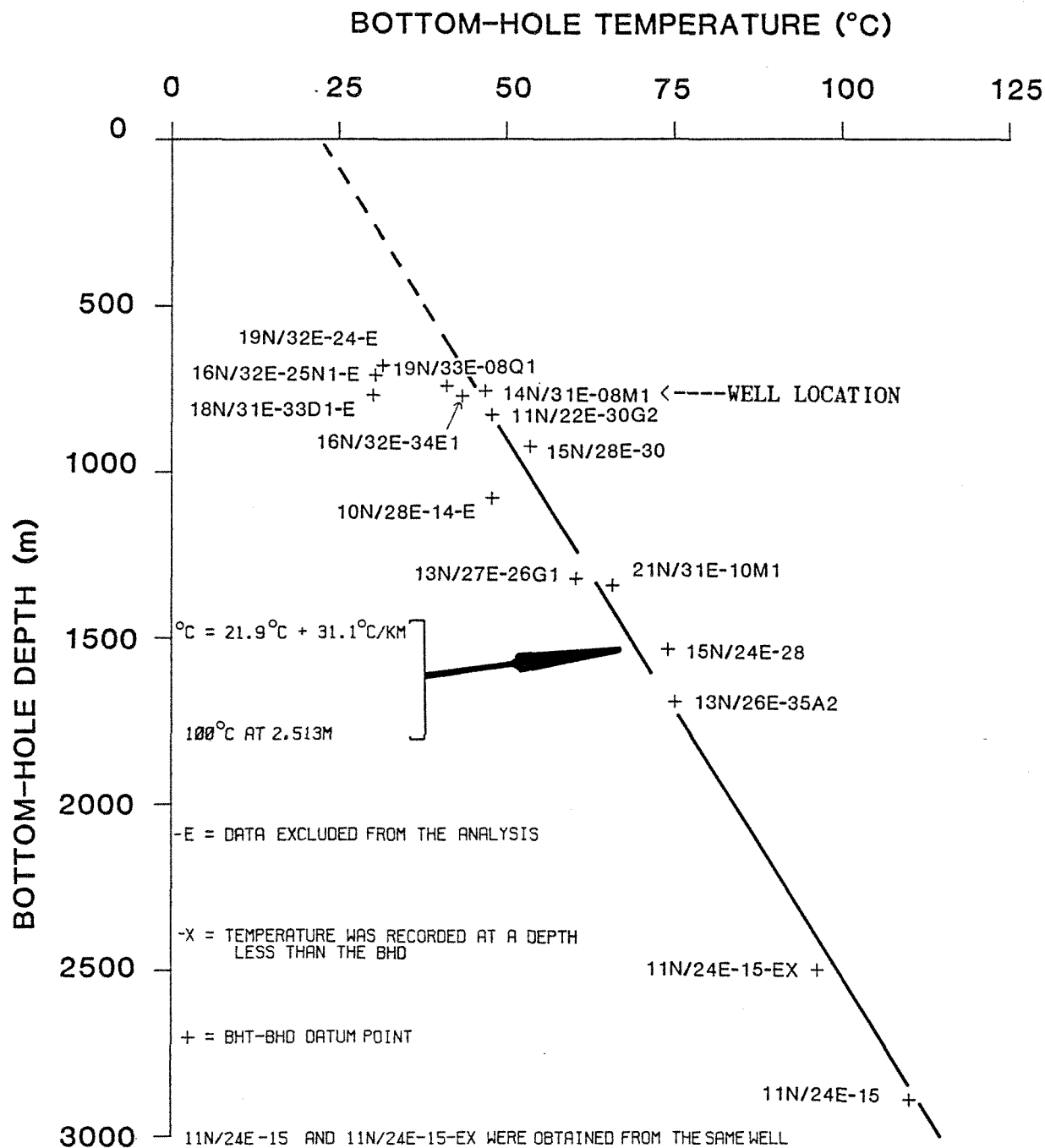


**FIGURE 56 PLOT OF BOTTOM-HOLE TEMPERATURE VS. BOTTOM-HOLE DEPTH FOR THE DEEP WELL DATA GROUP**

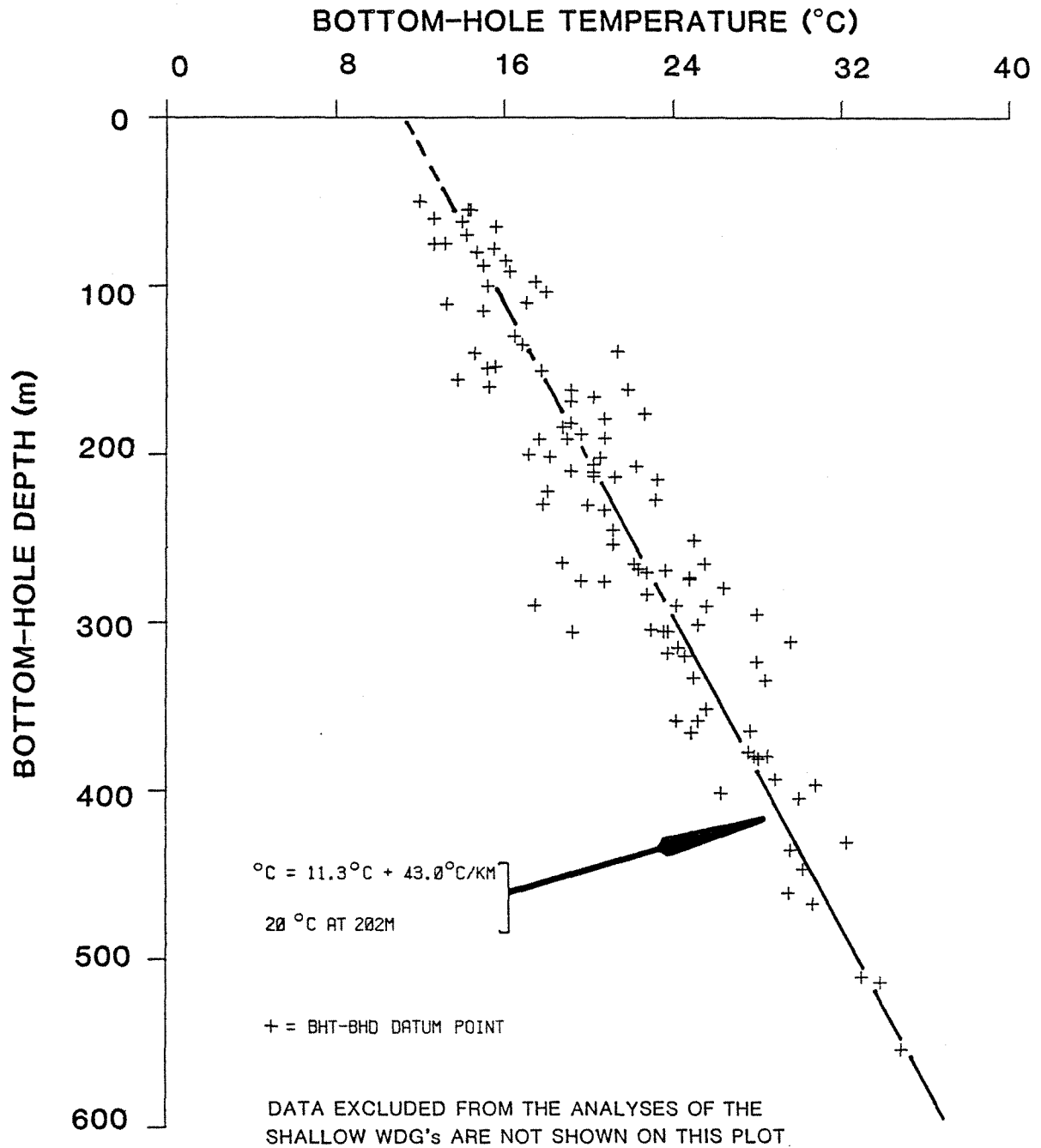


FIGURE 57 PLOT OF BOTTOM-HOLE TEMPERATURE VS. BOTTOM-HOLE DEPTH FOR THE SHALLOW WELL DATA GROUP.

somewhat arbitrary. A more accurate definition of the curvature and inflection point of the geothermal gradient cannot be formulated at this time because of relatively few BHT's from BHD's greater than 700m. A curvilinear analysis may prove more accurate than a linear analysis when more deep BHT data become available.

The magnitude of the error associated with the limited amount of deep BHT data, by the differences in geographic location, and by assuming a linear geothermal gradient does not appear to be large. This is suggested by the fact that the regression equations of the shallow and deep WDG's predict temperatures that differ by less than 2.3°C at a depth of 700m. The deep and shallow geothermal gradients predict equal temperatures, or intersect, at a depth of approximately 900m. The relationship between the deep and shallow geothermal gradients and projected LST's is shown in Figure 58.

The Yakima region and the area encompassed by the deep WDG are thought to act as recharge areas for the local and intermediate ground-water flow systems of the Columbia Plateau (Gephart and others, 1979). As reviewed previously in this report, the geothermal gradient would be expected to increase with depth in ground-water recharge areas. The geothermal gradient of south-central Washington appears to decrease with depth, as is shown in Figure 58, which suggests that downward (recharging) flow is not responsible for the apparent change in the gradient.

#### Heat Flow in the Yakima Region

The uncertainties involved in the value of the thermal conductivity of the lithologic units of the region cause calculation of the heat flow to be imprecise. Schmidt and others (1980) report that the thermal conductivity of the Grande Ronde, Umtanum, and Pomona basalts increases as the temperature and density of the basalt increases. Schmidt and others (1980) give the following equation which defines the basalt thermal conductivity,  $k$ , in terms of temperature,  $T$ , and density,  $\rho$ :

$$k = 0.58 + 0.045\rho + 0.00452T^{\circ}\text{C}(\rho - 1.77) \quad (10)$$

This relationship was developed from data obtained from the Grande Ronde and Umtanum basalts, and it also describes the thermal conductivity of the Pomona basalts at temperatures below 200°C. The difference in thermal conductivity as the density of basalt changes causes the thermal conductivity of the colonnade and entablature basalts to be greater than the interflow basalts (Schmidt and others, 1980). Equation (10) predicts a thermal conductivity of 0.814W/m°C, assuming a density of 2.75gm/cc and a temperature of 25°C.

A change which improved the testing method resulted in the measurement of a greater value of thermal conductivity for the Umtanum basalts (Foundation Sciences, Inc., 1981). FSI (1981) gives the following equation which defines the thermal conductivity of the Umtanum basalts,  $k_u$ , in terms of the temperature,  $T$ :

$$k_u = 2.16 + 0.0018(T^{\circ}\text{C}) \quad (11)$$

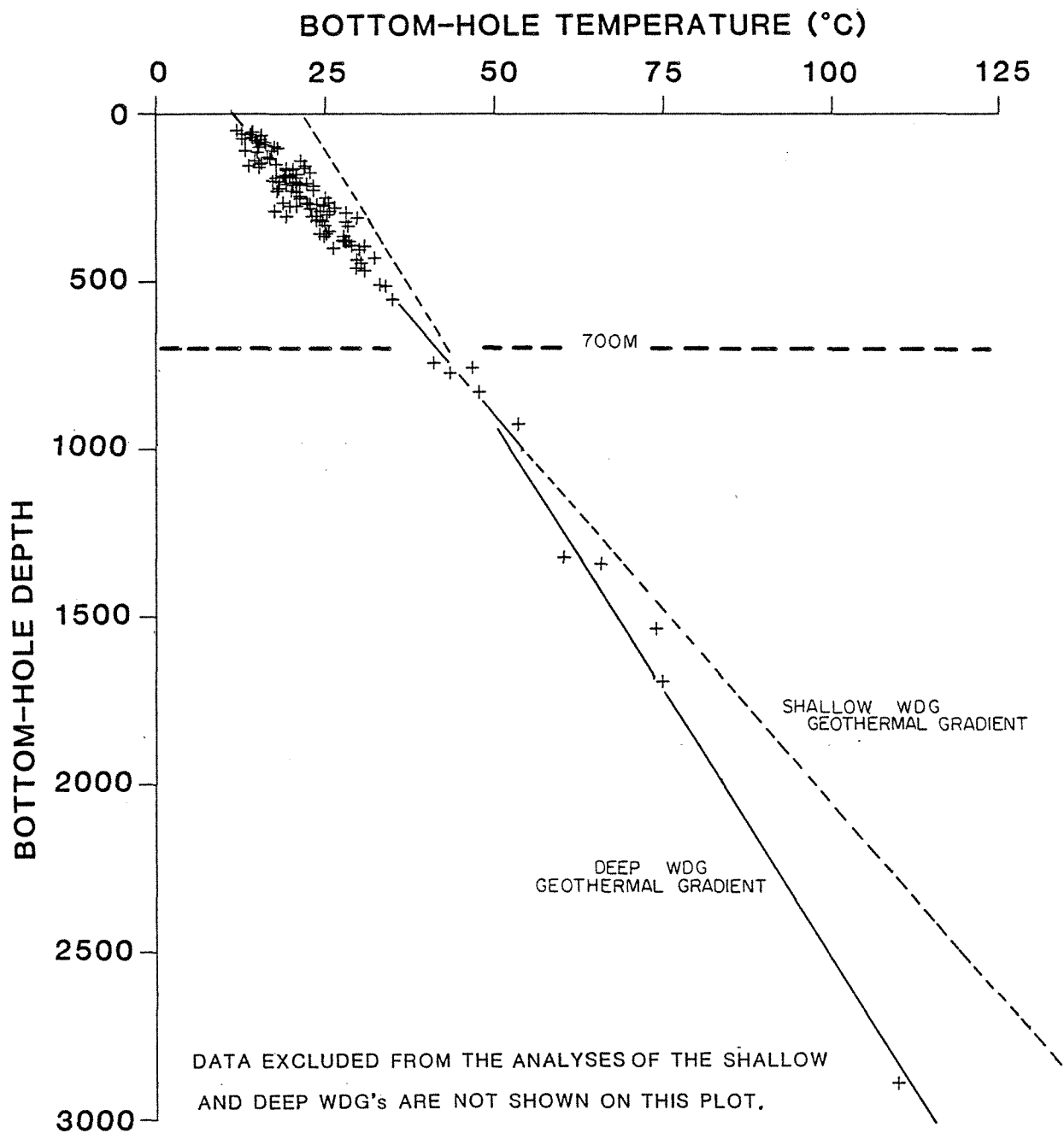


FIGURE 58 PLOT OF BOTTOM-HOLE TEMPERATURE VS. BOTTOM-HOLE DEPTH FOR THE SHALLOW AND THE DEEP WELL DATA GROUPS

Equation (11) predicts a thermal conductivity of  $2.205\text{W/m}^\circ\text{C}$  for the Umtanum basalts, assuming a temperature of  $25^\circ\text{C}$ . Thermal conductivities ranging from  $1.52$  to  $1.72\text{W/m}^\circ\text{K}$  have been used to determine the heat flow value of individual wells that bottom in the Columbia River basalts (Blackwell, 1980).

An approximation of the heat flow of the Yakima region can be made by assuming that the thermal conductivity varies from  $0.814$  to  $2.205\text{W/m}^\circ\text{C}$  and that the geothermal gradient equals  $43.0^\circ\text{C/km}$  (the shallow geothermal gradient). The resulting value of the heat flow, from equation (4), would range from  $35.0$  to  $94.8\text{mW/m}^2$ . A heat flow equal to about  $64.9\text{mW/m}^2$  would result if the assumed thermal conductivity were equal to  $1.510\text{W/m}^\circ\text{C}$ , a value midway between the reported extremes and closer to the values reported by Blackwell (1980).

The majority of the shallow BHT's and all of the deep BHT's were obtained within the CRBG. The apparent difference between the shallow and deep geothermal gradients may be partially explained by an increase in the thermal conductivity as the temperature and density of the basalt increases with increasing depths below the surface of the earth. Equation (4) indicates that the geothermal gradient will decrease in response to an increasing thermal conductivity if the heat flow is assumed to remain constant.

### Conclusions

The low-temperature geothermal resource of the Yakima region was described by analyzing the relationship between the BHT's and BHD's of two or more water wells. The fact that the BHT vs. BHD analysis could be successfully applied in the large geographic areas encompassed by the WDG's was not expected at the onset of this study.

Differences in the heat flow, thermal conductivity, and topography within a WDG might be expected to be great enough to produce a large variation in the geothermal regime of the individual wells and therefore cause a scatter of data on the plots of BHT vs. BHD. It should be apparent that the geothermal gradient and projected LST vary within the WDG, but the excellent correlation between the BHT and BHD data from the Yakima region suggests that the areal variation in the geothermal regime of a WDG is very small.

The ground-water flow system is at least partially responsible for the variation being as small as it appears to be. The effects of the flow system, especially the horizontal component, would tend to dampen the variation that results from differences in the heat flow, thermal conductivity, and topography. Topographic effects are also greatly reduced, if not eliminated, at the BHD's considered. In addition, the contrast in thermal conductivity was limited by the fact that most of the BHT's were obtained from the basalt aquifer.

Perhaps the greatest disadvantage of the BHT vs. BHD analysis is the requirement that at least three BHT's be available from the region before the assessment can be made with confidence. The results of any geothermal assessment which uses less than three BHT's by assuming an LST or by some other means would be subject to large errors. This is especially true when the calculated geothermal gradient must be projected to greater depths in order to reach production temperatures.

The BHT vs. BHD analysis should be applicable over even larger areas of the Columbia Plateau, considering the size of the WDG's of the Yakima region and the relatively small topographic relief of the plateau. If an LST must be assumed in order to calculate a geothermal gradient, then the BHT vs. BHD analysis should at least provide a guide to the assumed or projected LST.

### References

- Barker, R. A., 1979, Computer simulation and geohydrology of a basalt aquifer system in the Pullman-Moscow Basin, Washington and Idaho: Washington State Dept. of Ecology, Water-Supply Bulletin 48, Olympia, Wash.
- Bentley, R. D., 1977, Stratigraphy of the Yakima basalts and structural evolution of the Yakima ridges in the western Columbia Plateau, in Geological Excursions in the Pacific Northwest, Geological Society of America, 1977 Annual Meeting, E. H. Brown and R. C. Ellis, eds.: Western Washington Univ., Dept. of Geology, Bellingham, Wash.
- Bentley, R. D., and Farooqui, S. M., 1979, Left-lateral, strike-slip Riedel shears in the Yakima ridges, Columbia Plateau, Washington and Oregon: Rockwell Hanford Operations, Report RHO-BWI-SA-40-A, Richland, Wash.
- Bentley, R. D., Anderson, J. L., Campbell, N. P., and Swanson, D. A., 1980, Stratigraphy and structure of the Yakima Indian Reservation, with emphasis on the Columbia River Basalt Group: U. S. Geological Survey, Open File Report 80-200.
- Blackwell, D. D., 1971, The thermal structure of the continental crust, in The Structure and Physical Properties of the Earth's Crust, J. G. Heacock, ed.: American Geophysical Union, Geophysical Monograph 14, Washington, D. C.
- Blackwell, D. D., 1974, Terrestrial heat flow and its implications on the location of geothermal reservoirs in Washington, in Energy Resources of Washington: Washington State Dept. of Natural Resources, Div. of Geology and Earth Resources, Information Circular No. 50, Olympia, Wash.
- Blackwell, D. D., 1978, Heat flow and energy loss in the western United States, in Cenozoic Tectonics and Regional Geophysics of the Western Cordillera, R. B. Smith and G. P. Eaton, eds.: Geological Society of America, Memoir 152.
- Blackwell, D. D., 1980, Heat flow and geothermal gradient measurements in Washington through 1979, in The 1979-1980 Geothermal Resource Assessment Program in Washington, by M. A. Korosec and J. E. Schuster: Washington State Dept. of Natural Resources, Div. of Geology and Earth Resources, Open File Report 81-3, Olympia, Wash.
- Blackwell, D. D., Steele, J. L., and Brott, C. A., 1980, The terrain effect on terrestrial heat flow: Journal of Geophysical Research, vol. 85, no. B9, p. 4757-4772.
- Bloomquist, R. G., 1979, Geothermal energy in Washington, site data base and development status: Oregon Institute of Technology, Geo-Heat Utilization Center, Klamath Falls, Ore.

- Bolke, E. L., and Skrivan, J. A., 1981, Digital-model simulation of the Toppenish alluvial aquifer, Yakima Indian Reservation, Washington: U. S. Geological Survey, Open File Report 81-425, Tacoma, Wash.
- Brown, J. C., 1978, Discussion of geology and ground-water hydrology of the Columbia Plateau, with specific analysis of the Horse Heaven, Sagebrush Flat, and Odessa-Lind areas, Washington: Washington State Univ., College of Engineering, Research Report 78/15-23, Pullman, Wash.
- Brown, J. C., 1979a, Investigation of stratigraphy and ground-water hydrology, Columbia River Basalt Group, Washington: Washington State Univ., College of Engineering, Research Report 79/15-37, Pullman, Wash.
- Brown, J. C., 1979b, Geology and water resources of Klickitat County: Washington State Dept. of Ecology, Water Supply Bulletin No. 50, Olympia, Wash.
- Brown, J. C., 1980, Stratigraphy and ground-water hydrology of selected areas, Columbia Plateau, Washington: Washington State Univ., College of Engineering, Research Report 80/15-39, Pullman, Wash.
- Campbell, N. P., 1975, A geologic road log over Chinook, White Pass, and Ellensburg to Yakima highways: Washington State Dept. of Natural Resources, Div. of Geology and Earth Resources, Information Circular 54, Olympia, Wash.
- Campbell, N. P., 1976, Geologic map of the Yakima area: Washington State Dept. of Natural Resources, Div. of Geology and Earth Resources, Open File Report 76-11.
- Campbell, N. P., 1977a, Geology of the Selah area, Yakima County, Washington: Washington State Dept. of Natural Resources, Div. of Geology and Earth Resources, Open File Report 77-7, Olympia, Wash.
- Campbell, N. P., 1977b, Geology of the Snipes Mountain area, Yakima County, Washington: Washington State Dept. of Natural Resources, Div. of Geology and Earth Resources, Open File Report 77-8, Olympia, Wash.
- Campbell, N. P., and Bentley, R. D., 1979, Quaternary and Holocene faulting, Toppenish Ridge, south-central Washington, preliminary investigation: Rockwell Hanford Operations, Report RHO-BWI-SA-38-A, Richland, Wash.
- Cearlock, D. B., Cole, C. R., Foote, H. P., and Wallace, R. W., 1975, Mathematical ground-water model of the Ahtanum-Moxee subbasins, Yakima County, Washington: Battelle Pacific Northwest Laboratories, Richland, Wash.
- Cline, D. R., 1976, Reconnaissance of the water resources of the Upper Klickitat River Basin, Yakima Indian Reservation, Washington: U. S. Geological Survey, Open File Report 75-518, Tacoma, Wash.

- Crosby, J. W., III, Anderson, J. V., and Kiesler, J. P., 1972, Geophysical investigation of wells in the Horse Heaven Hills area: Washington State Univ., College of Engineering, Research Report 72/11-24, Pullman, Wash.
- Crosby, J. W., III, and Mellott, J. C., 1973, Physical characteristics of basalt aquifers: Washington State Univ., Water Research Center, Pullman, Wash.
- Diery, H. D., and McKee, B., 1969, Stratigraphy of the Yakima Basalt in the type area: Northwest Science, vol. 43, no. 2, p. 47-64.
- Diment, W. H., Urban, T. C., Sass, J. H., Marshall, B. V., Munroe, R. J., and Lachenbruch, A. H., 1975, Temperatures and heat contents based on conductive transport of heat, in Assessment of Geothermal Resources of the United States, 1975, D. E. White and D. L. Williams, eds.: U. S. Geological Survey, Circular 726, Washington, D. C.
- Donaldson, W. R., 1979, Washington climate for these counties--Grant, Kittitas, Klickitat, Yakima: Washington State Univ., Cooperative Extension Service, Publication EM 4422, Pullman, Wash.
- Eddy, P.A., 1971, Geology and ground-water availability, Selah area, Washington: Washington State Dept. of Ecology, Olympia, Wash.
- Foundation Sciences, Inc., 1981, Thermal/mechanical properties of Umtanum Basalt, borehole DC-2: Rockwell Hanford Operations, Report RHO-BWI-C-92, Richland, Wash.
- Foxworthy, B. L., 1962, Geology and ground-water resources of the Ahtanum Valley, Yakima County, Washington: U. S. Geological Survey, Water-Supply Paper 1598, Washington, D. C.
- Freeze, R. A., and Cherry, J. A., 1979, Groundwater: Prentice-Hall, Inc., Englewood Cliffs, N. J.
- Gephart, R. E., Arnett, R. C., Baca, R. G., Leonhart, L. S., and Spane, F. A., Jr., 1979, Hydrologic studies within the Columbia Plateau, Washington, an integration of current knowledge: Rockwell Hanford Operations, Report RHO-BWI-ST-5, Richland, Wash.
- Goguel, J., 1976, Geothermics: McGraw-Hill Book Co., New York, N. Y.
- Jhaveri, A. G., and Miller, J. A., 1980, Geothermal resources in the Yakima area, potential low temperature utilization, in Proceedings of the Geothermal Symposium, Low Temperature Utilization, Heat Pump Applications, District Heating, R. G. Bloomquist, ed.: Washington State Energy Office, Publication WAOENG 81-05, Olympia, Wash.
- Kinnison, H. B., and Sceva, J. E., 1963, Effects of hydraulic and geologic factors on streamflow of the Yakima River Basin, Washington: U. S. Geological Survey, Water-Supply Paper 1595, Washington, D. C.

- Korosec, M. A., Kaler, K. L., Schuster, J. E., Bloomquist, R. G., Simpson, S. J., and Blackwell, D. D., 1981, Geothermal resources of Washington: Washington State Dept. of Natural Resources, Div. of Geology and Earth Resources, Geologic Map GM 25, Olympia, Wash.
- Korosec, M. A., 1980, Well temperature information and locations in the state of Washington, in The 1979-1980 Geothermal Resource Assessment Program in Washington, by M. A. Korosec and J. E. Schuster: Washington State Dept. of Natural Resources, Div. of Geology and Earth Resources, Open File Report 81-3, Olympia, Wash.
- Lachenbruch, A. H., and Sass, J. H., 1977, Heat flow in the United States and the thermal regime of the crust, in The Earth's Crust, its Nature and Physical Properties, J. G. Heacock, ed.: American Geophysical Union, Geophysical Monograph 20, Washington, D. C.
- Lobdell, G. T., and Brown, J. C., 1977, Geophysical investigations of Washington's ground-water resources, annual report 1976/1977: Washington State Univ., College of Engineering, Research Report 77/15-76, Pullman, Wash.
- Long, P. E., Ledgerwood, R. K., Myers, C. W., Reidel, S. P., Landon, R. D., and Hooper, P. R., 1980, Chemical stratigraphy of Grande Ronde Basalt, Pasco Basin, south-central Washington: Rockwell Hanford Operations, Report RHO-BWI-SA-32, Richland, Wash.
- Luzier, J. E., and Burt, R. J., 1974, Hydrology of basalt aquifers and depletion of ground water in east-central Washington: Washington State Dept. of Ecology, Water-Supply Bulletin 33, Olympia, Wash.
- Luzier, J. E., and Skrivan, J. A., 1975, Digital-simulation and projection of water-level declines in basalt aquifers of the Odessa-Lind area, east-central Washington: U. S. Geological Survey, Water-Supply Paper 2036, Washington, D. C.
- MacNish, R. D., Myers, D. A., and Barker, R. A., 1973, Appraisal of ground-water availability and management projections, Walla Walla River Basin, Washington and Oregon: Washington State Dept. of Ecology, Water-Supply Bulletin 37, Olympia, Wash.
- Myers, C. W., Price, S. M., Caggiano, J. A., Cochran, M. P., Czimer, W. J., Davidson, N. J., Edwards, R. C., Fecht, K. R., Holmes, G. E., Jones, M. G., Kunk, J. R., Landon, R. D., Ledgerwood, R. K., Lillie, J. T., Long, P. E., Mitchell, T. H., Price, E. H., Reidel, S. P., and Tallman, A. M., 1979, Geologic studies of the Columbia Plateau, a status report: Rockwell Hanford Operations, Report RHO-BWI-ST-4, Richland, Wash.
- Myers, C. W., and Price, S. M., eds., 1981, Subsurface geology of the Cold Creek syncline: Rockwell Hanford Operations, Report RHO-BWI-ST-14, Richland, Wash.

- Parsons, M. L., 1970, Groundwater thermal regime in a glacial complex: Water Resources Research, vol. 6, no. 6, p. 1701-1720.
- Phillips, Earl L., 1970, Washington climate for these counties--Asotin, Benton, Columbia, Franklin, Garfield, Walla Walla: Washington State Univ., Cooperative Extension Service, Publication EM 3127, Pullman, Wash.
- Robinette, M. S., Robinette, M. J., and Brown, J. C., 1977, Geophysical investigations of Washington's ground-water resources, annual report 1975/1976: Washington State Univ., College of Engineering, Research Report 77/15-6, Pullman, Wash.
- Russell, I. C., 1893, A geological reconnaissance in central Washington: U. S. Geological Survey, Bulletin 108, Washington, D. C.
- Sass, J. H., and Lachenbruch, A. H., 1979, Heat flow and conduction-dominated thermal regimes, in Assessment of Geothermal Resources of the United States, 1978, L. J. P. Muffler, ed.: U. S. Geological Survey, Circular 790, Washington, D. C.
- Sceva, J. E., Watkins, F. A., Jr., and Schlax, W. N., Jr., 1949, Geology and ground-water resources of the Wenas Creek Valley, Yakima County, Washington: U. S. Geological Survey, Tacoma, Wash.
- Schmidt, B., Daly, W. F., Bradley, S. W., Squire, P. R., and Hulstrom, L. C., 1980, Thermal and mechanical properties of Hanford basalts, compilation and analyses: Rockwell Hanford Operations, Report RHO-BWI-C-90, Richland, Wash.
- Schmincke, H. U., 1967a, Flow directions in Columbia River Basalt flows and paleocurrents of interbedded sedimentary rocks, south-central Washington: Geologische Rundschau, vol. 56, p. 992-1020.
- Schmincke, H. U., 1967b, Fused tuff and peperites in south-central Washington: Geological Society of America Bulletin, vol. 78, p. 319-330.
- Schmincke, H. U., 1967c, Stratigraphy and petrography of four upper Yakima Basalt flows in south-central Washington: Geological Society of America Bulletin, vol. 78, p. 1385-1422.
- Schuster, J. E., 1974, Geothermal energy potential of Washington, in Energy Resources of Washington: Washington State Dept. of Natural Resources, Div. of Geology and Earth Resources, Information Circular No. 50, Olympia, Wash.
- Schuster, J. E., 1980, Geothermal energy potential of the Yakima Valley area, Washington, in Proceedings of the Geothermal Symposium, Low Temperature Utilization, Heat Pump Applications, District Heating, R. G. Bloomquist, ed.: Washington State Energy Office, Publication WAOENG 81-05, Olympia, Wash.

- Schuster, J. E., Blackwell, D. D., Hammond, P. E., and Huntting, M. T., 1978, Heat flow studies in the Steamboat Mountain-Lemei Rock area, Skamania County, Washington: Washington State Dept. of Natural Resources, Div. of Geology and Earth Resources, Information Circular 62, Olympia, Wash.
- Siems, B. A., Crosby, J. W., III, Anderson, J. V., Bush, J. H., and Weber, T. L., 1973, Final report 1972/73, Geophysical investigations of Washington's ground-water resources: Washington State Univ., College of Engineering, Research Report 73/15-58, Pullman, Wash.
- Smith, G. O., 1901, Geology and water resources of a portion of Yakima County, Washington: U. S. Geological Survey, Water Supply Paper 55, Washington, D. C.
- Smith, G. O., 1903, Description of the Ellensburg quadrangle (Washington): U. S. Geological Survey, Geological Atlas Folio 86, Washington, D. C.
- Stallman, R. W., 1963, Computation of ground-water velocity from temperature data, in Methods of Collecting and Interpreting Ground-Water Data, R. Bentall, comp.: U. S. Geological Survey, Water-Supply Paper 1544-H, Washington, D. C.
- Stevens, H. H., Jr., Ficke, J. F., and Smoot, G. F., 1975, Water temperature--influential factors, field measurement, and data presentation, Chapter D1, in Techniques of Water-Resources Investigations of the United States Geological Survey, Book I: U. S. Geological Survey, Washington, D. C.
- Swanson, D. A., 1966, Tieton volcano, a Miocene eruptive center in the southern Cascade Mountains, Washington: Geological Society of America Bulletin, vol. 77, p. 1293-1314.
- Swanson, D. A., 1967, Yakima basalt of the Tieton River area, south-central Washington: Geological Society of America Bulletin, vol. 78, p. 1077-1110.
- Swanson, D. A., and Wright, T. L., 1978, Bedrock geology of the northern Columbia Plateau and adjacent areas, in The Channeled Scabland, a Guide to the Geomorphology of the Columbia Basin, Washington, V. R. Baker and D. Nummedal, eds.: Planetary Geology Program, Office of Space Science, National Aeronautics and Space Administration, Washington, D. C.
- Swanson, D. A., Wright, T. L., Hooper, P. R., and Bentley, R. D., 1979a, Revisions in stratigraphic nomenclature of the Columbia River Basalt Group: U. S. Geological Survey, Bulletin 1457-G, Washington, D. C.
- Swanson, D. A., Anderson, J. L., Bentley, R. D., Byerly, G. R., Camp, V. E., Gardner, J. N., and Wright, T. L., 1979b, Reconnaissance geologic map of the Columbia River Basalt Group in eastern Washington and northern Idaho: U. S. Geological Survey, Open File Report 79-1363.

- Swanson, D. A., Brown, J. C., Anderson, J. L., Bentley, R. D., Byerly, G. R., Gardner, J. N., and Wright, T. L., 1979c, Preliminary structure contour maps on the top of the Grande Ronde and Wanapum Basalts, eastern Washington and northern Idaho: U. S. Geological Survey, Open-File Report 79-1364.
- Tanaka, H., Barrett, G., and Wildrick, L., 1979, Regional basalt hydrology of the Columbia Plateau in Washington: Rockwell Hanford Operations, Report RHO-BWI-C-60, Richland, Wash.
- Theis, C. V., Brown, R. H., and Meyer, R. R., 1963, Estimating the transmissibility of aquifers from the specific capacity of wells, in Methods of Determining Permeability, Transmissibility, and Drawdown, R. Bentall, comp.: U. S. Geological Survey, Water-Supply Paper 1536-I, Washington, D. C.
- U. S. Army Corps of Engineers, 1978, Yakima Valley regional water management study, Volume IV, Geology and Ground Water: Army Corps of Engineers, Seattle District.
- U. S. Geological Survey, 1974, Water resources of the Toppenish Creek Basin, Yakima Indian Reservation, Washington: National Technical Information Service, U. S. Dept. of Commerce, Report PB-243 749, Washington, D. C.
- Waitt, R. B., Jr., 1979, Forty late-Wisconsin catastrophic Lake Missoula backfloodings of Walla Walla and Lower Yakima valleys, southern Washington: Geological Society of America Abstracts with Programs, vol. 11, no. 3, p. 133.
- Waring, G. A., 1913, Geology and water resources of a portion of south-central Washington: U. S. Geological Survey, Water-Supply Paper 316, Washington, D. C.
- Waters, A. C., 1955, Geomorphology of south central Washington, illustrated by the Yakima East quadrangle: Geological Society of America Bulletin, vol. 66, p. 603-684.



## APPENDIX

LOCATIONS, DESIGNATIONS, BOTTOM-HOLE TEMPERATURES,  
AND BOTTOM-HOLE DEPTHS OF SELECTED WELLS  
IN THE YAKIMA REGION



Source <sup>1</sup>	TS/RG-SEC	Bottom-hole Depth (m)	Well Designation	Bottom-hole Temperature (°C)
3	08N/22E-01G1	329.0		23.0
1	08N/22E-11J1	161.5	Flower, B.	21.9
1	08N/24E-01J1	381.0	Prosser City	25.2
3	09N/21E-26L1	295.0		28.0
4	09N/21E-27R1	35.0		22.0
3	09N/22E-11H1	166.0		20.3
4	09N/23E-23G1	350.0		16.0
1	09N/23E-22J1	429.4	Grandview City	21.2
1	09N/25E-06B1	364.8	Prosser Experiment Station	24.9
2	10N/16E-26G1	135.0	Lawrence	16.9*
4	10N/17E-14D1	35.0		22.0
4	10N/17E-23L1	213.0		20.3
4	10N/17E-26J1	305.0		23.8*
4	10N/17E-27Q1	460.0		26.0
4	10N/17E-28B1	268.0		22.4
4	10N/17E-35B1	245.0		21.2
3	10N/18E-05Q1	202.0		20.6
4	10N/18E-31N1	318.0		23.8
4	10N/20E-03L1	244.0		14.8
4	10N/20E-04L1	312.0		22.6
3	10N/20E-09A1	256.0		20.5
4	10N/22E-25F1	480.0		20.0
1	10N/23E-17B1	359.6	Stout, B./Golob, D.	16.7
1	10N/23E-36A1	401.1	Evans, B.	25.6
1	10N/23E-36G1	282.8	White, J.	22.8
1	10N/25E-33N1	275.5	J and R Orchards	20.8
2	10N/28E-14	1079.9		47.8
1	11N/16E-25Q1	332.5	Pace, W. B.	25.0
4	11N/16E-34K1	139.0		21.4
4	11N/17E-01F1	358.0		24.2
4	11N/17E-02L1	265.0		25.5
4	11N/17E-03L1	301.0		25.2
4	11N/17E-16F1	302.0		31.6
4	11N/17E-16H1	233.0		20.8
4	11N/17E-30Q1	275.0		19.7
4	11N/18E-09N1	122.0		23.0
4	11N/18E-17B1	191.0		17.7
4	11N/18E-26L1	16.0		26.4
3	11N/18E-30H1	103.7		18.0
4	11N/19E-10Q1	233.0		18.4
4	11N/19E-10Q2	229.0		18.7
3	11N/19E-15A1	179.2		20.8
1	11N/20E-01M1	457.2	Johnson, F.	27.5
1	11N/20E-01R1	350.8	Lynch, B.	20.8
1	11N/20E-06A1	181.3	Peters, C.	19.2
1	11N/20E-13R1	333.7	Soost Brothers	28.4*
1	11N/21E-05B1	378.8	Weatherly, B.	28.5
1	11N/21E-06L1	364.2	Dahl, T.	27.7
1	11N/21E-06Q1	392.6	Dahl, T.	28.9

Source <sup>1</sup>	TS/RG-SEC	Bottom-hole Depth (m)	Well Designation	Bottom-hole Temperature (°C)
2	11N/21E-07A1	510.0	Clyde	33.0
1	11N/21E-16P1	380.4	Ramsier (DNR)	28.1*
2	11N/21E-17A1	273.0	Garretson	24.8
1	11N/21E-20M1	190.5	Hanrahan, P.	20.8
1	11N/21E-21B1	279.2	Ambrose, A.	26.4
1	11N/21E-22G1	303.9	Sandlin, J.	23.0
1	11N/21E-22G2	553.2	Sandlin, J., #2	34.9
1	11N/21E-22K1	319.4	Best, P.	24.6
1	11N/21E-34C1	173.7	Slagg, L.	18.5*
1	11N/21E-36K1	213.3	Gay, H.	21.3
2	11N/22E-21N1	207.0		22.3
1	11N/22E-26R1	466.3	Evans, B.	30.7
1	11N/22E-28A1	283.5	Kershaw, R.	16.6
1	11N/22E-29N1	434.3	Rowe Farms	29.6
1	11N/22E-30G1	188.1	de La Chapelle, C.	19.7
1	11N/22E-30G2	829.0	de La Chapelle, C.	47.8
4	11N/24E-15	2889.4	Rattlesnake Hills #1	110.0
2	11N/24E-15	2500.0	Rattlesnake Hills #1	96.3*
1	12N/16E-12N1	268.8	Shelton, C. L.	24.4
2	12N/16E-13B1	70.0		14.2
1	12N/16E-15E1	179.2	White, H.	10.5
1	12N/16E-18A1	108.2	Meyer, C.	19.7
3	12N/17E-02G1	85.0		16.1
1	12N/17E-02J1	27.4		19.4
1	12N/17E-07E1	191.4	Gilbert, C.	11.1
3	12N/17E-07L1	79.3		19.5
1	12N/17E-07M1	201.5	Bates, K. P.	18.2
2	12N/17E-11D1	130.0		16.5
4	12N/17E-16A1	265.0		22.2
4	12N/17E-16R1	329.0		17.0
2	12N/18E-01F1	62.0		14.0
2	12N/18E-26R1	184.0	Douglas	18.8
4	12N/18E-27G1	305.0		23.6
4	12N/18E-27H1	311.0		29.6
4	12N/18E-31R1	479.0		22.2
4	12N/18E-32H1	358.0		25.2
3	12N/18E-32L2	379.0		27.9
4	12N/18E-33A1	290.0		25.6
1	12N/18E-33B1	323.1	Mt. Adams Feed #3	28.0
4	12N/19E-01Q1	404.0		30.0
1	12N/19E-27H1	168.5	Stepniewski, S.	19.2*
1	12N/19E-28J1	91.4	Sunnyside Dam	16.3
1	12N/20E-13R1	376.4	Charron, S.	27.6
2	12N/20E-16H1	415.0	Elephant Mountain (DNR)	29.2
1	12N/20E-27N1	396.2	Logan, W.	30.8
3	12N/20E-27M1	409.0		27.5
2	12N/20E-31J1	110.0	Brooks	17.1*
1	12N/20E-34N1	274.0	Estes, M.	24.8
1	12N/20E-34N2	429.7	Estes, M.	32.3

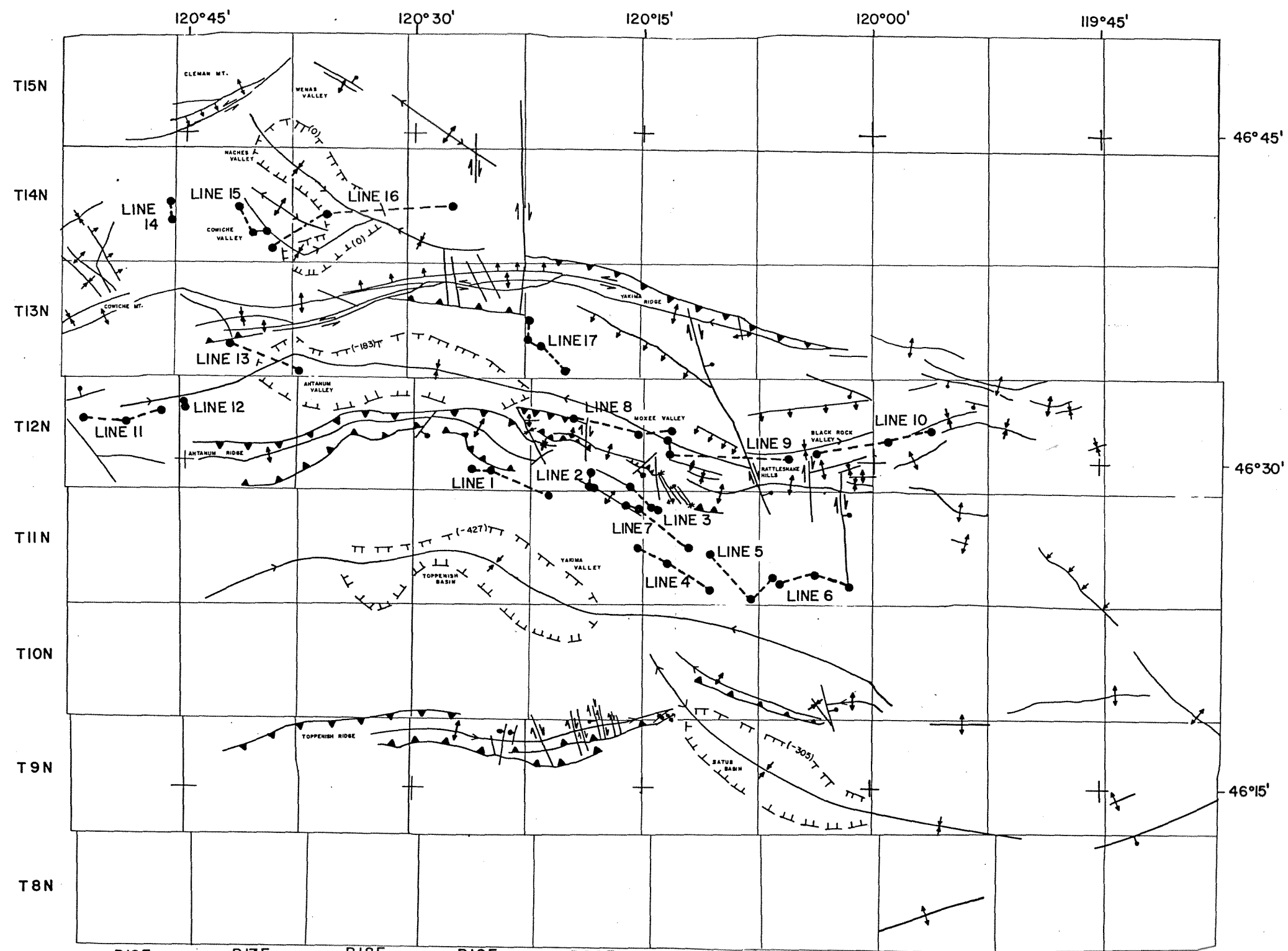
Source <sup>1</sup>	TS/RG-SEC	Bottom-hole Depth (m)	Well Designation	Bottom-hole Temperature (°C)
1	12N/20E-36P1	407.8	Cheyne Road (DNR)	25.6
2	12N/21E-16R1	235.0	DNR	25.1
1	12N/21E-17L1	472.7	Martinez, D.	28.3
1	12N/21E-20D1	143.9	Martinez, D. T., #1	21.4*
1	12N/21E-20P1	314.5	Griswald, P.	25.2
2	12N/22E-13	460.0	Changala	29.5*
3	12N/22E-14C1	149.0		15.2
2	12N/22E-20K1	210.0	Martinez	19.2
1	12N/22E-21R1	270.0	Marley Orchards	22.8
1	12N/22E-29B1	430.1	Changala, S.	23.0
1	12N/23E-16J1	350.8	Blackrock #1 (DNR)	25.6
2	12N/23E-16J2	100.0		15.2*
2	12N/23E-17P1	206.0		20.3*
1	12N/23E-19A1	229.5	Taggares Ranches	17.9
1	12N/24E-05A1	254.2	Tramel, J. D.	23.0
1	13N/17E-28B1	170.7	C-6 (DOE)	13.9
2	13N/18E-01F1	28.0	Silvercove	8.4
3	13N/18E-12A1	201.0		24.8
2	13N/18E-15L1	55.0	Nazerene	14.4*
4	13N/18E-24	513.0	Creamery	33.9
2	13N/19E-11K1	162.0		19.2
2	13N/19E-12N1	97.5	Hill	17.5*
1	13N/19E-13Q1	251.1	Terrace Heights	25.0
2	13N/19E-14A1	210.5	Watkins	20.3
3	13N/19E-22M1	82.0		20.0
2	13N/19E-23B1	78.0	Watkins	15.5
2	13N/19E-23C1	80.0	Watkins	14.7
3	13N/19E-24B1	230.0		44.5
2	13N/19E-24A1	230.0		20.0
4	13N/19E-31B1	191.0		19.0
1	13N/20E-18N1	292.0	Riebe, J.	16.3
1	13N/20E-19N1	253.3	Sundquist Fruit	21.2
2	13N/20E-20C1	65.0	Coppornall	15.6
2	13N/20E-20F1	215.0	Champoux	23.3
3	13N/20E-29D1	176.0		22.7
1	13N/20E-30A1	289.2	Yergen, R.	24.2
1	13N/20E-33L1	227.1	Coombs, B.	23.2
1	13N/20E-33M1	446.2	Coombs, B., #2	30.0
2	13N/21E-12D1	45.0		11.7*
1	13N/21E-34H1	310.9	Martinez, D. T., #2	21.2
1	13N/22E-13B1	516.9	Changala, S., #2	30.7
4	13N/26E-35A2	1691.6	ARH DC-1	75.0
1	13N/27E-26G1	1323.7	DC-6	60.2
2	14N/15E-29M1	67.0	Troutlodge	13.6
2	14N/16E-01B1	111.0	Englund	13.3*
2	14N/16E-01H1	170.0	Huck	13.1*
2	14N/16E-01J1	115.0	Marmion	15.0*
2	14N/16E-01K1	200.0	Shearer	17.2
1	14N/16E-13K1	147.8	Keller Fruit/Cold Stor. #2	15.6

Source <sup>1</sup>	TS/RG-SEC	Bottom-hole Depth (m)	Well Designation	Bottom-hole Temperature (°C)
1	14N/16E-24K1	264.6	Keller Fruit/Cold Stor. #1	18.6
4	14N/17E-04H1	305.0		14.4
2	14N/17E-06F1	160.0	Perham	15.3*
2	14N/17E-13H1	132.0	Murray	19.5*
1	14N/17E-15N1	155.7	Majnarich, F.	13.8
2	14N/17E-19K1	75.0	Knutson	12.7
2	14N/17E-19Q1	150.0	Mansperger	19.9
2	14N/17E-20P1	60.0	Dardon	12.7*
1	14N/17E-26G1	305.4	Allen, B.	19.3*
1	14N/17E-27A1	160.0	Zuetenhorst, W.	17.4
1	14N/17E-35H1	289.5	Hargrave, H.	17.5
2	14N/18E-07K1	50.0	Murray	12.0*
1	14N/18E-20G1	324.6	Zirkle, W. H.	29.5
2	14N/18E-29K1	55.0	McFarlane	14.3
1	14N/19E-16N1	268.2	Roche Fruit Company	22.5
4	14N/19E-28B1	183.0		21.0
2	14N/20E-16B1	29.0	Yakima Firing Center #2	12.1*
3	14N/20E-20N1	183.5		17.0
1	14N/31E-08M1	758.0	Rathbun, C.	46.8
2	15N/17E-02K1	90.0	Picatti	15.8
2	15N/17E-23B1	222.0	Day	18.1
2	15N/17E-24H1	155.0	Day	10.3
2	15N/17E-36A1	598.0	Wenas (DNR)	29.2
2	15N/18E-28A1	140.0	McNeilly	14.6
2	15N/18E-28R1	88.0	McNeilly	15.0
1	15N/18E-30G1	145.7	Boyd, J.	8.7
2	15N/18E-28M1	75.0	Young	13.2
1	15N/19E-22L1	121.9	Burbank Creek (USGS)	24.3
1	15N/19E-22P1	392.9	Larson Fruit	31.5
1	15N/24E-28	1534.3	DH-5	74.0
1	15N/28E-30	924.1	DH-4	53.5
1	16N/32E-25N1	709.2		30.4
4	16N/32E-34E1	772.9		43.4
1	18N/31E-33D1	771.0		30.0
1	19N/32E-24	680.3		31.5
4	19N/33E-08Q1	741.8		41.0
1	21E/31E-10	1342.5		65.8

<sup>1</sup>Source:

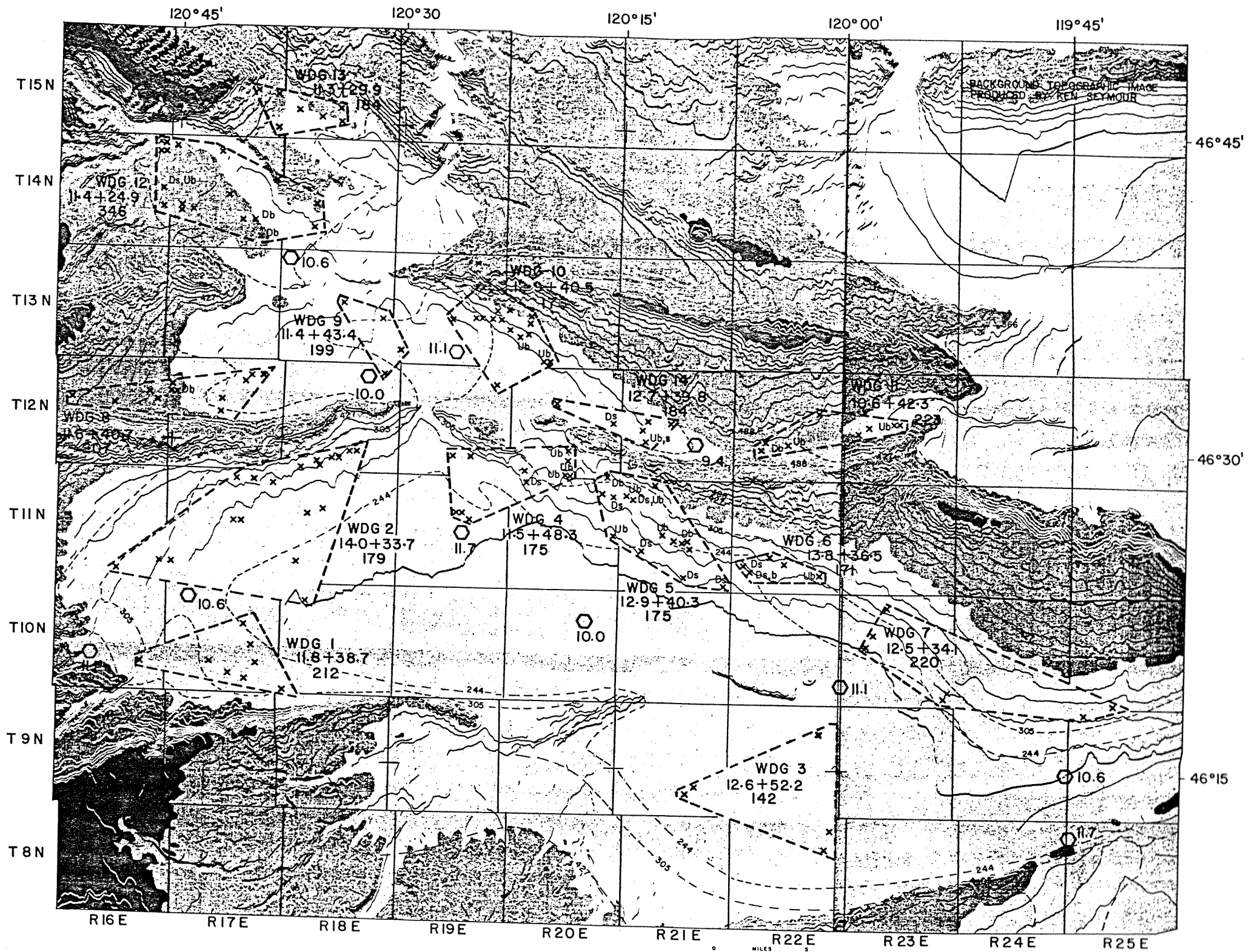
- 1 = Washington State University Geological Engineering Section
- 2 = Southern Methodist University Department of Geological Sciences
- 3 = U. S. Geological Survey
- 4 = others

\*= not a bottom-hole temperature



R16E R17E R18E R19E R20E R21E R22E R23E R24E R25E  
 PRELIMINARY STRUCTURAL GEOLOGY FROM SWANSON AND OTHERS (1979), (west of 120°) AND MYERS AND OTHERS (1979), (east of 120°)  
 FAULT ——— STRIKE SLIP FAULT ———  
 HIGH ANGLE FAULT BAR AND BALL ON DOWNTHROWN SIDE ———  
 THRUST FAULT ———  
 CRESTLINE OF ANTICLINE ———  
 TROUGHLINE OF SYNCLINE ———  
 ABRUPT CHANGE OF DIP ———  
 DIP INCREASES IN THE DIRECTION OF ARROWS ———  
 DIP DECREASES IN THE DIRECTION OF ARROWS ———  
 STRATIGRAPHIC CORRELATION LINE ———  
 STRUCTURE CONTOUR ON TOP OF THE WANAPUM AND GRANDE RONDE BASALTS ——— (ELEVATION IN METERS) ———

**PLATE 1 PRELIMINARY STRUCTURAL GEOLOGY AND LOCATIONS OF STRATIGRAPHIC CORRELATION LINES**



MAP LEGEND { WELL DATA GROUP NUMBER  
 PROJECTED LAND SURFACE TEMPERATURE(°C) + GEOTHERMAL GRADIENT(°C/km)  
 DEPTH(m) TO THE 20°C ISOTHERM

○ - MEAN ANNUAL ATMOSPHERIC TEMPERATURE(°C) (FROM PHILLIPS, 1970 AND DONALDSON, 1978)  
 x - LOCATION OF BOTTOM-HOLE TEMPERATURE DATA  
 D - DOWNHOLE } BOREHOLE FLOW DIRECTION  
 U - UPHOLE }  
 b - BASALT } AQUIFER FROM WHICH THE  
 s - SEDIMENTARY } BOREHOLE FLOW ORIGINATES  
 ( ) - ELEVATION IN METERS - GROUND WATER STATIC LEVEL (AFTER TANAKA AND OTHERS, 1978)  
 - - - - - WELL DATA GROUP BOUNDARY

PLATE 2 WELL DATA GROUP LOCATIONS AND PERTINENT PARAMETERS

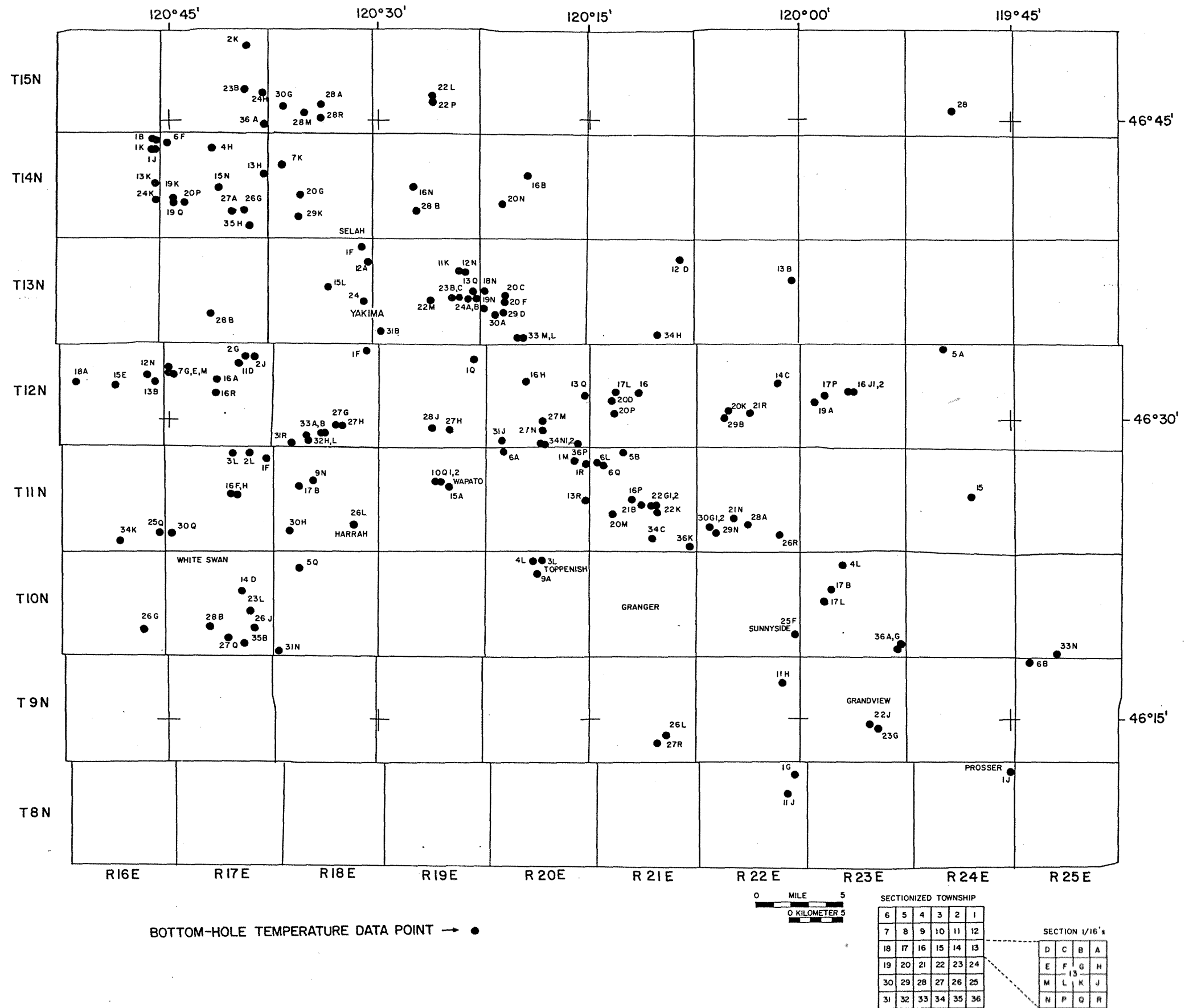
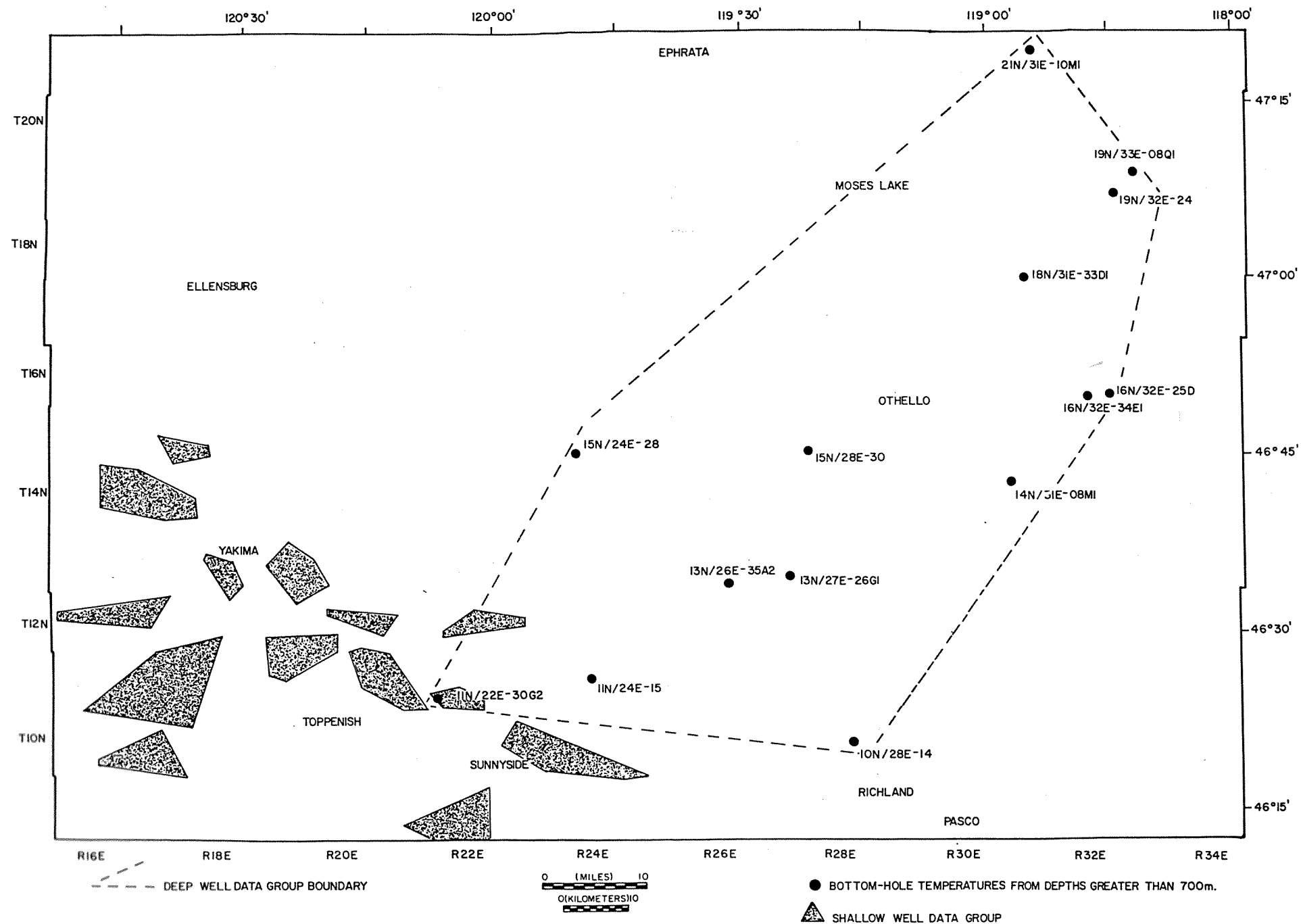


PLATE 3 LOCATION OF BOTTOM-HOLE TEMPERATURE DATA POINTS



**PLATE 4 LOCATION OF BOTTOM-HOLE TEMPERATURE DATA POINTS FROM DEPTHS GREATER THAN 700M**